Master Thesis

Experimental evaluation of an adsorbent under direct air capture conditions

carried out for the purpose of obtaining the degree of Master of Science (MSc or Dipl.-Ing. or DI), submitted at TU Wien, Faculty of Mechanical and Industrial Engineering, under the direction of Univ.Prof. Dipl.-Ing. Dr.techn. Hermann Hofbauer

by

Florian Maximilian Chimani

Mat.Nr.: 01604990

[redacted]

[redacted]

under the supervision of

Dipl.-Ing. Dr.techn. Josef Fuchs

Vienna April 28, 2022

Affidavit

I declare in lieu of oath, that I wrote this thesis and performed the associated research myself, using only literature cited in this volume. If text passages from sources are used literally, they are marked as such.

I confirm that this work is original and has not been submitted elsewhere for any examination, nor is it currently under consideration for a thesis elsewhere.

I acknowledge that the submitted work will be checked electronically-technically using suitable and state-of-the-art means (plagiarism detection software). On the one hand, this ensures that the submitted work was prepared according to the high-quality standards within the applicable rules to ensure good scientific practice "Code of Conduct" at the TU Wien. On the other hand, a comparison with other student theses avoids violations of my personal copyright.

City and Date	*Signature*

Acknowledgements

This work would not have been possible without the knowledge taught to me at the Institute of Process Engineering, Environmental Engineering and Technical Biosciences at the Vienna University of Technology, for which I would like to express my sincere thanks.

I would like to thank Prof. Hermann Hofbauer as well as Dr. Dipl.-Ing. Josef Fuchs and Dr. Dipl.-Ing. Johannes Fuchs for their trust and valuable scientific support.
Thank you, Josef, for the numerous discussions, the time and the patience you gave me, whether it was about literature advice or the operation of the experimental facility and the Laboratory plant. Thank you, Johannes, for your extensive support in the commissioning of the experimental plant. Your wide-ranging expertise, especially in industrial-plant engineering, was essential to the success of this work.

I would like to express my deepest gratitude to my whole family, without them my studies would not have been possible in this form.

Kurzfassung

Direct air capture (DAC) kann einen wesentlichen Beitrag leisten, schwer zu vermeidende CO_2 Emissionen zu reduzieren. Die großmaßstäbliche Umsetzung von DAC erfordert allerdings ernsthafte staatliche, private und unternehmerische Unterstützung und Investitionen, insbesondere zum Ausgleich der Kapital- und Betriebskosten. Weitere Optimierungen können in der Wahl der Energiequelle sowie in Fortschritten bei der CO_2-Abscheidungstechnologie gefunden werden, z. B. Materialien mit hoher CO_2 Kapazität und Selektivität, schnellere Kinetik und einfache Wiederverwendbarkeit.

Am Institut für Verfahrenstechnik, Umwelttechnik und technische Biowissenschaften an der TU Wien wurde ein Temperaturwechseladsorptionsverfahren auf Basis eines Festbett-betriebes im Labormaßstab untersucht. Die Basis für das ausgewählte Verfahren liefert eine umfassende Literaturrecherche. Dabei werden die wichtigsten Technologien, welche für DAC verwendet werden, vorgestellt und miteinander verglichen. Ein Hauptaugenmerk dieser Arbeit ist die Co-Adsorption von CO_2 und H_2O. Die Adsorption von CO_2 kann mit dem Toth Modell ausreichend gut beschrieben werden[1]. Gleiches gilt für die Beschreibung der Adsorption von H_2O, welche basierend auf dem Mehrschicht-Ansatz von Brunauer, Emmet und Teller (BET) angewendet werden kann[2]. Allerdings ist es zurzeit nicht möglich die CO_2-H_2O Adsorption mathematisch exakt zu beschreiben, da die zugrundeliegenden chemischen Vorgänge in der Literatur nicht ausreichend untersucht wurden. Für weiterführende Experimente und erste Versuchsdaten reicht die empirische Methode, welche in dieser Arbeit beschrieben wurde, allerdings aus.

Der Forschungsbereich Brennstoff- und Energiesystemtechnik und die darin enthaltene DAC Arbeitsgruppe plant basierend auf dieser und weiterer Arbeiten den Bau eines Prototyps. Um die Auslegung und zugrundeliegende Technologie der geplanten DAC Prototyp-Anlage festlegen zu können, wurde eine Evaluierung laufender DAC-Projekte aus diversen Forschungsgruppen durchgeführt. Dabei wurden die wichtigsten Start-ups nach diversen Kriterien wie verwendete Technologie, vorhandene Patente, Investments etc. untersucht. Diese Evaluierung bestätigt das Potential von auf festen Aminen basierten Adsorptionsmittel für das Prototyp-Design.

Abstract

DAC can make a significant contribution to reduce CO_2 emissions which are hard-to-avoid. However, large-scale implementation of DAC requires serious government, private, and corporate support and investment, especially to offset capital and operating costs. Further optimization may be found in energy source selection and advances in CO_2 capture technology, such as materials with high capacity and selectivity, faster reaction kinetics, and reusability.

At the Institute of Process Engineering, Environmental Engineering and Technical Biosciences at the Vienna University of Technology, a temperature swing adsorption process based on a fixed bed operation was investigated on a laboratory scale. The basis for the selected process is provided by a comprehensive literature review. The most important technologies used for DAC are presented and compared. An important part of this work is the co-adsorption of CO_2 and H_2O. The adsorption of CO_2 can be described sufficiently well with the Toth model[1]. The same can be said about the adsorption of H_2O, which can be described based on the multilayer approach of Brunauer, Emmet and Teller (BET)[2]. However, it is currently not possible to describe the CO_2-H_2O adsorption in a mathematically more advanced way because the underlying chemical processes have not been sufficiently investigated in the literature. However, the empirical method described in this thesis is sufficient for the discussion of experiments and the corresponding data.

Based on this and further work, the DAC-team of the TU plans to build a prototype DAC-unit. In order to be able to determine the design and underlying technology of the planned prototype, an evaluation of the DAC competition was conducted. In this process, the most important start-ups were examined according to various criteria such as technology used, existing patents, investments, etc. This evaluation confirms the potential of solid amine-based adsorbents for the prototype design.

Table of content

1 INTRODUCTION 1

2 STATE OF THE ART OF DAC 2

2.1 CARBON CAPTURE THEORY 2

2.2 DAC TECHNOLOGY 6

2.3 ADSORPTION 15

2.4 PURE COMPONENT ADSORPTION 18

2.5 EVALUATION OF COMPETITION 22

2.6 OVERVIEW OF DAC COMPETITION 28

3 EXPERIMENTAL WORK 30

3.1 LABORATORY PLANT SETUP 30

3.2 CALCULATION OF FIXED BED OPERATION 37

3.3 LABORATORY PLANT PROCEDURE 39

3.4 ADSORBENT EVALUATION WITH LAB PLANT 43

3.5 EXPERIMENTAL DAC PLANT SETUP 50

4 DISCUSSION OF LABORATORY PLANT DATA 55

4.1 DESORPTION 55

4.2 ADSORPTION 57

4.3 DATA VALIDATION WITH EXPERIMENTAL DAC PLANT 61

5 CONCLUSION 65

6 DIRECTORIES 67

6.1 LIST OF ABBREVIATIONS AND SYMBOLS 67

6.2 LIST OF TABLES 69

6.3 LIST OF FIGURES 70

6.4 LITERATURE 73

1 Introduction

CO_2 concentrations in the atmosphere have been steadily increasing from 280 ppm in pre-industrial times to more than 410 ppm today mainly due to anthropogenic emissions. It is common agreement among scientists that limiting the CO_2 concentration in the atmosphere is necessary in order to stay within the 1.5 °C temperature increase limits. Therefore, the classical approach for CO_2 capture is based on point source carbon capture, where the CO_2 is separated from a CO_2-rich flue gas stream. In contrast to this classical approach direct air capture (DAC) can be used to manage emissions from distributed sources, such as cars or breathing air. Like any technology, DAC has its challenges too: humidity, changing weather conditions and high energy demand.

A novel research project at TU Wien focuses on the development and commercialization of a DAC prototype. Through retrofitting the DAC technology to commercial heating, ventilation and air conditioning (HVAC) systems, the above-mentioned problems should be solved. Additionally, HVAC systems could be the source of air that is less diluted in CO_2 than typical ambient air. Furthermore, in contrast to typical ambient air being affected changing weather conditions, air release by HVACs is mostly consistent in temperature and conditions. Finally, DAC blower energy requirements could be reduced by using the same air removed by the HVAC blower.

2 State of the art of DAC

2.1 Carbon Capture Theory

Due to the "Paris agreement" of the UN Climate Conference COP21, society is required to make a comprehensive and rapid transformation of our climate strategy with a significant reduction in greenhouse gas emissions. An imperative way to reduce the rise of global temperature is to stabilize atmospheric CO_2 levels.

The Intergovernmental Panel on Climate Change (IPCC) states that by 2050 CO_2 emissions must be reduced by 30-85% just to stabilize atmospheric CO_2 between 350 and 440ppm. This would require to not only stop emissions from coal-fired power plants, but also significantly reduce emissions produced by all other fossil fuels. To achieve full stabilization of the atmospheric CO_2 concentration beyond 2050, global CO_2 emissions would have to decrease to levels approaching zero. Some research even suggests that it is necessary to reduce the amount of CO_2 below levels currently in the atmosphere. [3]–[5]

Achieving climate goals requires careful demand management, global decarbonization, and the development and deployment of negative emissions technologies (NETs). NETs must no longer be seen as a last option; they must be deployed to offset hard-to-decarbonize sectors and stabilize the planet's carbon reserves.[6]

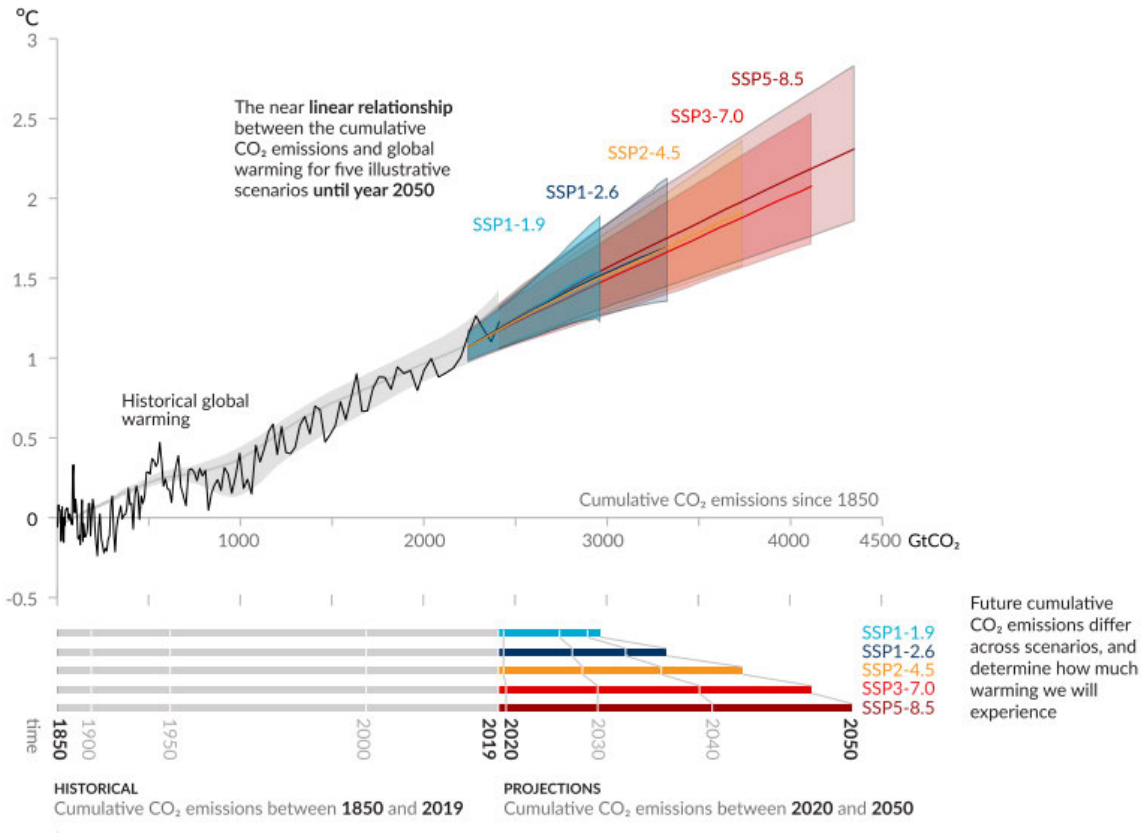

Figure 1: Global surface temperature increase since 1850-1900 as a function of cumulative CO_2 emissions [7]

2.1.1 Carbon dioxide capture from concentrated sources

Capturing carbon dioxide from concentrated sources is essential to significantly reduce emissions. Typically, flue gases from fossil burning power plants contain between 5 and 15% CO_2. These power plants could be retrofitted with post combustion CO_2 capture facilities. There are also huge amounts of CO_2 emitted in the iron, steel, aluminium, and cement industry. Therefore, it is inevitable that great efforts must be made to develop technologies to separate the emitted carbon dioxide.

Today the sequestration of carbon dioxide from conventional power plants happens at different points in the process chain and with different methods. One way to distinguish those methods is by the starting point of separation.

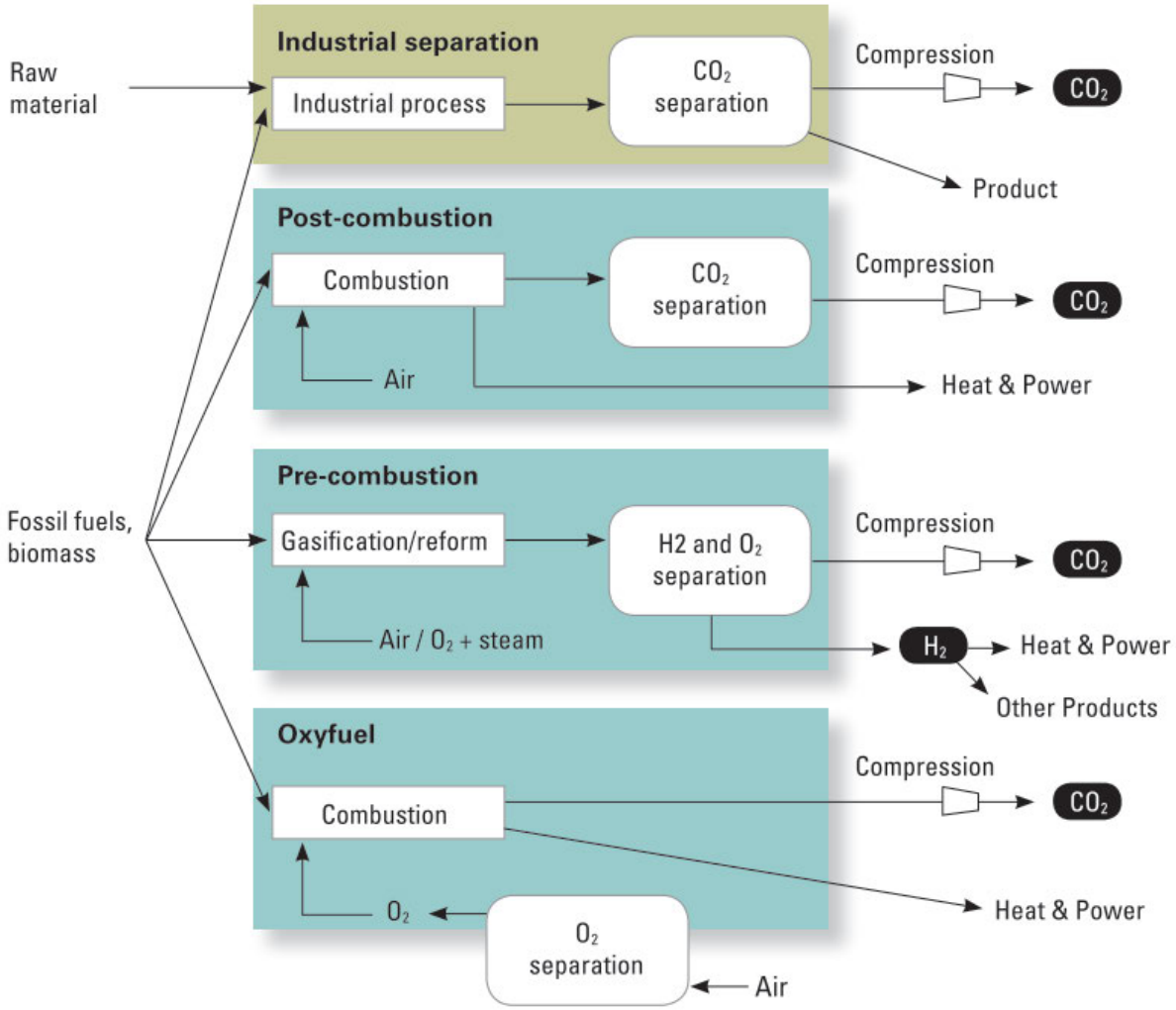

Figure 2: Types of carbon capture scenarios[8]

All those methods offer different advantages and disadvantages. One major advantage of post combustion systems and the separation at the end of industrial process chains is the ability to retrofit emitting plants. While the use of pre-combustion and oxyfuel technologies in some cases requires considerable changes in the process chain, in the best case nothing needs to be changed in previous steps at existing plants in order to implement a separation concept in the exhaust gas.[8]

There are three main technologies for the post combustion capture of CO_2 from flue gas:

Absorption with liquid solvents: Liquid solvents are used for the separation of CO_2 since the early 1950 and are thus among the most advanced available technologies. The most common solvents are based on chemical reactions with various amines, which show reversible reactions with CO_2 to form soluble carbonate salts. Other solvents are based on the likewise reversible reaction of alkali metal carbonates to the corresponding hydrogen carbonates ($Na_2CO_3 \rightarrow NaHCO_3$). Advantages of these technologies are, for example, the advanced stage of development and the ability to be used even at low concentrations. Disadvantages include high energy costs for regeneration, the possible degradation of the solvents over longer cycle times and the corrosive effect on equipment.[9]

Adsorption with solid adsorbents: Solid sorbents can be divided into physical or chemical adsorbents according to their functionality. The main advantage of solid adsorbents is the lower energy expenditure for regeneration, which can be explained mainly by the absence of water and the tendency of the adsorbents to have a lower heat capacity. In the case of thermal regeneration, this saves a considerable part of the energy expenditure that is not directly put into the desorption of CO_2 in the case of liquid solvents.[3]

Membranes: Separation is achieved by means of selective membranes which are, for example, made of polyvinyl amine with a large surface area. On one side of the membrane the compressed flue gas (feed) flows and on the other side a partial pressure difference is built up by vacuum pumps, which should lead to sufficient passage and enrichment of the CO_2 on the permeate side. Thus, in addition to investment costs, the costs of this technology lie primarily in the mechanical work required to achieve the necessary pressure differentials. An advantage of this technology is the elimination of energy-intensive regeneration cycles and the adsorbent as such. Disadvantages are the high investment costs and the significantly increased effort to separate high purity CO_2.[10], [11]

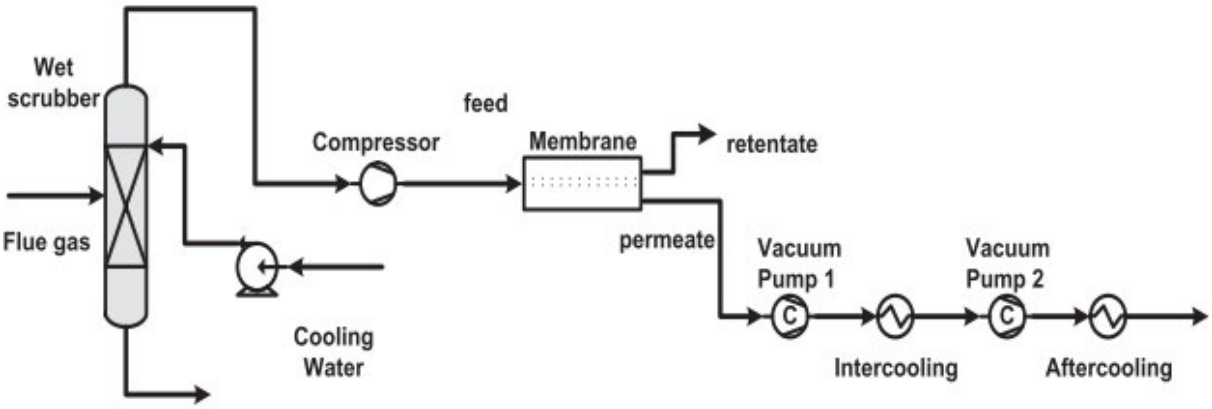

Figure 3: Schematic of a membrane separation process[10]

2.1.2 History of capturing CO_2 from air

Ever since the concept of direct air capture came up, there has been a heated discussion over the advantages and disadvantages. The concept of capturing CO_2 from air for climate change mitigation was first proposed by Lackner in 1999[12]. After the introduction of DAC, the subsequent decade produced several papers and analysis in an effort to present the topic to a broader community. These papers mainly discuss if DAC is a viable option for reducing greenhouse gas levels. [12]–[17]

Now, in the second decade of research on DAC, we can see a clear shift to more experimental work. Also the number of publications has risen from roughly 25 in the first decade, to >100 in the subsequent decade.[18] There is no denying, that DAC is a rapidly growing technology in the environmental sector. The number of academics turning their attention to developing new sorbent materials and processes for this technology is increasing, alongside several start-up companies which are gathering millions in funding to push their prototype plants from lab scale to demonstration scale.

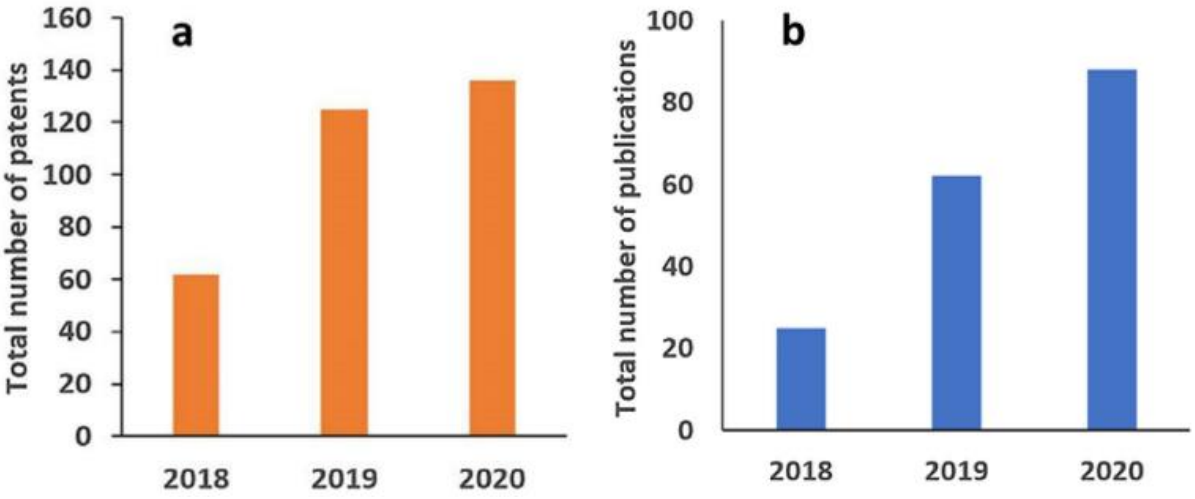

Figure 4: (a) Cumulative number of patents and patent applications and (b) Total number of publications on Direct Air Capture since 2018[19]

2.1.3 Why capture carbon from the air?

The AR6 report from the IPCC reaffirms that there is a near-linear relationship between cumulative anthropogenic CO_2 emissions and the global warming they cause. Every 1000 Gt of CO_2 emissions is assessed to likely cause a 0.27°C to 0.63°C increase in global surface temperature with a best estimate of 0.45°C. Every year humanity is adding an additional 40+Gt of CO_2 to the atmosphere with a rising tendency. The amount of anthropogenic CO_2 emissions can be divided into two main sources roughly the same size: One is the result of large industrial sources such as power plants, steel and cement factories, the other half originate from small, distributed sources such as private homes, office heating/cooling and the transportation sector. Collecting CO_2 from millions even billions of small fossil fuel- burning sources would be a very difficult task, if possible, and is therefore considered not economically feasible. [20]

For example, Capturing CO_2 onboard cars or airplanes would not be feasible because of the added weight and thus the increased amount of fuel required to operate. Not only that, but once the CO_2 is captured, there would be a massive infrastructure network required to transport the CO_2 to a sequestration site. Therefore, a solution is needed in which the captured CO_2 does not have to be transported for further processing, but in which the CO_2 is extracted directly where it is needed. Capturing CO_2 from the atmosphere would overcome this obstacle, because the atmosphere has roughly the same CO_2 levels everywhere. Furthermore, extracting CO_2 from the atmosphere enables disposal sites which would normally not be of any practical interest.

2.2 DAC Technology

There are a variety of technologies to capture CO_2 from a concentrated sources as mentioned in chapter 2.1. To capture CO_2 from ambient air however, more technologically sophisticated methods are required. Due to the fact that CO_2 is present in the air at a very low concentration of ~400ppm only, the presence of water and the fact that it has to operate near room temperature and ambient pressure, most methods for capturing CO_2 from concentrated sources can be ruled out.

Most direct air capture technologies proposed in the last few years suggest the use of sorbent materials. Since CO_2 is very dilute in the air, any CO_2 capture process must be designed to use little to no energy to pre-treat air for the capturing process. Sorbents have the advantage that the air drawn in does not need to be heated, cooled, or compressed. The required energy is shifted to a more favourable process phase where higher CO_2 concentrations are present.[21]

Physical adsorbents such as zeolites, activated carbon and alumina cannot be used at atmospheric pressure, because of their low selectivity for CO_2. Also, the presence of moisture and very low heat of adsorption, would lead to very low adsorption capacities. While sorbents investigated for CO_2 capture from concentrated sources are both physisorbent and chemisorbent materials, chemisorbent materials are proven to be much more effective for DAC processes.[18][20]

2.2.1 Aqueous hydroxide sorbents

Since CO_2 is ultra-dilute in our atmosphere, chemisorbents with very high CO_2 binding affinity are used for the DAC process. One example proposed by Lackner in 1999, who is considered the initiator of today's DAC research, is the use of a calcium hydroxide solution[12]. This solution is known to have a very high binding energy with carbon dioxide and therefore forms calcium carbonate (1).

The calcium carbonate must then be separated and dried. This is followed by a process step also known as calcination. At temperatures above 700°C, calcium oxide is formed, and a concentrated stream of carbon dioxide is released (2). Finally, to close the cycle, Calcium hydroxide is regenerated in a slaking process via hydration of calcium oxide (3).

$$Ca(OH)_2 + CO_2 \rightarrow CaCO_3 + H_2O \qquad \Delta H = -109\ kj\ mol^{-1} \qquad (1)$$

$$CaCO_3 \rightarrow CaO + CO_2 \qquad \Delta H = +179.2\ kj\ mol^{-1} \qquad (2)$$

$$CaO + H_2O \rightarrow Ca(OH)_2 \qquad \Delta H = -64.5\ kj\ mol^{-1} \qquad (3)$$

Most of the energy required in this process, is used to regenerate the sorbent. This is a trade-off that must be made, because of the considerable binding energy from CO_2 to calcium hydroxide. As can be seen in equation 2, the drying and calcining of calcium carbonate requires the most energy in calcium hydroxide systems.

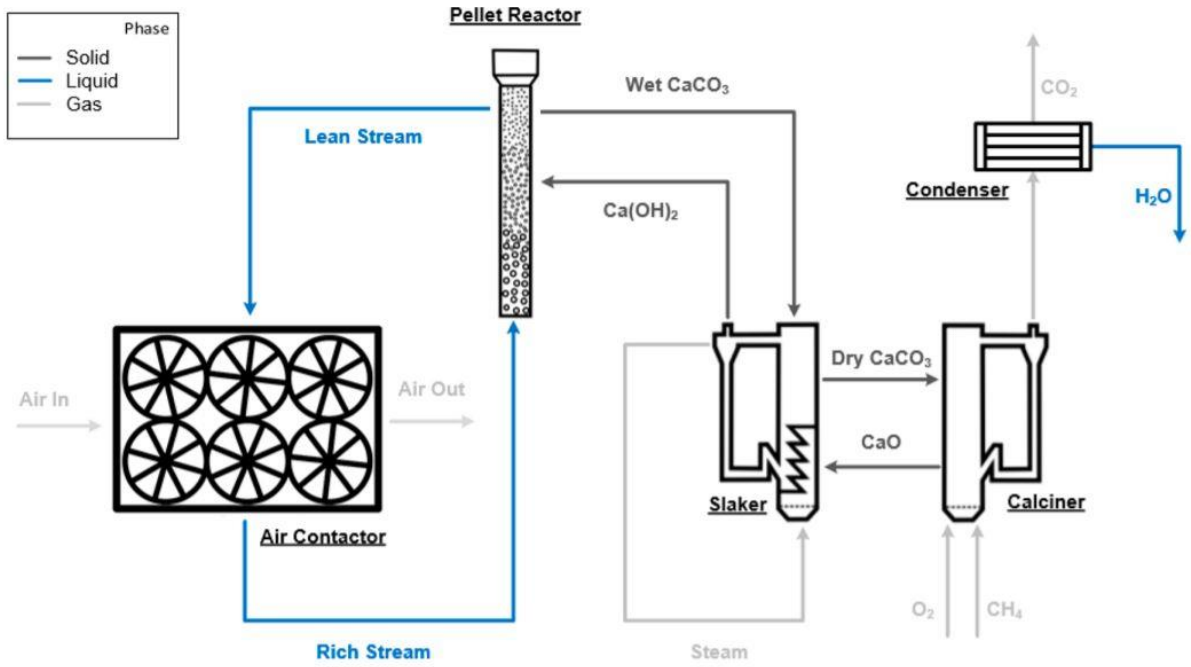

Figure 5:Simplified flowsheet of a DAC process with a liquid solvent [22][23]

2.2.2 Solid sorbent alkali carbonates

Using solid inorganic bases instead of solutions for atmospheric Carbon dioxide removal has mainly been studied and proposed by Steinfeld and co-workers.[21]

Using thermodynamic and thermogravimetric analysis, the team compared three different Na-based sorbents. Using air containing 500ppm of CO_2 the carbonation of solid NaOH at 25°C was very slow and only reached a conversion of 9% after a 4h reaction. The carbonation of $NaHCO_3$ performed even worse with a conversion of 3.4% in a flow of water saturated air. The desorption process of $NaHCO_3$ and Na_2CO_3 was performed at 90–200°C and 1000–1400°C, respectively. Consequently, the process was rendered technically and economically unfeasible because of the low carbonation rate as well as the large mass flow required.

However, results obtained with Ca-based adsorbents carried out by the same team were found to have more promising kinetics. The carbonation of $Ca(OH)_2$ and CaO in presence of water in the air stream

was much faster. The conversion of CaO to $CaCO_3$ eq. (4) reached levels of up to 80%. A big drawback was the substantially higher reaction temperature needed for the carbonation. 300–450°C and 200–425°C for CaO and $Ca(OH)_2$, respectively. The need to heat a large volume of air to aforementioned temperatures for the carbonation step makes this approach impractical as well.[24]

$$CaO(s) + CO_2(g) \leftrightarrow CaCO_3 \quad (4)$$

$$Ca(OH)_2(s) + CO_2(g) \leftrightarrow CaCO_3 \quad (5)$$

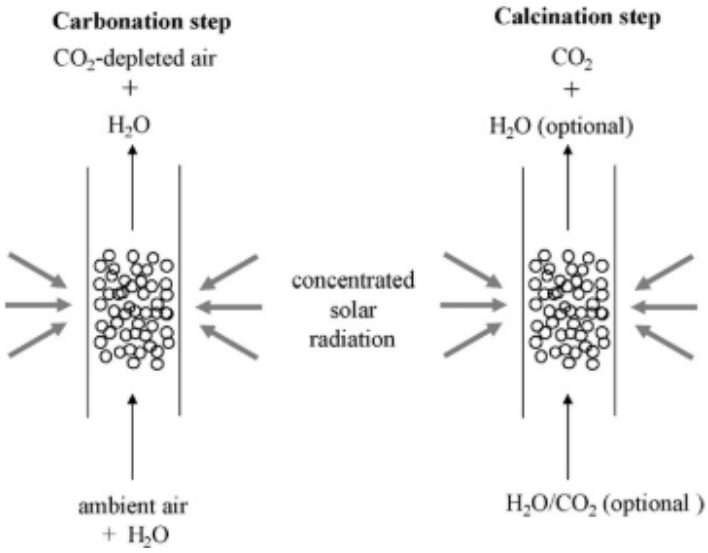

Figure 6:Schematic of a solar fluidized-bed reactor for the consecutive conduction of the carbonation and calcination steps using solar energy (ETH Zurich)[21]

2.2.3 Solid sorbent amines

By far the highest quantity of reports investigating sorbents for DAC have focused on the use of solid-sorbent amine materials. In those supported amine materials, a chemical reaction takes place between the amines and CO_2, thus creating strong bonds and allowing for significant carbon dioxide uptakes even at low CO_2 partial pressures. Accordingly, the selectivity toward CO_2 and the heat of sorption are higher than for physical sorbents. These characteristics makes the use of organic–inorganic hybrid materials for direct air capture highly suitable.[18]

In general, amine containing sorbents can be divided into three classes:

- Class 1 sorbents: prepared by impregnating amines into the pores of a support structure
- Class 2 sorbents: consisting of amines covalently bonded to the walls of porous materials
- Class 3 sorbents: amine monomers are polymerized in situ, resulting in polyamine structures tethered to the walls[20][25]

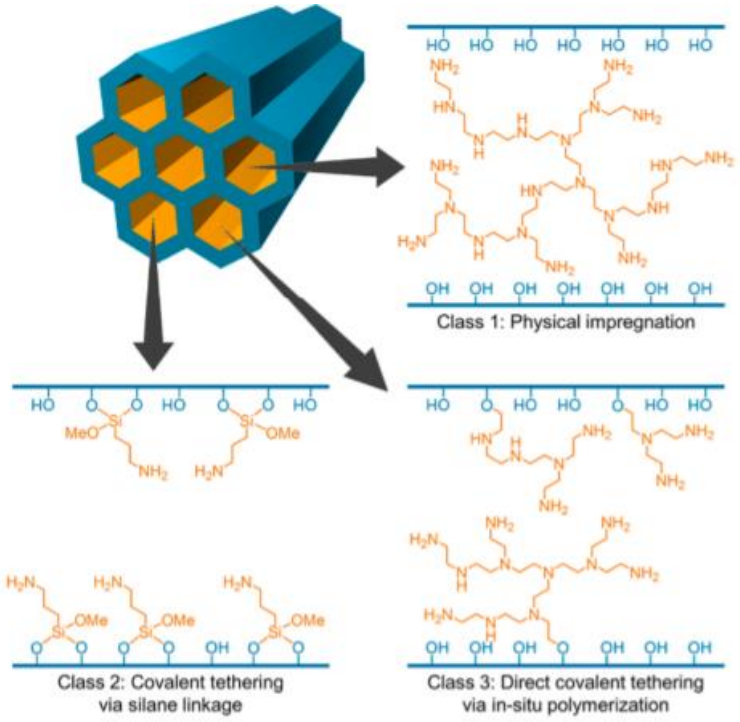

Figure 7: Display of the three classes of amine adsorbent materials[25]

Class 1 sorbents:

Due to their simple preparation procedure, Class 1 adsorbent materials have been studied in detail for CO_2 adsorption. In general, they consist of a solid support structure such as polymers, silica, mesoporous mate- rials, carbon fibres and physically loaded monomeric or polymeric amines.

Amines such as pentaethylenehexamine (PEH), tetraethylenepentamine (TEP), monoethanolamine (MEA) and diethanolamine (DEA) have low molecular weights and low boiling points. However, they showed leaching from the solid absorbents. In contrast, silica supported polyethylenimines (PEIs), especially branched low-molecular-weight and high molecular weight PEIs were found especially suitable for CO_2 adsorption in terms of CO_2 uptake and stability. [20]

Olah et al.[26] found that branched PEI is outperformed by linear PEIs which shows an adsorption capacity of 173 mg CO2 per g, however a higher degree of sorbent leaching was also observed. A linear and a branched PEI structure can be seen in Figure 8. It was considered that the readily accessible amino groups at each chain end led to the high sorption capacities of class 1 adsorbents containing PEI.

In summary, PEIs are easy-to-produce, low-cost hybrid adsorbents that exhibit remarkable CO_2 adsorption capacities, improved kinetics under both dry and wet conditions, and good regenerability.

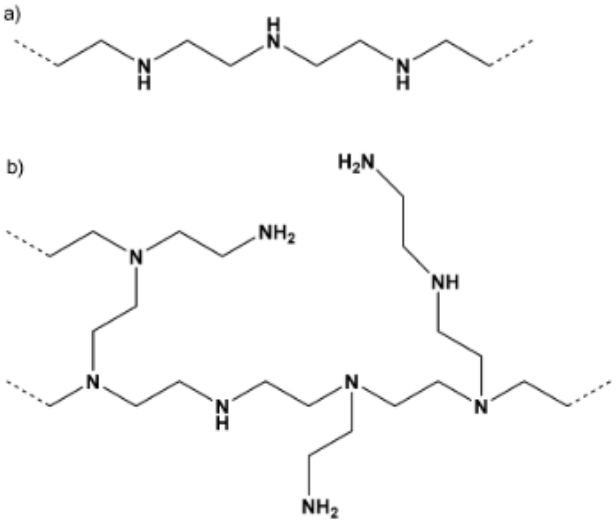

Figure 8: a) Linear PEI structure and b) branched PEI structure[21]

Class 2 sorbents:

Class 2 sorbents are more stable during regeneration than Class 1 sorbents because of amine functional groups which are chemically grafted onto the support surface. There are various methods Class 2 sorbents can be prepared, involving the attachment of amines to material surfaces:

- Silane chemical reactions: siloxane groups of amine-containing silanes are first hydrolysed (or alcoholated). They then bind to active hydroxy groups as they condense on the surfaces of the porous material. This creates a single layer of amine groups.
- Binding to coupling agents: coupling agents are chemicals able to bind themselves to a porous material on one side and to an amine-bearing compound on the opposite side.

The most commonly used method to prepare amine-grafted sorbents for CO_2 capture from air is through silane chemical reactions. With this method sorbents can be prepared by reacting an aminosilane with a premade supporting porous material.[27] There are three silanes which are most commonly used for this purpose:

- 3-aminopropyltrimethoxysilane-(AP)
- 3-(2-aminoethyl) aminopropyltrimethoxysilane (DAP)
- 3-[2-(2-aminoethyl)aminoethyl]aminopropyltrimethoxy-silane (TAP)[21]

Wurzbacher et al.[28] were the first to demonstrate a cyclic temperature-vacuum swing (TVS) process to separate CO_2 from atmospheric air using a class 2 sorbent. The proposed cycle can operate in dry and humid air. Using a solvent free procedure, the sorbent, [N-(2-aminoethyl)-3-aminopropyl] trimethoxysilane (AEAPTMS), was grafted onto silica gel beads with a diameter ranging from 2–5 mm. To recover the CO_2 captured from an air flow with 40% relative humidity, the sorbent material was heated to temperatures ranging from 74 to 90°C at 150 mbar pressure. Even after 40 consecutive sorption/desorption cycles the sorbent demonstrated remarkable stability (Figure 9).

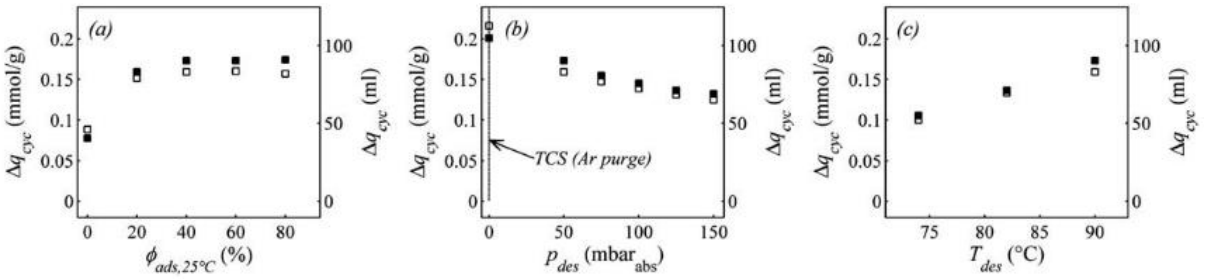

Figure 9: Variation of cyclic CO_2 adsorption (open symbols) and desorption (closed symbols) capacity of SI-AEATPMS as a function of: (a) adsorption humidity, (b) desorption pressure and (c) desorption temperature [28]

Class 3 sorbents:

Class 3 sorbents were first reported by Choi et al. [29] as a new class of amine-based solid sorbents. They described them as hyperbranched aminosilica (HAS) materials. These sorbents work based on the integration of covalently bound polymeric amines into porous substrates. HAS sorbents are also known as class 3 supported amine sorbents. Because of the larger number of amines in the HAS materials the working capacity of these sorbents is higher than Class 2 amine-based sorbents. Because of the covalent tethering of the amines onto the sorbents, they exhibit an excellent regeneration ability in successive operations.

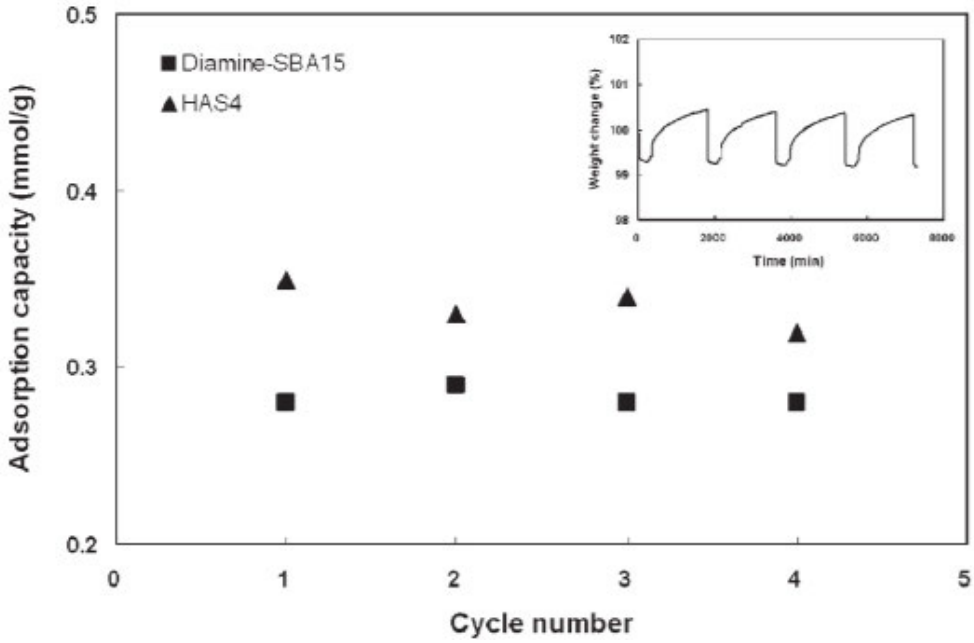

Figure 10: Cyclic regenerability of the HAS4 adsorbent compared to a representative class 2 adsorbent[29]

Using humid gas mixtures, the CO_2 adsorption capacity of the obtained hyperbranched aminosilica (HAS) adsorbents were measured. With a CO_2 content of 10% and 400 ppm in Ar simulating flue gas and ambient air, it was found that the CO_2 uptake increased from 0.16 mmol/g to 1.72 mmol/g as the amine loading increased from 2.3 mmol/g (HAS1) to 9.9 mmol/g (HAS6). This demonstrates the tunability of air capture capacities of HAS, by controlling the organic content.

However, it should be mentioned that because of the more pronounced pore blocking and mass transfer limitations, adsorption kinetics became slower with higher organic content. This was reflected by increased adsorption half times. More importantly, the drop of the inlet CO_2 concentration from 10% to 400 ppm was less affecting the air capture capacities of HAS adsorbents with higher amine loadings. Furthermore, even after four adsorption (25 °C)/ desorption (110 °C) cycles, the tested novel hybrid materials showed almost no changes in air capture capacity (Figure 10).

2.2.4 Electrochemical carbon dioxide capture

Capturing CO_2 directly from the atmosphere electrochemically is another interesting approach which is getting more and more attention of researchers due to its flexibility, ability to address decentralized emissions (e.g., ocean and atmosphere) and its fit in an electrified industry. Most of these methods build upon the concept of ‘‘pH-swing’’ and its effect on the CO_2 hydration/ dehydration equilibrium. By shifting the pH of a working fluid between basic and acidic pH, CO_2 can be captured and recovered. A ‘‘pH-swing’’ can be applied electrochemically through bipolar membrane electrodialysis, capacitive deionization, electrolysis, and reversible redox reactions.[30]

Electrolysis:

Electrolysis causes the pH-swing at the two electrodes, as shown in Figure 11. Membrane electrolysis for CO_2 capture is used for the regeneration of alkali absorbers with possible simultaneous H_2 production. The cost of CO_2 capture can partially be offset by H_2 production through water electrolysis. Stucki et al. [31] first proposed the adsorption of CO_2 from a flue gas in a KOH absorbent via electrolysis. The resulting bicarbonate solution is fed into the electrolyser (for alkaline regeneration). The CO_2 is recovered and H_2 is produced following equation (6):

$$2H_2O + K_2CO_3(aq) \rightarrow 2KOH(aq) + CO_2(g) + H_2(g) + 0{,}5O_2(g) \qquad (6)$$

When KOH is used as an absorbent for capturing CO_2, it turns into K_2CO_3(aq), which can be fed again to the electrolysis system, thus completing the cycle.

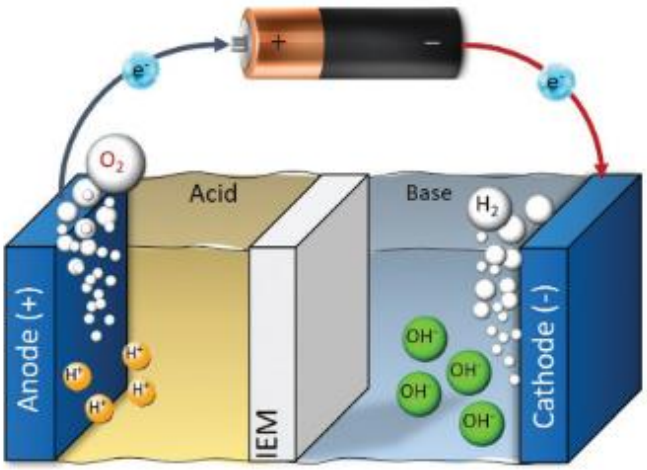

Figure 11: Schematic of water electrolysis. [30]

Bipolar membrane electrodialysis (BPMED):

A bipolar membrane (BPM) consists of two exchange layers which are laminated together. An anion (AEL) and a cation (CEL) layer. The BPM dissociates water into OH^- and H^+ when a sufficient electric field is applied. This produces a controllable ΔpH over the membrane as shown in Figure 12.

When using a bipolar membrane, the thermodynamic minimum voltage required is 0.829 volts for this water dissociation to produce ΔpH = 14. This means a 2.5 times lower voltage required than that of water electrolysis for the same ΔpH = 14 (1.23 + 0.829 at minimum). The reason for this is that no gas evolution takes place using a bipolar membrane. For smaller ΔpH over the membrane the thermodynamic voltages over the BPM are even lower. In 1995 Bandi et al. [30] showed the feasibility of pH-swing based CO_2 capture using bipolar membrane electrodialysis. They used a two compartment BPMED cell, containing a BPM and a cation exchange membrane to regenerate alkaline KOH and acidic H_2SO_4.

After CO_2 is captured from air in a KOH absorbent, it can be recovered through acidification and regenerated in the BPMED cell to get the desired acid and base.

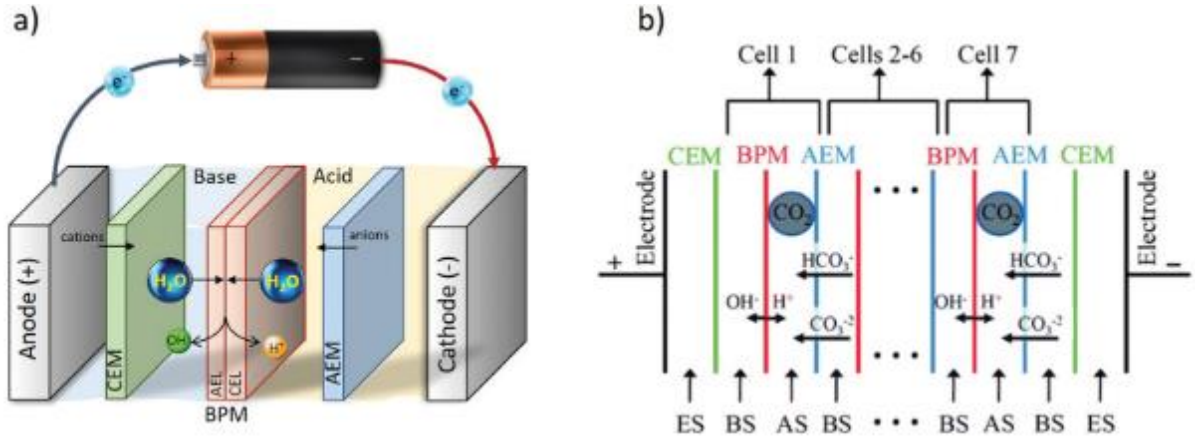

Figure 12: (a) BPMED schematic. (b) BPMED for CO_2 recovery; (ES) electrode solution = KOH; (AS) acid solution of KH_2PO_4 +H_3PO_4; (BS) base solution of six different mixtures of $KHCO_3$,K_2CO_3 and KOH.[30]

Redox-active carriers and electrode reactions:

Electrochemically mediated separation strategies using specific redox-active sorbent carriers are an alternative to BPMED and electrolysis for CO_2 capture. These redox-active carriers can be used to separate CO_2(g) from a gas mixture by chemical bonding Fig. 13a or through the pH-swing route Fig. 13b. Both variants have been demonstrated feasible, yet only on a laboratory scale.

Chemical bonding:

In this variant, the suitable carrier is activated at the cathode and bonds with the target species in its reduced state. In this case the target species is the CO_2 molecule. Subsequently, while the carrier is regenerated, the captured CO_2 can be released at the anode by oxidation of the carrier. Also referred to as ‘‘electrochemical CO_2 pumping’’, this process is can be broken down into four steps: [32]

- Sorbent activation through oxidation or reduction.
- CO_2(g) capture on the activated sorbent.
- Sorbent deactivation through the reverse electrochemical process.
- CO_2(g) release.

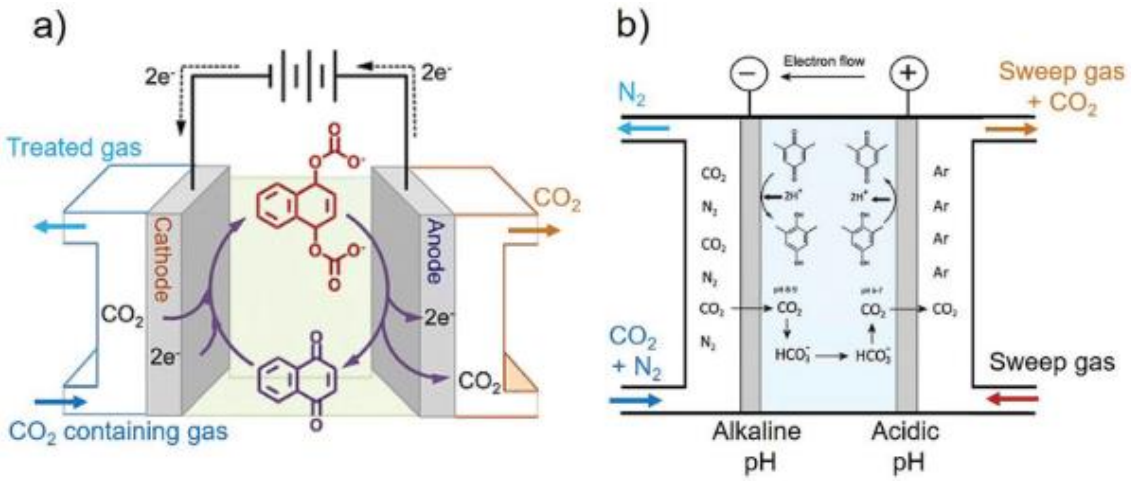

Figure 13: (a) Electrochemical CO_2 separation using gas diffusion electrodes (GDE) through binding with quinone redox-active carrier (i.e., no pH-swing is created). (b) Combination of pH-swing with the chemistry of redox active carriers through (PCET) reaction using mixture of hydroquinone, quinone, and sodium bicarbonate [30]

2.3 Adsorption

Hereinafter, a brief introduction is given to the most important theoretical principles of adsorption. The different binding forces between physical and chemical bonding are described. Furthermore, the most important adsorption models and evaluation methods are considered in more detail regarding the adsorption isotherm.

2.3.1 Fundamentals of adsorption

Adsorption refers to the binding of selected components from a fluid, gaseous or liquid phase to a solid surface. The inverse process, the removal of the previously adsorbed molecules on a solid surface, is called desorption. The driving force for selective separation in a technical process is always an imbalance caused by external forces. These external forces can be triggered either by changes in temperature, pressure, or concentration. The behaviour and the change of the equilibrium are usually described thermodynamically. In technical processes mainly porous solids are used. Due to their large inner surface area, they create ideal conditions for various adsorption processes. The porous solid that binds the adsorbing molecules to itself is generally referred to as the adsorbent. The molecule to be adsorbed, which is in the fluid phase, is called adsorptive and the molecule already bound to the adsorbent is called adsorpt. The entire interface, consisting of adsorbent and adsorptive, is summarized under the term adsorbate.[33]

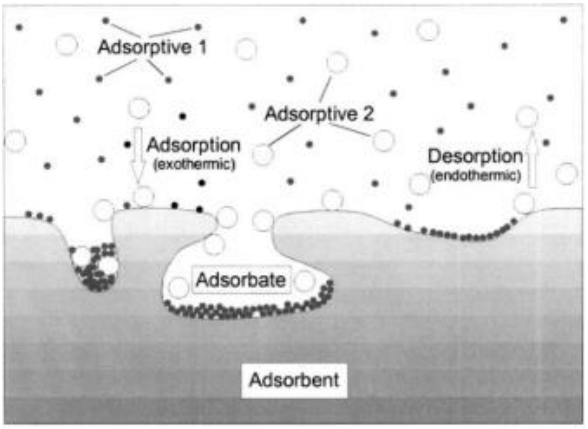

Figure 14: Adsorption and Desorption system of a two-component gas phase on a solid sorbent material. Extracted from Keller and Staudt [34]

Adsorption is an essential basic operation in thermal process engineering and is therefore used in many technical processes. In addition to the chemical and similar branches of industry, its use is becoming increasingly important, especially in environmental technology. In environmental engineering, adsorption can be used for waste and drinking water treatment, but it is especially interesting in the field of exhaust gas purification. Basically, adsorption is always an exothermic process in which the adsorption enthalpy is released. Depending on the type and strength of the bond between the adsorbent and adsorbate, a distinction is made between physisorption (physical adsorption) and chemisorption (chemical adsorption). [34]

2.3.2 Physisorption and chemisorption

In general, the loading depends on the partial pressure of the adsorbed substance in the gas phase and on the temperature. Adsorption is always exothermic, desorption endothermic. In physisorption, the strength of the bond between adsorbent and adsorbate is based on relatively weak physical forces. The physical forces include, in addition to van der Waal's dipole forces, dispersion and induction forces. Due to the weak bond between adsorbent and adsorbate, the binding energy only corresponds to less than <50 kJ/mol. Physisorption is a reversible process since no chemical change, of the adsorbent or the adsorptive takes place and the adsorption process is relatively fast. In physisorption, the loading of the adsorbent occurs either monocularly or multi-layered. Physisorption is mainly favoured by low temperatures. [35]

In contrast to physisorption, a real electron transfer takes place in chemisorption. In this process, a chemical bond occurs between adsorbent and adsorbate and significantly more adsorption enthalpy is released, since the binding forces are significantly stronger. For example, chemisorbents typically have adsorption enthalpies in the range of -60 to -100 kJ/mol. The loading of the adsorbent is purely monomolecular compared to physisorption. An important distinguishing feature in chemisorption is the chemical change in the surface of the adsorbent, which is why the process is sometimes irreversible. Physisorption and chemisorption can only be reversed by the application of heat and/or vacuum. [36]

Though the higher adsorption enthalpy of chemisorption also results in an increased energy demand for desorption compared to physisorbents, the stronger bonds also enable typically higher adsorption capacities at lower partial pressures. In addition, adsorbents with a low adsorption enthalpy, such as physisorbents, require a higher temperature increase for desorption. In the case of adsorption, a precise separation between physisorption and chemisorption is difficult in practice, since the transition often occurs smoothly.[37]

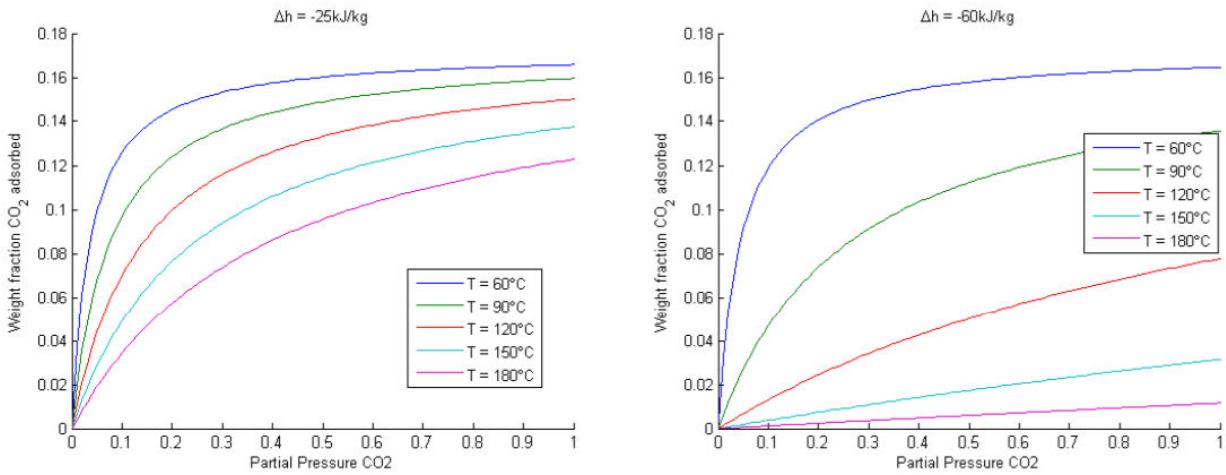

Figure 15: Adsorption isotherms of a physisorbent (left, active char) and a chemisorbent (right, amine functionalized sorbent)[36]

2.3.3 Desorption methods

As already mentioned in the previous chapter, the reverse process of adsorption i.e., the removal of the previously adsorbed molecules, is called desorption and it is based on the principle of Le Chatelier. To regenerate a loaded adsorbent, it is important to shift the previously established thermodynamic equilibrium between adsorption and desorption into a desorption favouring direction. Taking into account that adsorption proceeds preferentially at low temperatures, high pressures and a high concentration of the adsorptive, the following processes can be used.[33]

PSA - Pressure Swing Adsorption:

The loading of the adsorbent increases with increasing pressure. Therefore, if there is a pressure reduction in the adsorber, the previously adsorbed molecules are removed again. If the set pressure is below atmospheric pressure, the process is also called vacuum swing adsorption (VSA). Pressure swing adsorption is based on four process steps: 1.) Adsorption with pressure build-up, 2.) Depressurization of the gas, 3.) Desorption by purge gas flow, 4.) repeated pressure build-up. These four process steps result in one cycle. The duration of a typical cycle ranges from 30 seconds to only a few minutes and is much faster compared to TSA (temperature swing adsorption). Pressure swing adsorption is not only used for capturing carbon dioxide but in various other applications, including the recovery of oxygen or nitrogen from air.

TSA - Temperature Swing Adsorption:

When using the temperature swing adsorption, the regeneration of the adsorbent bed takes place by increasing the temperature. This shifts the loading equilibrium to lower values and the attached molecules desorb. The temperature increase causes a jump to another isotherm, which has a higher temperature and a lower loading capacity. To heat the adsorbent and overcome binding forces, energy input in the form of thermal energy is required. The thermal energy can be supplied in different ways. Hot flushing media such as steam, air or even nitrogen are predominantly used. Depending on the process, the temperatures at which the purge gases are introduced into the adsorber vary. Due to the low specific heat capacity of the purge gas, higher temperatures are preferred. In addition to heating the adsorber by introducing purge gas, heat exchangers can also be used. The heating elements can be placed either externally around the adsorbent bed or directly inside the adsorbent bed. Furthermore, thermal management plays a crucial role in the TSA process. Since adsorption is an exothermic process, the process of adsorption requires active cooling of the adsorbent material to maintain the desired temperature. In turn, the same amount of energy must be supplied to the endothermic desorption to maintain the level.[38]

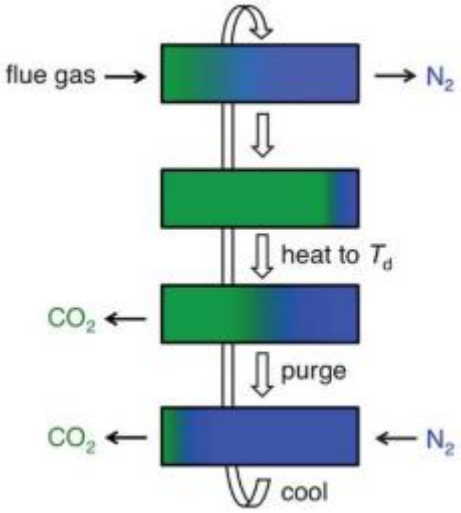

Figure 16: Schematic diagram of an idealized temperature swing adsorption (TSA) process[39]

CSA - Composition Swing Adsorption:

Composition swing adsorption is essentially based on the change of composition in the fluid phase. Regeneration can be achieved by flushing with an adsorptive-free gas. In this case, the loaded fixed bed is flushed with an adsorptive-free gas, which causes the temperature in the adsorber to drop and a new equilibrium to be established. On the other hand, regeneration by displacement is another possibility. The component which was previously adsorbed is displaced by an additional component and takes its place in the adsorbent.[38]

2.4 Pure component adsorption

2.4.1 CO_2 isotherms

Isotherm models typically describe adsorption equilibrium of species onto a solid surface. CO_2 adsorption on amine-functionalised adsorbents has previously been described by the temperature-dependent Toth isotherm, a standard isotherm model used for amine functionalised silica, cellulose, and the product Lewatit VP OC 1065.[40][41]

The Toth isotherm is based on the Langmuir isotherm with an empirical extension added, to improve the fit at the highest and lowest-pressure ranges. This is especially relevant for amine functionalised sorbents due to their high affinity for CO_2 at low partial pressure. The following equations describe the temperature dependent form of the Toth isotherm.

$$q_{CO_2}(T, p_{CO2}) = \frac{q_\infty(T) * b(T) * p_{CO2}}{[1+(b(T)*p_{CO2})^{\tau(T)}]^{\frac{1}{\tau(T)}}} \quad (7)$$

$$q_\infty(T) = q_{\infty,0} * \exp\left(X * \left(1 - \frac{T}{T_0}\right)\right) \quad (8)$$

$$b(T) = b_0 * \exp\left(\frac{-\Delta H_0}{RT}\right) \quad (9)$$

$$\tau(T) = \tau_0 + \alpha(1 - \frac{T_0}{T}) \quad (10)$$

Table 1: Description of parameters for adsorption Isotherms

Variable	Description	Unit
T/T_0	Temperature/Temperature at t=0	K
R	Gas konstant	J/molK
q_{co2}	loading of CO_2 on the adsorbent	mol/kg
q_∞	maximum CO_2 capacity	mol/kg
b	affinity of CO_2 on the adsorbent	Pa^{-1}
p_{co2}	partial pressure of CO_2	Pa
τ	exponential factor describing the heterogeneity of the adsorbents	-
X	temperature dependency	-
ΔH_0	the isosteric heat of adsorption	J/mol
α	factor which describes the temperature dependency	-

2.4.2 H_2O isotherms

For CO_2 capture applications, adsorption of water onto solid species is an essential field of study. The work of Hefti et al.[42] shows that water adsorption on Lewatit VP OC 1065 follows a Type 3 isotherm according to the IUPAC classification[43]. This also fits the behaviour described for monolayer-multilayer adsorption of water onto favourable sites of a macroporous adsorbents.

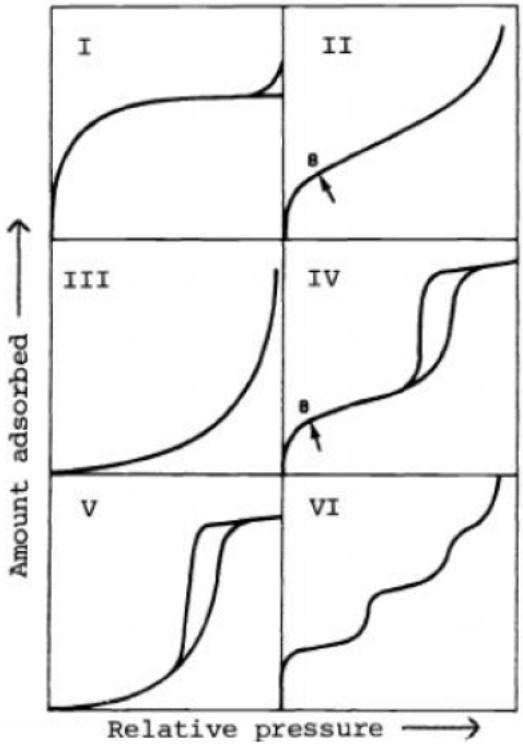

Figure 17:IUPAC classification of physisorption isotherms. Extracted from Sing et al. [43]

An isotherm model that fits this behaviour is the Guggenheim-Anderson-de Boer (GAB) model which is an extension to the more commonly utilised Brunauer–Emmett–Teller (BET) equation[44]. The GAB isotherm model is presented in Equation (11):

$$q_{H_2O}(x) = \frac{q_m K_{ads} c_G x}{(1-K_{ads}x)(1+(c_G-1)K_{ads}x)} \quad (11)$$

Table 2: Description of parameters for H_2O isotherms

Variable	Description	Unit
q_{H2O}	loading of water	mol/kg
q_m	loading corresponding to a monolayer	mol/kg
x	Relative humidity	-
K_{ads}	affinity parameter	-
C_G	affinity parameter	-

2.4.3 Water-CO_2 co-adsorption models

It has been shown that on amine-functionalised adsorbents, CO_2 has little to no impact on H_2O equilibrium adsorption up to a relative humidity of < 60%. On the other hand, previous studies have shown that H_2O improves CO_2 adsorption significantly.[40]

To explain the co-adsorption of CO_2 and H_2O on amine-functionalised sorbents mathematically, the underlying chemical mechanism needs to be understood in detail. Only one attempt has been made so far, to develop an empirical mathematical description by Stampi-Bombelli et al.[44].

Wurzbacher et al. used an empirical approach to describe the co-adsorption of CO_2 in humid conditions via introducing an enhancement factor [45]. While the results can be used for certain data points, it does not correctly represent to all of them. Therefore Stampi-Bombelli et al. suggest a new isotherm model which accounts the dependency of the water loading to describe CO_2 uptake in binary conditions. The isotherm model shown in the following equation, uses the Toth isotherm as a basis. It accounts for the water adsorption dependency in the maximum uptake term, n_s, and in the affinity coefficient, b:

$$q_{CO_2}(T, p_{CO2}, q_{H_2O}) = q_\infty(T, q_{H_2O}) \frac{b(T,q_{H_2O})p_{CO2}}{(1+(b(T,q_{H_2O})p_{CO2})^{\tau(T)})^{\frac{1}{\tau(T)}}} \quad (12)$$

$$q_\infty(T, q_{H_2O}) = q_\infty(T) \left[\frac{1}{1-\gamma q_{H_2O}}\right] \quad \gamma > 0 \quad (13)$$

$$b(T, q_{H_2O}) = b(T)\left(1 + \beta_{q_{H_2O}}\right) \quad \beta > 0 \quad (14)$$

γ [—] and β [—] are parameters that describe co-adsorption, therefore do not have specific physical meaning. The authors suggest fitting them to wet parameters and to be greater than 0. However, if you consider that the overall CO_2 capacity can decrease due to site blockage, γ could have a negative value.

[46][44]

As there may be multiple mechanisms in play on one adsorbent, there is no one adsorption mechanism valid for different amine-functionalised sorbents.

There are three main effects which should be considered for water-CO_2 co-adsorption:

- At high water loadings, hydrogen-bonded water structures blocking CO_2 access to amine sites may be limiting amine efficiency
- Ammonium bicarbonate forming rather than ammonium carbamate due to the presence of water and thus increasing the stoichiometric ratio
- The presence of water changes the heat of adsorption of the adsorbed CO_2 species and thus the affinity [46]

2.5 Evaluation of Competition

Direct air capture companies are demonstrating early success. The companies mentioned below are using direct air capture to remove carbon dioxide from the air today and utilizing it for commercial purposes in a rapidly expanding CO_2 market.

2.5.1 Climeworks

Climeworks was founded in 2009 by two ETH Zurich alumni in Switzerland and is now considered the leader in DAC technology. By 2013 they developed the first working prototype of their DAC technology. In 2017 Climeworks commissioned the world's first commercial scale direct air capture plant based on solid sorbent technology and opened the first service to offer carbon removal to individual customers just two years later. In September 2021 they launched the world's largest direct air capture and storage plant in Iceland, called Orca.

Climeworks has publicly set an ambitious goal of removing 225 million tons of CO_2 from the atmosphere by 2025 which corresponds to approximately 1% of total worldwide emissions. Climeworks' 2025 goal will require roughly 450 TWh of energy at an estimated energy consumption of 2000 kWh per tCO_2. The capital cost of constructing have the largest impact on the price of CO_2 capture. For Climeworks' Hinwil DAC system, which captures 900 tCO_2/yr., it was $3–4 million which amounts to a levelized capture price of $500–600 per ton of CO_2.[47]

Over the years Climeworks has managed to sign partnerships with renowned companies such as:

Table 3: List of Climeworks partners

Accenture	**The Economist**	**Shopify**
Audi	**Microsoft**	**Square Inc.**
Boston Consulting Group	**Ocado**	**Stripe**

2.5.1.1 Technology

Figure 18 shows a representative process flow diagram of the packed bed solid sorbent DAC process used by Climeworks.

This process uses fans to push air through the contactor unit where the CO_2 adsorbs onto the solid sorbent at ambient conditions. The apparatus operates in adsorption mode until the solid sorbent is saturated with CO_2 or the desired CO_2 uptake is reached. At this stage the apparatus is switched from adsorption to desorption mode and the contactor is closed off from the surrounding environment. To prevent dilution of the produced CO_2 by the remaining oxygen and nitrogen in the contactor, a vacuum pump evacuates residual air from the contactor. In addition, this is crucial to minimize amine degradation from air.

Previous literature suggests that the vacuum stage decreases the temperature requirements for

regeneration; the mentioned vacuum pressure is on the order of 30 mbar[48]. After the desired pressure is reached, the sorbent is heated to a regeneration temperature of roughly 80-120°C. The required heat can be supplied in many ways, Climeworks uses steam created through industrial waste heat or geothermal energy. During this process, CO_2 is released from the contactors and flushed out of the apparatus by the steam. Finally it is separated from water in the condenser and sent to compression for subsequent storage, transportation, or further processing.[6]

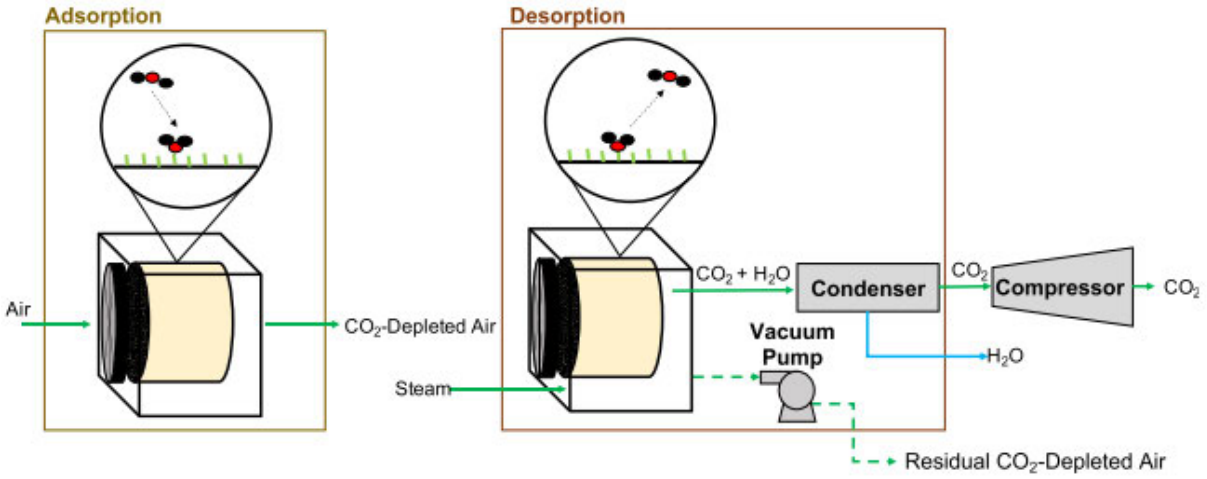

Figure 18: Representative process flow diagram for solid sorbent DAC. Green lines represent gaseous flows and blue lines liquid flows [6]

2.5.2 Carbon Engineering

Founded in 2009 by Harvard Professor David Keith, Carbon Engineering is the first commercial entity to pursue solvent DAC technology and has been removing CO_2 from the atmosphere at its pilot plant in British Columbia since 2015. The company developed a continuous carbon capturing process using a potassium hydroxide solvent coupled to a calcium caustic recovery loop.

In 2017 they took a step further incorporating fuel synthesis capability into their existing pilot plant, being among the first companies to produce carbon neutral fuels using CO_2 from the atmosphere. In 2022, Carbon Engineering aims to begin construction of a DAC plant in the Permian Basin with 1PointFive, a development company formed by Oxy Low Carbon Ventures. The projects ambitious goal is to have the capacity to capture and store up to 1 million tons of CO_2 per year. [49]

Carbon Engineering's long-term goal is to deploy DAC and carbon neutral fuel facilities in leading markets with the highest corporate and government targets, and the strongest policies that favour permanent sequestration of atmospheric CO_2 and clean fuels.

2.5.2.1 Technology

The liquid solvent DAC system used by Carbon Engineering consists of two loops: the contactor loop and the calciner loop. In the contactor loop, air is pushed horizontally through long contactor units measuring roughly 200 m by 20 m by 5–8 m. To capture around 1 $MtCO_2$/yr., ten of these units are

required. In more recent designs, a fan pulls the air horizontally through the packing material and pushes it out vertically working similar to a crossflow forced draft cooling tower. A 2 molar KOH solution flows in the contactors vertically through packing material, reacting with the CO_2 from the airstream to form potassium carbonates in solution (K_2CO_3). This solution is then pumped out of the contactor to a central regeneration facility in which, the K_2CO_3 undergoes an anionic exchange with calcium hydroxide ($Ca(OH)_2$). In the regeneration facility (pellet reactor) calcium carbonate ($CaCO_3$) is formed and the KOH solution is regenerated which can be circled back to the contactors.

The pellet reactors produce large $CaCO_3$ crystals (<0,85mm) through controlled precipitation reactions. Before the $CaCO_3$ from the pellet reactors reaches the calciner, it is fed into a steam slaking unit, where heat from the calciner products is used to dry the $CaCO_3$ pellets. Finally, the dry $CaCO_3$ is heated to 900 °C in the calciner where it undergoes a decomposition reaction to form calcium oxide (CaO) and CO_2.

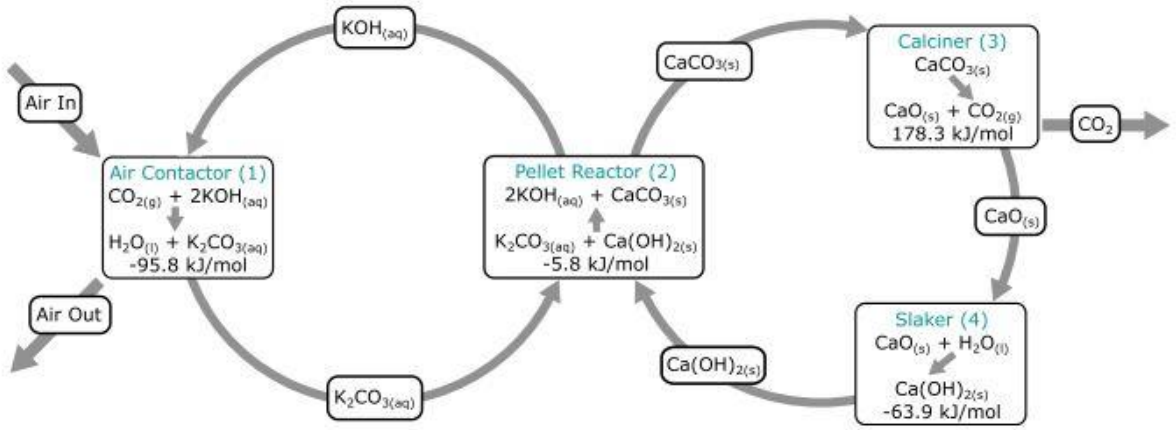

Figure 19:Process chemistry and thermodynamics of Carbon Engineering's DAC process[22]

To obtain the required temperature in the calciner, Carbon engineering currently uses natural gas and oxygen. The result is a gaseous mixture consisting primarily of CO_2 and water. The CaO formed in the calciner is then fed into the steam slaker where it is hydrated to $Ca(OH)_2$. To close the loop, the $Ca(OH)_2$ is fed back into the pellet reactors, thus being again available for the anionic exchange. The gas produced at the calciner, containing mostly CO_2 and water is sent through a condenser to remove most of the water present. The resulting high purity CO_2 is compressed and can be further processed.

When CO_2 is delivered at 15MPa, this design has an energetic requirement equivalent to either 8.81 GJ natural gas or 5.25 GJ natural gas coupled with 366 kWh of electricity per ton of CO_2 captured. Carbon Engineering estimates the cost for this process to capture a ton of CO_2 to be between $94 and $232.[22]

A representative process flow diagram of Carbon Engineering's DAC system is provided in Figure 20.

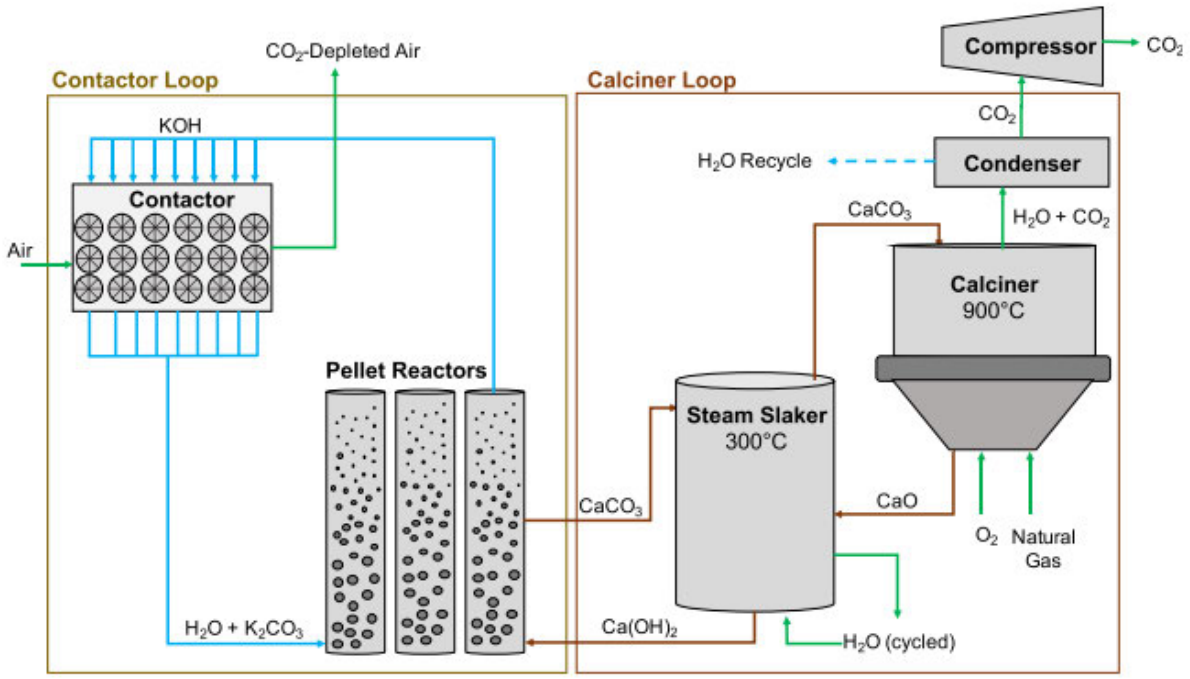

Figure 20: Representative process flow diagram for the solvent process.[6]

2.5.3 Global Thermostat

New York based Global Thermostat was founded in 2010 by Dr. Graciela Chichilnisky and Professor Peter Eisenberger. The company uses amine-based sorbents bonded to ceramic monoliths which absorb CO_2. The captured CO_2 is later released through low temperature steam near 100°C up to roughly 130°C, with the preferred range being 105–120°C[50]. Currently, Global Thermostat has two pilot DAC plants with the potential to capture 3000–4000 tonnes of CO_2/yr. The captured carbon dioxide from their pilot plant in California is sold for use in greenhouses, food and beverages, desalination, biofertilizers, and chemicals.

In 2019 Global Thermostat announced a collaboration with Exxon mobile to help them bring their commercially viable CO_2 removal technology to the scale necessary to pull one million tons of carbon out of the atmosphere per year.

2.5.4 Soletair Power

The Finnish company was founded in 2016 and is the first in the world to integrate DAC with HVAC systems in buildings. It captures CO_2 from ventilation units inside buildings to improve air quality. The companies unique selling point is, that they not only reduce carbon emissions but also can improve human's cognitive function. Their arguments are heavily based on a study from Harvard University, reporting that human cognitive function starts to decline by 20% for each 400 ppm increase of CO_2.[51]

2.5.4.1 *Technology*

Table 4: Technical specifications of Soletair's DAC unit

Rated CO_2 production	**3800 g/d**
Max. air flow	1500 m3/h
Air temp. for blowers	(−40) to 80 °C
Vacuum (desorption, min)	5 mbar
Max. water temp.	100 °C
Cartridge content	Amine-funct. polymer resin
Number of cartridge/beds	8
Mass of adsorbent/cartridge	30 kg
Temp. of operation	ambient to 90 °C
Pressure (adsorption)	1.005 bar

The operating principle of Soletair's DAC process is shown in Figure 21. There are two identical beds which are operated in parallel, therefore are subject to the same stage of operation simultaneously. To heat the bed during the desorption step, a brush type heat exchanger is immersed in the bed of adsorbent.

Soletair uses a TVSA (temperature vacuum swing adsorption) process which can be divided into four stages. The first stage of the carbon capture process is the adsorption stage that lasts for ca. 20 h (Figure 21a). To maximize mass transfer in the bed, air is led through the column via a flow distribution plate.

In the second stage (Figure 21b), the remaining air from the adsorption process containing mainly O_2 and N_2 is removed using a two-stage vacuum pump. This stage (purging) lasts for 15 min and is crucial to achieve high-purity CO_2 gas required for the synthesis.

The next stage of the process is the heating stage, and it lasts for 30 min (Figure 21c). A 3-kW boiler pumps a warm glycol-water mixture (20% ethylene glycol) to the intra-bed heat exchanger to preheat the bed. At the same time some gases already desorb in preparation for the next step, shown in Figure 21d.

Finally, after pre- heating is complete, CO_2 is sucked out of the bed through the product gas line. The hot gases from the beds are cooled in an ambient-air-heat exchanger and pass through a water trap (right water trap) before being drawn through the product vacuum pump. Then, the product gas, containing mainly CO_2 at this stage, passes through the ambient-air-cooled heat exchanger again and a second water trap (left water trap) for drying and additional cooling before being compressed.[52]

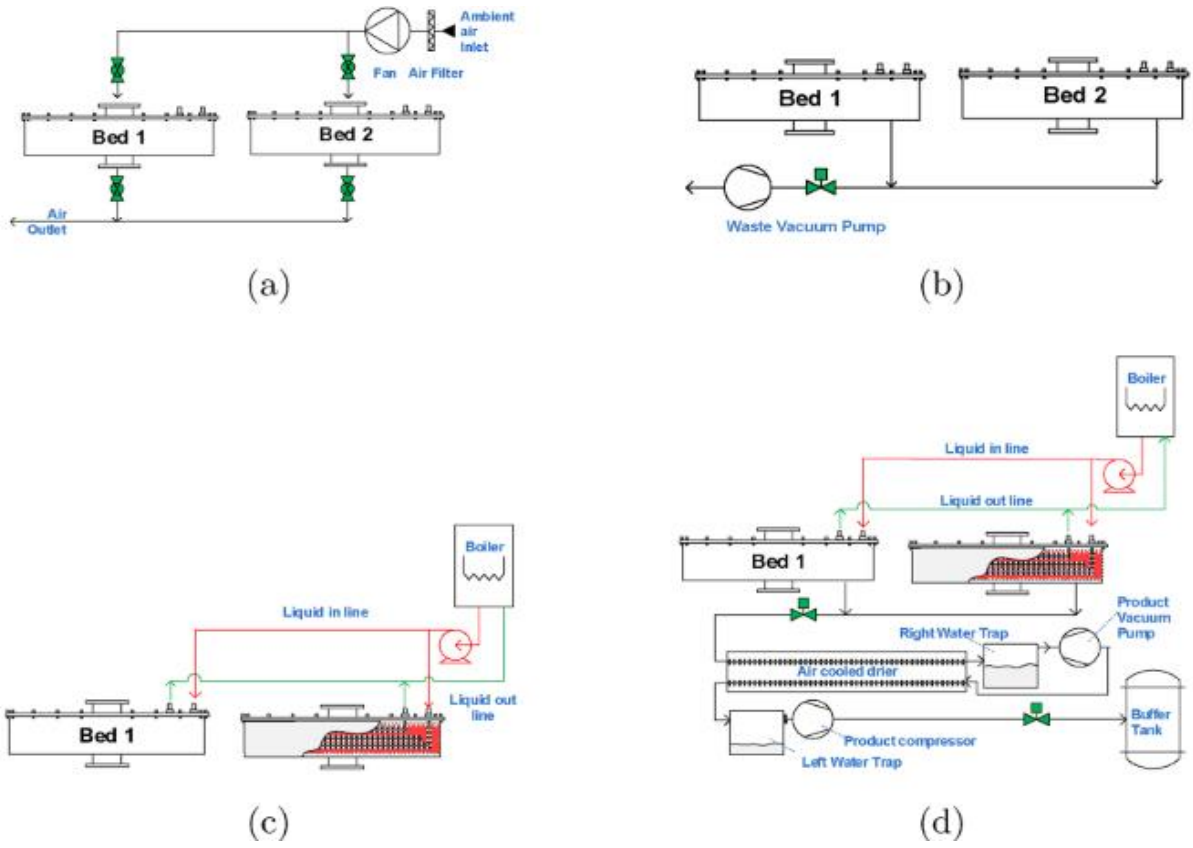

Figure 21: Stages of TVSA operation of the DAC unit. (a) Adsorption. (b) Purging. (c) Heating. (d) Desorption[52]

2.5.5 RepAir

Founded 2020 in Tel Aviv RepAir uses electrical current and a selective membrane to separate CO_2 from the air. They are currently in the testing phase with their lab scale prototype. The advantage of RepAirs process is that they don't need high temperature or significant pressure differentials.

Their process starts from the electrochemical generation of OH^-/H^+, with protons being produced from water in an anodic reaction eq. (15). Simultaneously in its paired cathodic reaction, hydroxyl groups are produced eq. (16). If a gas stream containing O_2 is supplied (air from the atmosphere) to the cathode, the more favourable reaction takes place to form hydroxyl groups eq. (17). Subsequently, CO_2 supplied from a gas stream can react with these hydroxyl groups, thus being captured in the aqueous solution eq. (18). [18]

$$2H_2O \rightarrow O_2 + 4e + 4H^+ \quad (15)$$

$$4H_2O + 2e \rightarrow 2H_2 + OH^- \quad (16)$$

$$O_2 + 2H_2O + 4e \rightarrow 4OH^- \quad (17)$$

$$CO_2 + OH^- \rightarrow HCO_3^- \quad (18)$$

This approach for capturing Carbon dioxide shows promising results regarding energy consumption. Nevertheless, this technology is far from being commercially applicable and needs a lot more research.

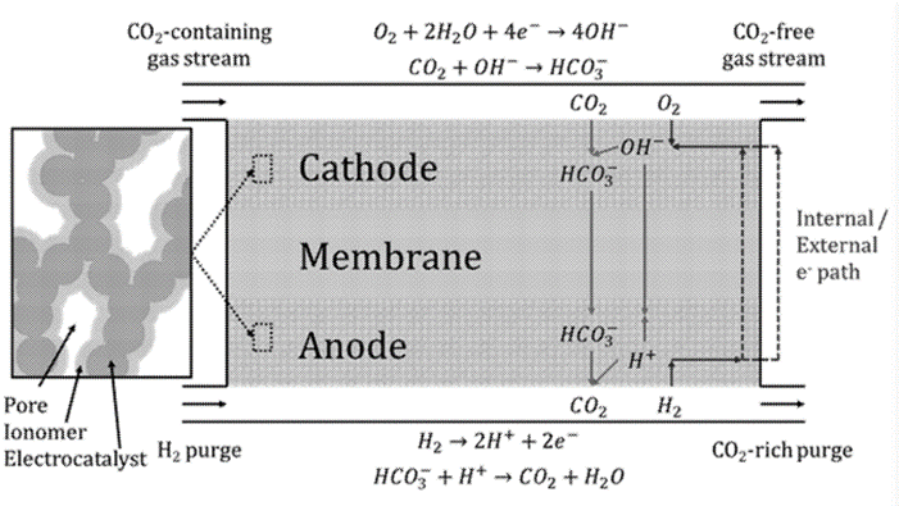

Figure 22: Electrochemical DAC membrane (RepAir)[53]

2.6 Overview of DAC competition

Figure 23 provides an overview of operational and non-operational companies divided into the three main carbon capture technologies. It is easy to see that companies based on solid sorbent technology predominate. A reason for this could be that a process using liquid solvent is hardly scalable and investment costs are significantly higher than for solid sorbent technology. Furthermore, as explained in the description of technology above, electrochemical direct air capture needs a lot more research to enter this competitive market.

The size of the operating companies varies greatly from a few small companies with less than 10 employees to bigger ones like Climeworks or Carbon Engineering with more than 150 employees. The size of the company and the number of employees is unsurprisingly directly related with the investment received. Most of the companies mentioned in Figure 23 focus primarily on the storage of CO_2 extracted from the atmosphere and on the processing of so-called carbon neutral fuels. Some companies also focus on selling their CO_2 to the food and beverage industry.

The use of DAC technology in conjunction with HVAC systems is largely untouched, with the exception of Soletair Power. However, it should be noted that Soletair Power focuses more on removing CO_2 from office air to improve air quality and productivity and less on capturing the CO_2 as a product itself.

Start-Ups	Company size (employees)	Operational since	Product available	Total funding	Latest update	Target market
Solid sorbent						
Climeworks	<150	2009	Yes	$138.7m	2021: Orca, world's largest direct air capture plant	Carbon capture and storage; renewable fuels
Carbon Capture	~15	2019	No	$35m	2021: Series A funding $35m	Renewable fuels; building materials; food and beverage
Global Thermostat	~25	2006	Yes	$2.5m	2020: $15m supplied by Exxon	Biofertilizers; building materials; food and beverage; desalination
Carbfix	~10	2006	Yes	$3.9m	2021: 3.9m€ EU innovation fund	Carbon capture and storage, (technology from Climeworks)
Infinitree	/	2014	No	-----	No update since 2018	Greenhouse applications
Skytree	~10	2010	No	$15k	No update since 2019	Electric cars (range, air quality)
Carbon Collect	~10	2018	No	N/A	2021: Rebranding of Company to Carbon Collect Limited	Renewable fuels; building materials; food and beverage, sequestration
Soletair Power	~10	2016	Yes	$1.5m	2021: 1m€ seed funding	Health (indoor air quality); HVAC; Power to X
Liquid solvent						
Carbon Engineering	<125	2009	Yes	$110.4m	2021: Engineering begins on large-scale commercial facility in Canada to produce fuel from air	Carbon capture and storage; renewable fuels
Carbon Clean	<70	2009	Yes	$64.4m	2021: CEMEX and Carbon Clean work on carbon capture project in Germany	Carbon capture and storage
Electrochemical						
RepAir	>10	2020	No	$1.5m	2021: $1.5m seed funding	No defined market yet
Prometheus Fuels	>25	2019	No	$150k	2021: $150k funding series B	Renewable fuels

Figure 23: Overview of existing DAC Start-up companies

3 Experimental work

3.1 Laboratory plant setup

The space required to set up the test facility was provided by the Vienna University of Technology in the Technikum laboratory. This laboratory fulfils all safety-relevant conditions as well as all process relevant parameters required for the experiments. This includes the presence of compressed air containing 400ppm CO_2, a nitrogen and CO_2 supply that can be regulated to 6 bar to fit the flow meter demand as well as test gas for the calibration of the measuring equipment used.

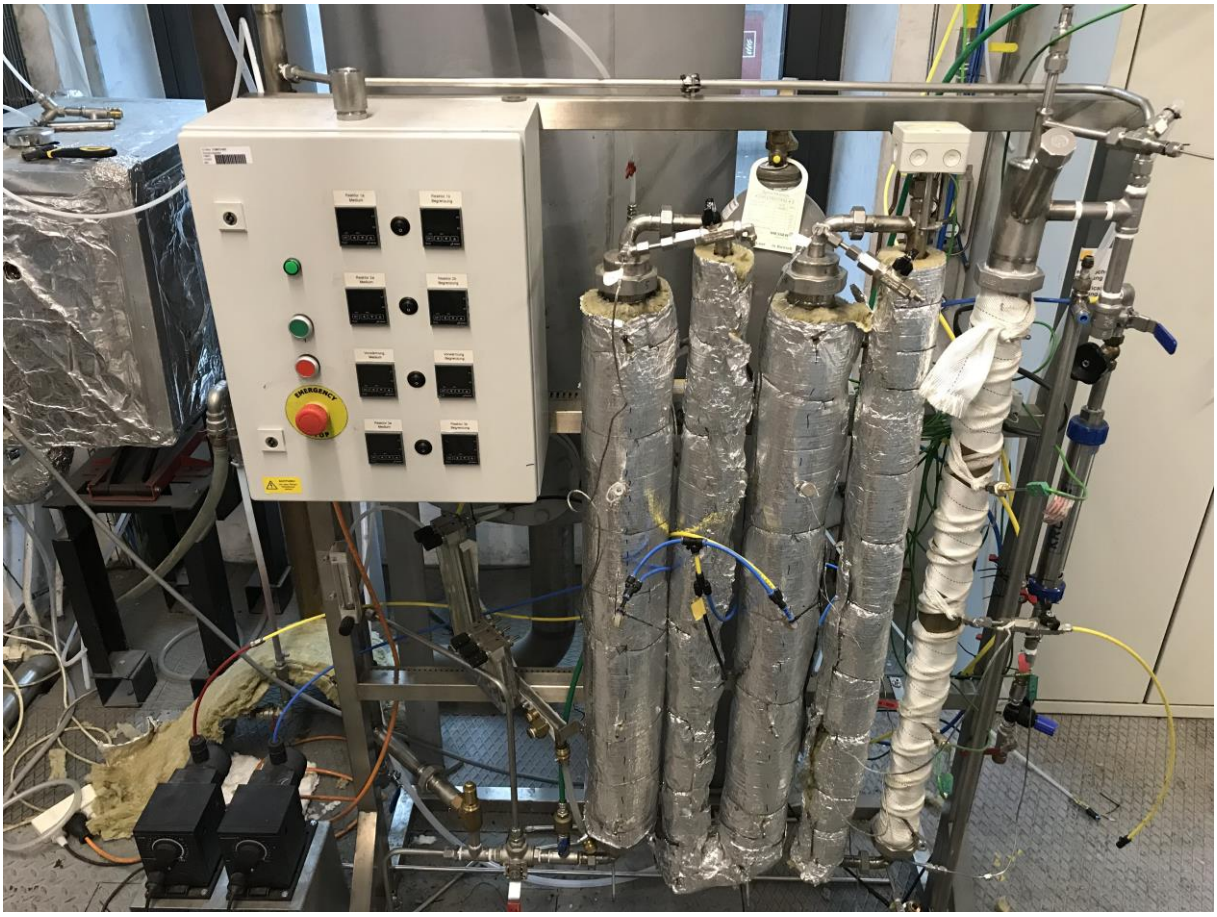

Figure 24: Testing facility Technikum TU Vienna

The laboratory plant consists of a reactor and two additional columns, through each of which a gas stream flows from bottom to top with the adsorption or desorption medium. The reactor as well as the columns can be heated from the outside by separately controllable heating coils and are covered with insulation to minimize heat losses. In addition, a heat exchanger is installed in the reactor which pumps a tempered medium from a cryostat through the inside of the reactor. This heating from the inside and from the outside brings the adsorbent to the desired temperature.

Figure 24 shows the two columns and the reactor, from which the insulation wool has been removed for better visualization. In the lower left corner of the picture, the membrane pumps can be seen, which can be used for humidification of the desorption medium. This is essential because the adsorbent Lewatit

must not be gassed with a completely dry gas stream. The process gases used for the experiments are metered via the rotameters (0.02- 0.2|0.2-2.0 Nm³/h) and fed into the first column.

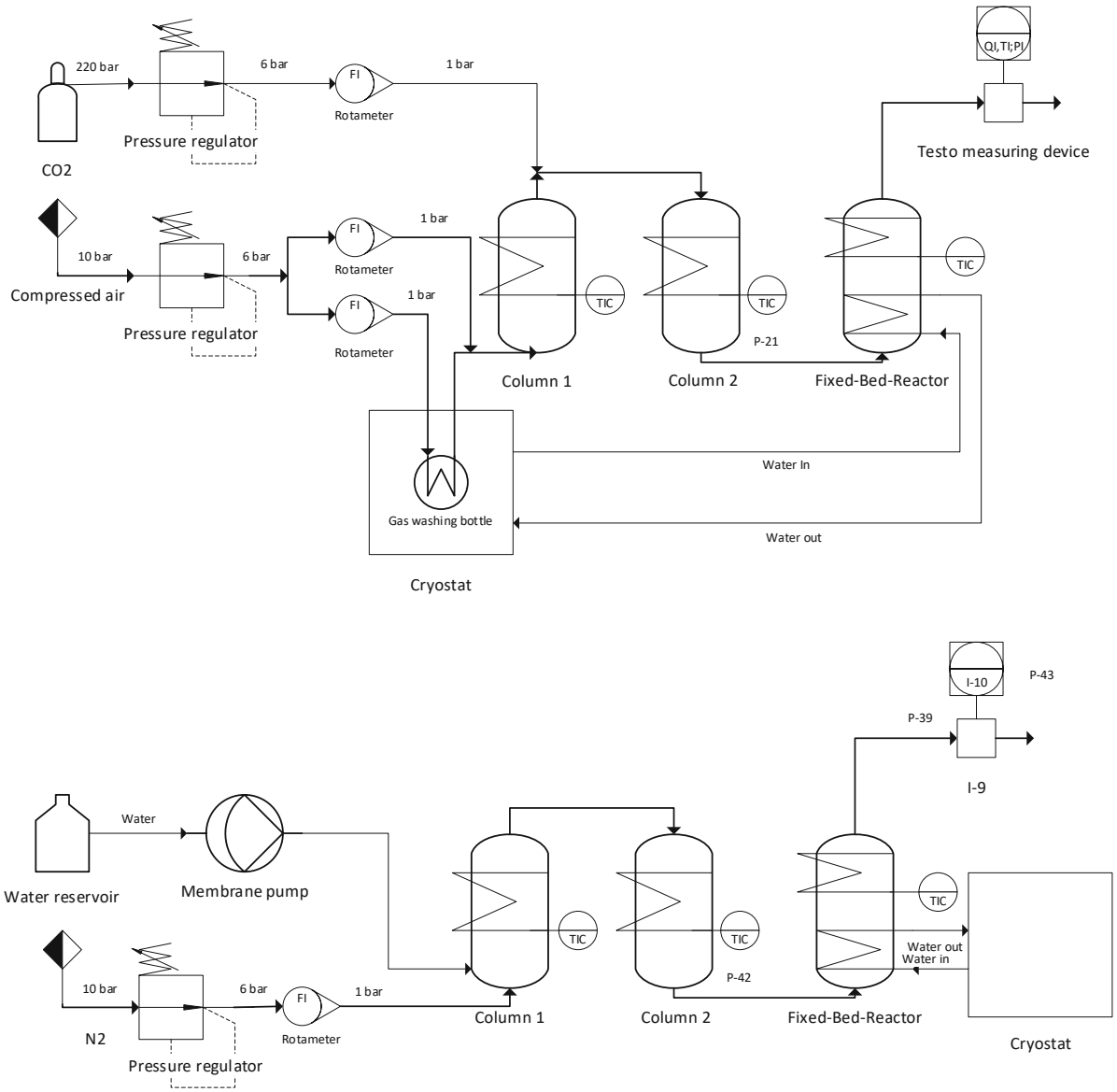

Figure 25: Flow diagram of the fixed bed adsorption (upper) and desorption (lower) apparatus

The gases used and their supply sources are listed below:

- CO_2 technically pure; obtained from Messer Austria GmbH
- N_2 technically pure; obtained from Messer Austria GmbH
- Compressed air; obtained and compressed in-house from ambient

To measure the temperature inside and outside of the heating coil, each column and the reactor are fitted with K-type thermocouples. Two K-tpye thermocouples are used to measure the temperature of the fixed bed and in the head of the reactor. The thermocouples inside the heating coil centered on the reactor and inside the reactor head are used to control the reactor temperature. These temperatures are only used for process monitoring and are not recorded electronically.

The measuring device Testo CO_2 probe with Bluetooth (Serial Nr.: 0632 1551) is used to record the measurement data (Figure 26). This device is used for measuring the concentration of CO_2, the relative as well as absolute humidity and the temperature of the flue gas at the end of the reactor. The measurement data is stored by the device and can be transferred directly to a PC for data processing via USB cable. The measuring device as well as the associated measuring probe are operated by AA batteries and can record a maximum test duration of approximately 10h.

Figure 26: Testo measuring device and measuring probe

Table 5: Technical data for Testo measuring device and measuring probe

Property	Value
Measurement range	0 … +50 °C
	5 … 95 % r.H.
	0 … 10000 ppm CO_2
	700 … 1100 hPa
Accuracy	± 0.5 °C
	± 50 ppm CO_2

To set a desired moisture content during adsorption, the compressor air can be divided into two streams. One of these streams is conveyed through a gas washing bottle. In order to be able to reproduce different environmental scenarios, the gas washing bottle is additionally tempered with a cryostat. This makes it possible to simulate a relative humidity ranging from 25 to 75% as well as atmospheric temperatures of 20 to 35°C.

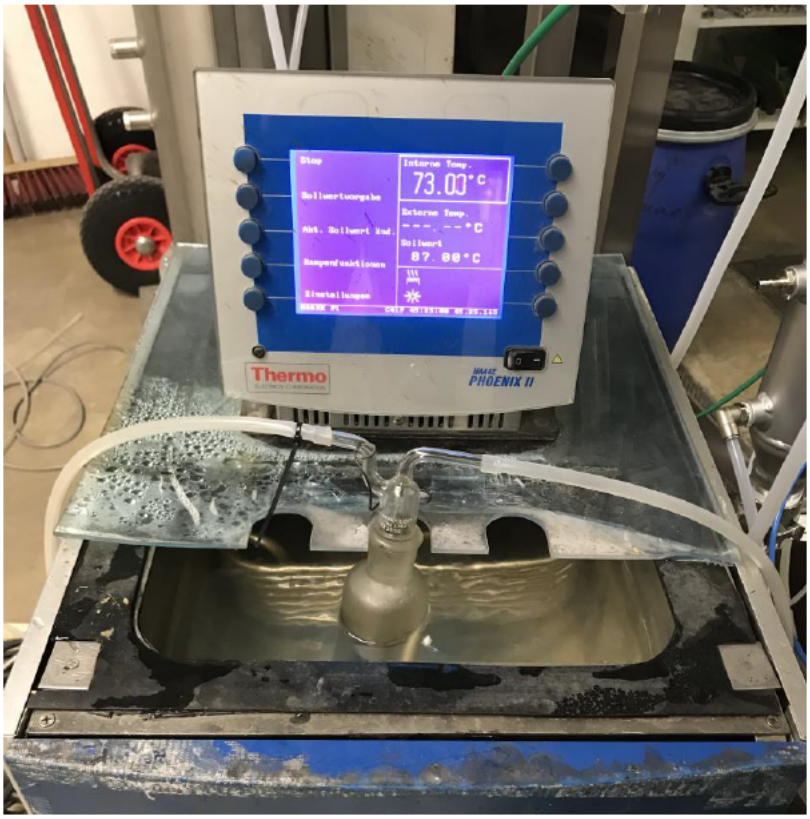

Figure 27: Cryostat with gas washing bottle

3.1.1 Adsorbent: Lewatit VP OC 1065

The adsorbent used for the experiments is commercially available and is manufactured by the Lanxess company under the trademark Lewatit VP OC 1065. The material consists of a polystyrene polymer and featuring only primary amine groups, which are covalently bonded to the macroporous support. This support is cross-linked with divinylbenzene and functionalized with a benzylamine group, through a phthalimide process[54].

Table 6: Material data of Lewatit [55]

Lewatit VP OC 1065	
Composition	Cross linked polystyrene functionalized with primary amines
Matrix	Styrenic
Structure	Macroporous
Uniformity coefficient	Max. 1.8
Range of size for >90 vol% of all beads	0.3-1.25 mm

Effective size	0.52 (+/-0.05) mm
Average pore diameter	25 nm
Bulk density	630-710 kg/m³

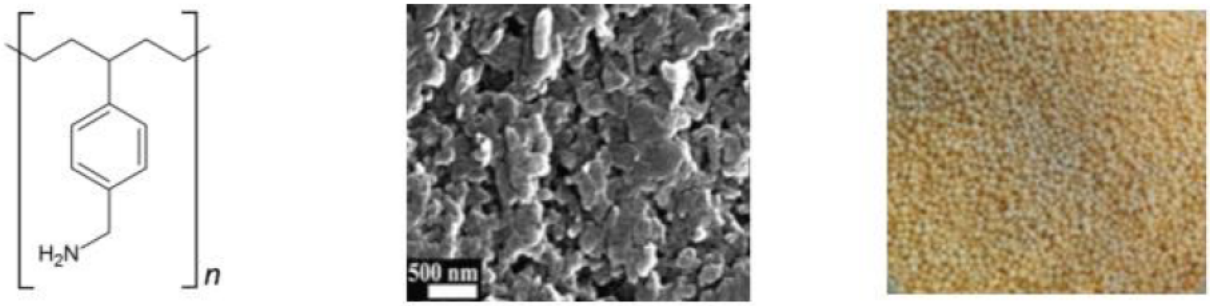

Figure 28:Molecular structure and surface of Lewatit VP OC 1065

Veneman et al. [56] proposed this adsorbent for the application in continuous TSA CO_2 capture processes. Several studies showed, that this material is thermally and mechanically stable and shows excellent CO_2 capture properties.[57][58]

Furthermore, the same material was used before for studies regarding CO_2 capture from flue gas by the Future Energy Technology group at the Institute of Chemical, Environmental and Bioscience Engineering at the TU Vienna.

However, so far Lewatit has not been considered for utilization in direct air capture applications, except by Buijs et al.[59]. In their simulation for a DAC process using Lewatit VP OC 1065 they calculated that a flow of~1400 m3 of air through ~23 kg of resin is required to capture 1 kg of CO_2. As you can see in Figure 29 at 40 Pa (400 ppm) of CO_2 and T= 293K, the capacity of the resin is still ~1.1 mol CO_2/kg which is crucial for application in a DAC process.

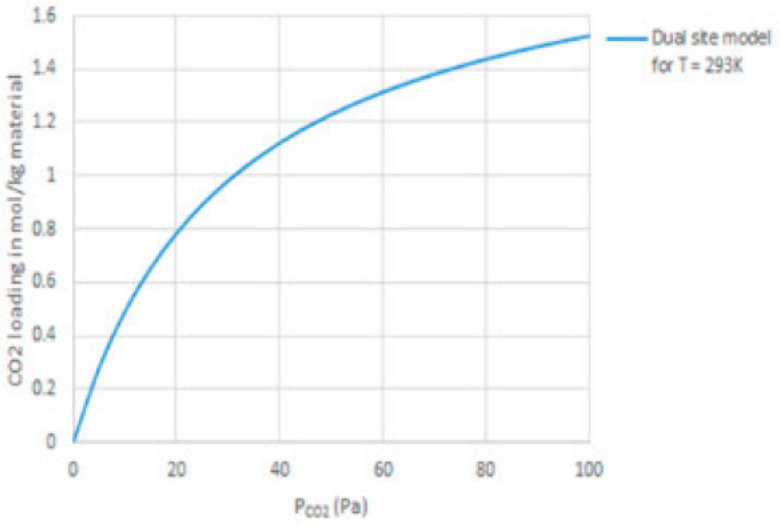

Figure 29: Calculated CO2 capacity at direct air capture conditions for VP OC 1065[59]

Yu et al. [60]evaluated the chemical and thermal stability of Lewatit VP OC 1065 with respect to potential strategies of regenerating this sorbent in CO_2 removal or capture applications. They studied the effect of long-term continuous purging with air, concentrated CO_2, different $O_2/CO_2/N_2$ mixtures, and steam on the CO_2 adsorption rate at different temperatures and exposure time for both wet and dry conditions.

To avoid thermal degradation, sorbent regeneration should be carried out in absence of oxygen when operating at temperatures above 70 °C and below 150 °C. If the partial pressure of CO_2 reaches 1 bar, the maximum temperature must not get higher than 120 °C, otherwise carbamide formation is unavoidable. Humidity helps to prevent urea formation up to a certain level but cannot stop it let alone reverse it. Furthermore, the application of water vapor or pure steam, did not have a negative influence on the sorbent capacity.

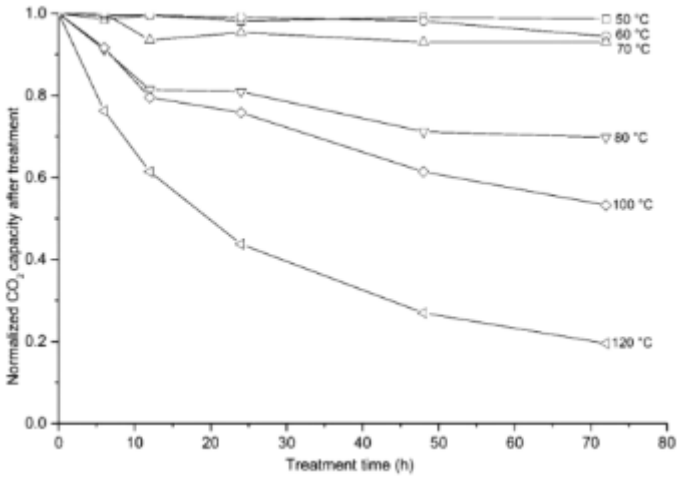

Figure 30:Effect of temperature in dry air exposure on the CO_2 adsorption capacity (evaluated at 15 vol % CO_2, 40 °C) as a function of treatment time[60]

E. Zerobin et.al [37]conducted an extensive research about the obtained Lewatit VP OC 1065. The key findings and the data obtained are summarized following section.

CO_2 capacity:

A variety of adsorption experiments were carried out for Lewatit, using thermogravimetric analysis (TGA) and a fixed bed reactor. The measurements for the CO_2 capacity were carried out by gradually increasing the partial pressure of CO_2. To reach an equilibrium loading for each partial pressure maintaining isothermal conditions was crucial. The CO_2 adsorption isotherms generated by the data points obtained from these equilibrium loadings are displayed in Figure 31. The isothermal measurements were carried out at temperatures ranging from 40°C to 95°C/102°C. The highest measured capacities for this sorbent at the highest investigated CO_2 partial pressure of 0.5 bar were reached at 40°C with 2.5 mol kg^{-1}. Lewatit performed especially well at CO_2 contents below 12%. A high CO_2 equilibrium loading at low CO_2 partial pressures is obviously an advantage from this sorbent material and is therefore promising for capturing air containing low CO_2 concentrations. The CO_2

adsorption enthalpy for Lewatit (76 kJ mol^{-1}) was calculated for a reference temperature of 50°C and a loading of 1.8 mol $kg^{-1}$by using the Clausius-Clapeyron equation. These results are similar to experiments and data reported by Li et al. [61] and Veneman et al. [40].

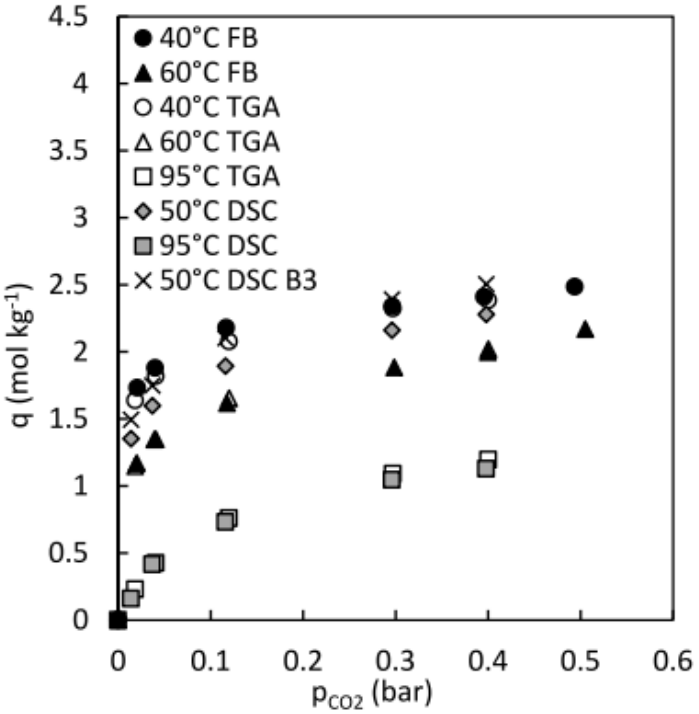

Figure 31: CO_2 adsorption isotherms for Lewatit obtained from FB and TGA measurements [37]

Thermal degradation:

To evaluate the loss of adsorption capacity or thermal stability of the adsorbent material, TGA tests were performed, to figure out the limits of the desorption temperature. The experiment was carried out by heating up adsorbent samples from ambient temperature to 190°C at a heating rate of 1°C min^{-1}. The mass loss of the sample was measured and considered as an indication for degradation effects. Two experiments were conducted with the adsorbent material.

In the first experiment, the samples inside the TGA chamber were exposed to a purge gas containing only nitrogen. For the second experiment the purge gas was switched to synthetic air containing oxygen. The data was compared to assess whether the presence of oxygen results in an increased degradation of the adsorbent sample. Displayed in Figure 32 is the relative mass loss referred to the dry sample mass. When purged with N_2, Lewatit did not have significant mass loss up to 110°C. However, when purged with air a slight mass loss was already detected at 90°C. Furthermore, when purged with Nitrogen and heated to temperatures beyond 160°C no further mass loss was detected. The adsorbents manufacturer guarantees in the material data sheet a thermal stability up to 100°C. Nevertheless, to get further details on the effects of thermal degradation on the adsorption behaviour of Lewatit under certain conditions, additional analyses would be needed. To summarize the findings of the obtained results: When using Lewatit, the desorption temperature must be limited to around 100°C.

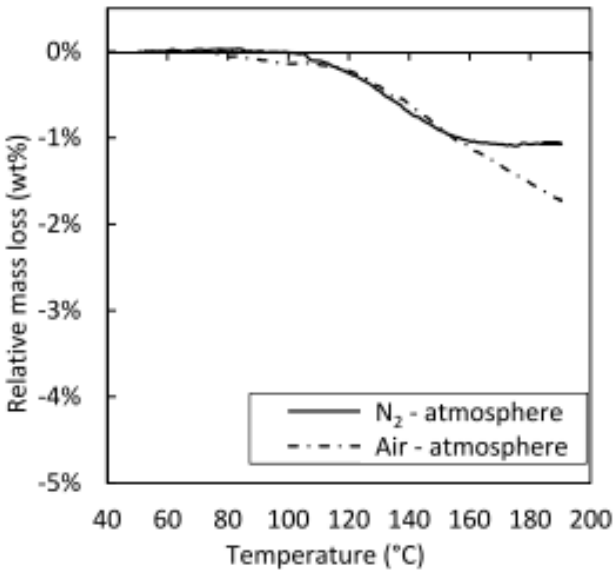

Figure 32: Thermal stability of Lewatit

3.2 Calculation of fixed bed operation

In order to avoid the formation of a fluidized bed in the test reactor, or to prevent particle discharge out of it, the minimum fluidization velocity must be calculated before operation starts. The minimum fluidization velocity represents the boundary velocity between the fixed bed and the fluidized bed and can be calculated using Ergun's equation.[62][63]

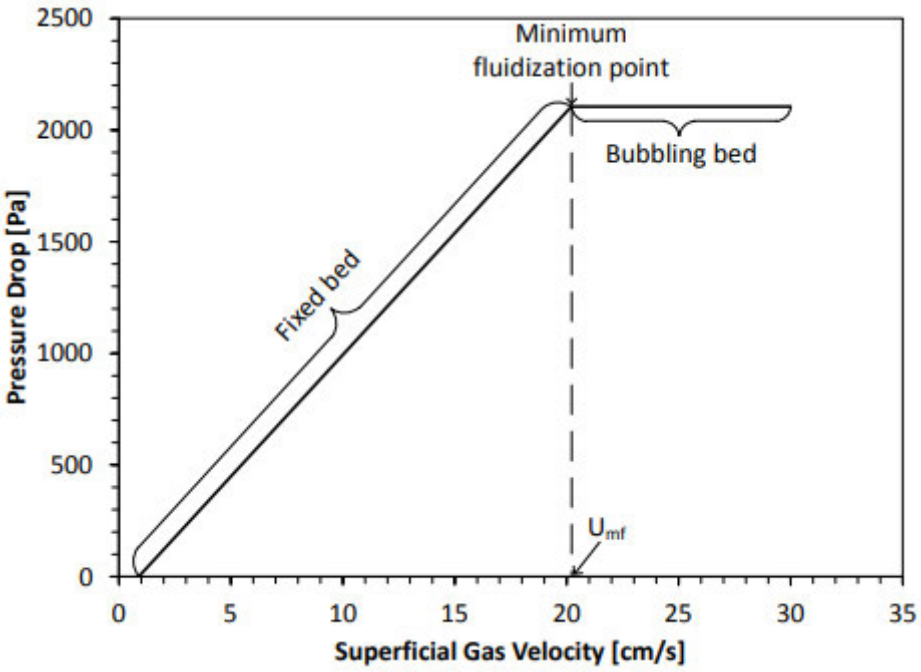

Figure 33: Minimum fluidization velocity[64]

The following equation is a simplification of Ergun's equation with an empirical approach and is valid for a Reynolds number range from 0.001 to 4000. This approach has worked well in practice for a wide range of materials and grain diameters:

$$U_{mf} = \frac{\mu}{\rho_{g*} d_{sv}} * [\sqrt{33.7^2 + 0.0408 * Ar} - 33.7 \quad (19)$$

where the Archimedes number is to be used as follows:

$$Ar = \frac{\rho_g * {d_{sv}}^3 * (\rho_p - \rho_g) * g}{\mu^2} \quad (20)$$

From the calculation using these formulas, a minimum fluidization velocity of 0.097 m/s can be determined. Multiplying this velocity by the cross-sectional flow area of the reactor yields the maximum allowed flow rate.

$$\dot{V}_{max} = U_{mf} * A_{reactor} \quad (21)$$

Table 7: Description of parameters for calculation of the fixed bed operation

Variable	Description	Unit
$\dot{V}_{max}$	Maximum allowed flow rat	Nm^3/s
U_{mf}	Minimum fluidization velocity	m/s
Ar	Archimedes number	/
μ	Dynamic viscosity	kg/ms
ρ_g	Gas density	kg/m^3
ρ_p	Particle density	kg/m^3
d_{sv}	Surface/Volume related diameter	m
A_{rector}	Cross-sectional flow area	m^2
g	Gravitational acceleration	m/s^2

3.3 Laboratory plant procedure

At the beginning of a series of experiments, the reactor is filled with pebbles up to half of its height. The pebble has the advantage that it stores heat very well and thus avoids temperature fluctuations in the fixed bed. It also allows precise placement of the adsorbent in the reactor, as the height of the fixed bed would not be sufficient for this. The precise placement of the fixed bed is so important because the thermocouple leading centrally into the reactor must be surrounded by the adsorbent.

Before filling the adsorbent into the reactor, the required amount is weighed out precisely so that the results can be compared over several tests. To ensure that the adsorbent is correctly distributed in the reactor and that the thermocouple is surrounded by the fixed bed, an optical check is carried out using an endoscope camera. After each series of experiments, the adsorbent must be completely desorbed in a nitrogen atmosphere.

3.3.1 Desorption

Desorption is an important part of the entire experiment, as it serves to regenerate the adsorbent. In order not to damage the adsorbent or to be able to ensure complete desorption, it is important to adhere to the desorption parameters.

Table 8: Desorption parameters

Desorption	
Temperature	~80 °C [max 90°C]
Purge gas	Nitrogen
Volumetric flow	0.5 Nm^3/h
Relative humidity	>5 %

Desorption proceeds as follows:

- Turning on the nitrogen supply and setting the volume flow through the columns and the reactor
- Switching on the heating coils and setting the temperature limit of the surface temperature for each column
- Connection of the diaphragm pump and feeding of water into the first column to prevent the adsorbent from drying out
- Heating the fixed bed inside the reactor with the heat exchanger which is connected to the cryostat

Recording of the desorption data starts as soon as the air supply from the compressor is turned off and the nitrogen supply is turned on. Only at this point may the heating of the experimental plant by means of heating coils and cryostat be switched on. The heating process of the cold system takes about 2 hours. This also corresponds to the total desorption time. Desorption is carried out until no CO_2 can be measured in the exhaust gas for a few minutes. In almost every measurement, the CO_2 content in the

exhaust gas already drops to zero before the maximum temperature is reached. In this sense, these temperatures are not to be understood as a minimum, but rather as a certainty for complete desorption, since the desorption enthalpy itself prevents the adsorbent from rising to the desired temperature of 80°C.

Figure 34 shows a desorption process in which the adsorbent was not introduced into the reactor until the entire test system was at the desired temperature. The temperature curve shows very clearly that desorption draws energy from the system in the form of heat, and the fixed bed is only at the desired temperature after desorption is almost complete. When the regeneration of the adsorbent (desorption) is completed, i.e., no more CO_2 is measured in the measuring instrument, the preheating of the columns and the cryostat are turned off. The adsorbent is cooled down further in a nitrogen atmosphere to the desired temperature for the subsequent adsorption. During the entire desorption as well as the following cooling phase, it is very important to ensure that a constant volume flow of water is conveyed into the column, otherwise high temperatures may cause the adsorbent to dry out and thus be damaged.

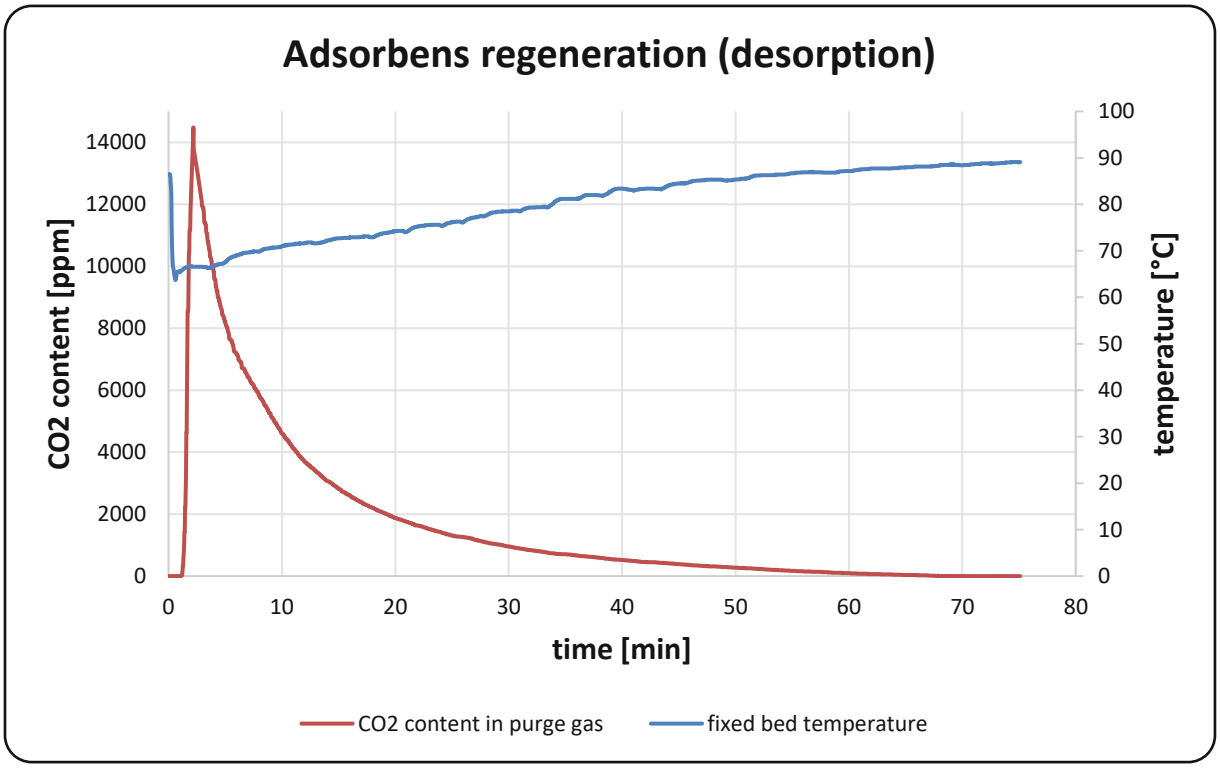

Figure 34: Display of desorption enthalpy influence

3.3.2 Adsorption

In this work and the associated experiments, the main focus was placed on adsorption. This is due to the fact that the process parameters for adsorption are essential for further design of a DAC pilot unit and are easy to achieve in the case of DAC, and these can also be reproduced very well with the available laboratory apparatus. Different adsorption conditions, which can occur in the case of DAC, were investigated.

Table 9: Adsorption parameters

Adsorption	
Temperature	20-35 °C
Purge gas	Atmospheric air
Volumetric flow	0.5 Nm^3/h
Relative humidity	25-75 %

As already noted, before the measurement data recording begins, the adsorbent must be brought to the correct temperature under a nitrogen atmosphere. Likewise, the carrier gas flow is measured before each adsorption. At the end of the experiment, the indicated CO_2 volume flow must be equal to that of the pure carrier gas flow. This is the only way to verify complete loading of the adsorbent.

After reaching the temperature required for the adsorption, the desired carrier gas volume flow is set. Subsequently the dry volume flow rate as well as the humid volume flow rate conveyed through the temperature-controlled wash bottle are set manually at the same time. At this point, the exact CO_2 partial pressure is still unknown. Normally, during adsorption experiments, the temperature in the reactor increases due to the adsorption heat released. However, since the CO_2 content in the atmosphere is so low and the associated duration of adsorption is very long, this phenomenon can unfortunately not be recorded.

However, as can be seen in Figure 35, the uptake of water in the fixed bed can be demonstrated very well. In addition, this graph shows that the complete adsorption of water is completed much faster (approx. 40 min) than that of CO_2 (approx. 400 min).

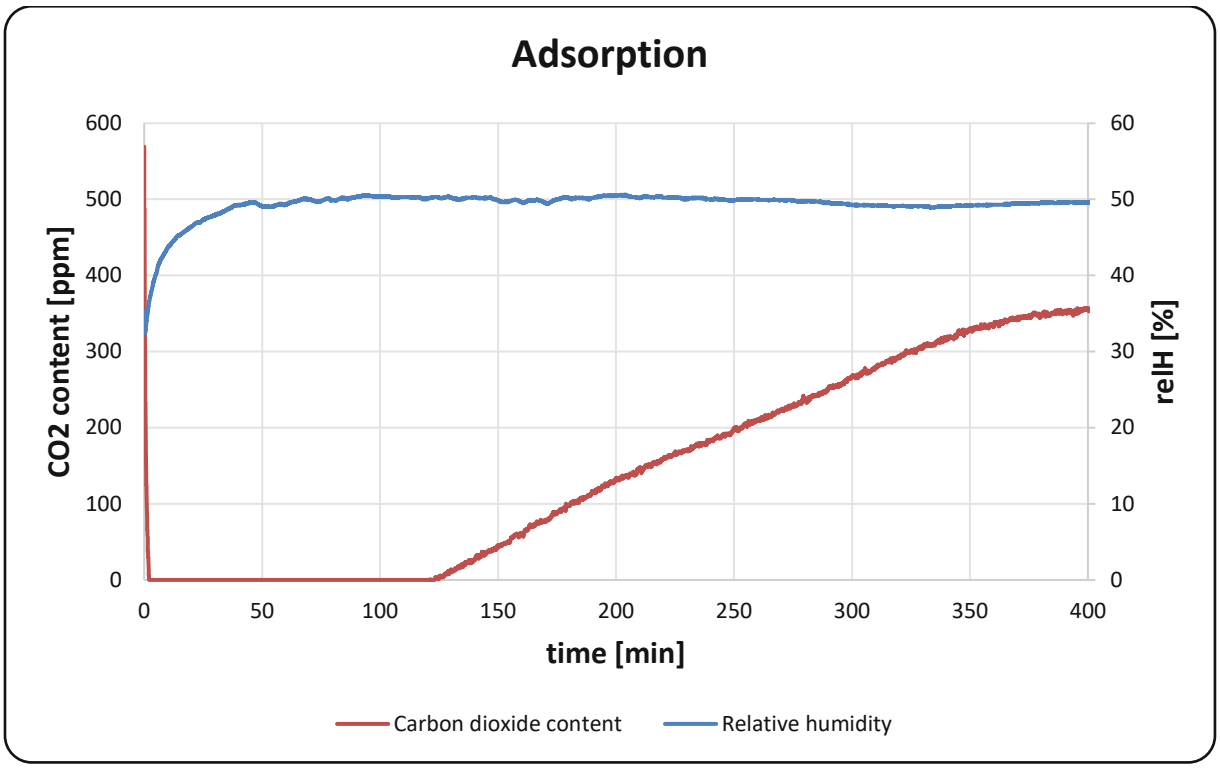

Figure 35: Displayed water adsorption of the adsorbent

The CO_2 content in the exhaust gas can be read off the measuring device. However, since the ambient air itself is measured before each test run, the large dead volume of the system and the delay of the measuring device itself result in a strong measurement inaccuracy at the beginning of each test. This is taken into account by not including the first 120 seconds when evaluating the adsorption process. The adsorption is operated until a steady state is reached over a longer period (approx. 30 min).

At this point, the connection of the measuring probe is changed so that the gas is measured before instead of after the reactor. This ensures that the partial pressure of CO_2 reached, corresponds to the equilibrium state. The CO_2 concentration in the airstream before reaching the reactor is noted and used in the evaluation of the mass balance. After reaching the end of the adsorption process, the air supply from the compressor is turned off and the feed gas is switched to nitrogen. Subsequently, the heating of the apparatus is switched on and the regeneration of the adsorbent starts.

3.4 Adsorbent evaluation with lab plant

The following chapter describes the evaluation of the test data and the calculation of the test-relevant characteristic parameters.

3.4.1 Determined parameters

The results presented below are based on adsorption- (Figure 36) and desorption (Figure 37) curves. These are used to plot the CO_2 concentration (and hence the CO_2 partial pressure) $CO_{2,out}$ at the reactor outlet over time. A typical data set is used to explain how the results presented below are obtained from it. In this section, only the determination of the characteristic values and their presentation will be discussed.

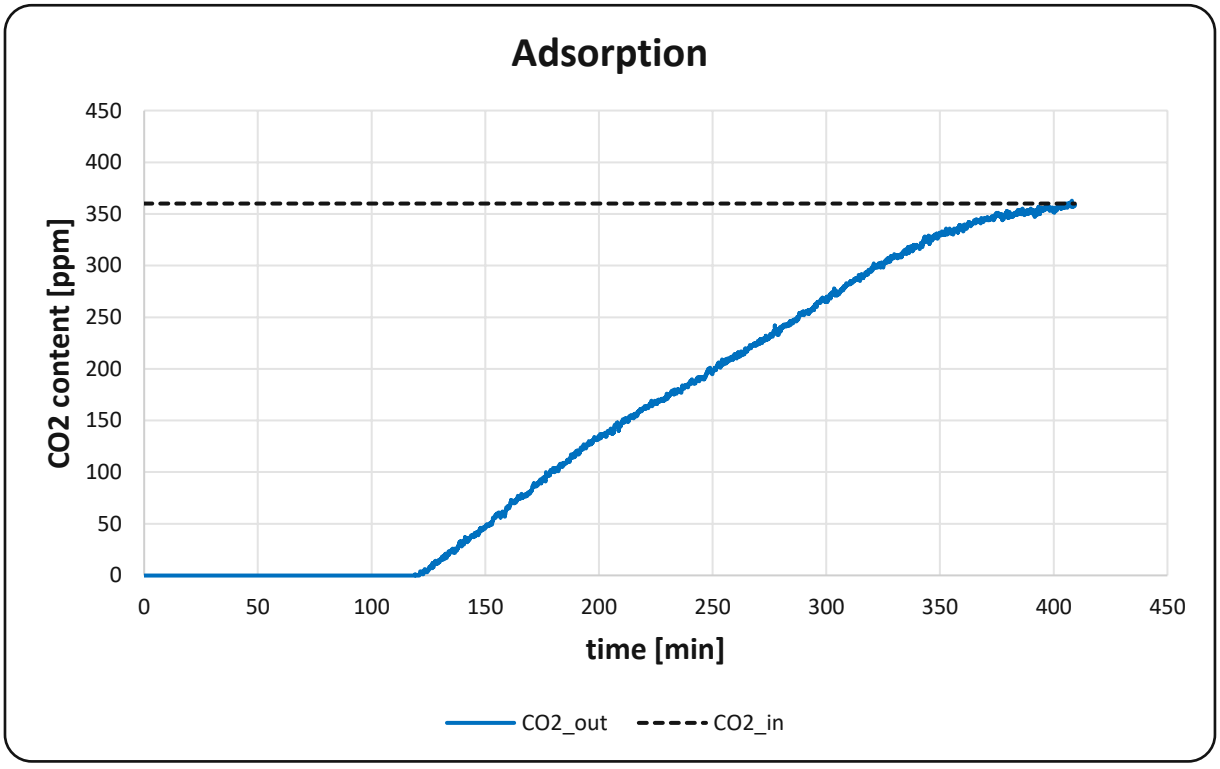

Figure 36: Typical adsorption curve

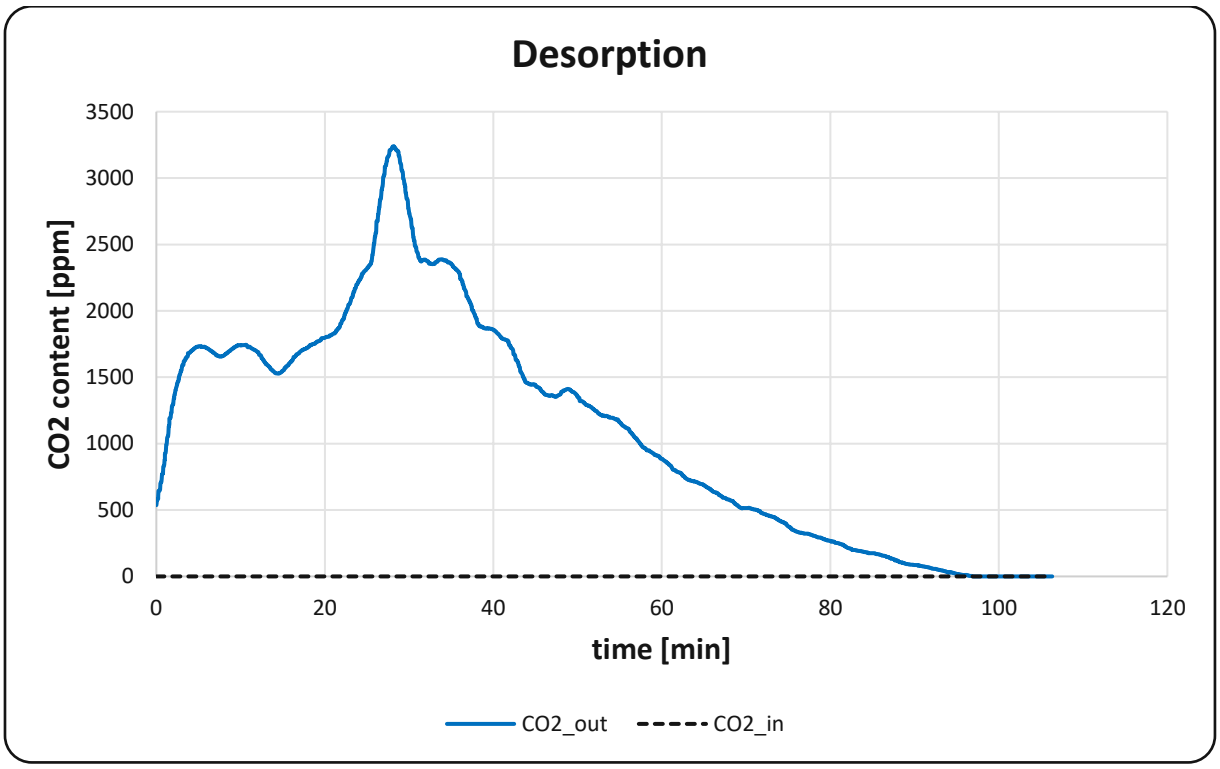

Figure 37: Typical desorption curve. CO_2 content measured in N_2 purge gas flow of 0.5 Nm^3/h

3.4.2 Adsorption equilibrium

The equilibrium loading is determined by balancing according to (22). Adapted for CO_2, the formula is as follows.

$$X_{CO_2} = \frac{m_{CO_2,ad}}{m_{adsorbens}} = \frac{m_{CO_2,in} - m_{CO_2,out}}{m_{adsorbens}} \quad (22)$$

For the entire duration of the experiment (about 420 minutes in Figure 36), it is assumed that there is a constant mass of CO_2 flowing into the reactor and thus the total mass of incoming CO_2 $m_{CO2,in}$ can be calculated. This assumption is justified because no change is made to the reactor inlet during this time. To do this, the duration of adsorption is multiplied by the concentration measured at the bypass upstream of the reactor after the experiment, using the ideal gas equation.

$$m_{CO_2,in} = \frac{\Delta t * c_{CO_2,in} * \dot{V}_{dry} * p * M_{CO_2}}{R * T} \quad (23)$$

The same procedure can be followed for the mass of CO_2 leaving the reactor. Here, the total duration of the adsorption is divided into discrete time intervals with a length of 2s since the measuring probe only records in this time interval. For these n time intervals, the concentration measured at the outlet is then used to determine an outgoing mass in this time interval. These partial masses are summed up as shown in equation (24).

$$m_{CO_2,out} = \sum_{i=0}^{n} \frac{\Delta t_i * c_{CO_2,in_i} * \dot{V}_{dry_i} * p * M_{CO_2}}{R * T} \quad (24)$$

Using equations (22), (23) and (24), the equilibrium loadings shown in the following three tables (Table 10,Table 11,Table 12) have been determined.

Table 10: Adsorption equilibrium at 25°C

Relative humidity	Description	Unit	25 %	50 %	75 %
$m_{CO2,in} - m_{CO2,out}$	Mass adsorbed	g	1,23	1,42	1,66
X_{CO2}	Equilibrium loading	$kg_{CO2}/kg_{Adsorbent}$	0,041	0,047	0,056
q_{CO2}	Adsorption equilibrium	mol/kg	0,93	1,07	1,28

Table 11: Adsorption equilibrium at 35°C

Relative humidity	Description	Unit	25 %	50 %	75 %
$m_{CO2,in} - m_{CO2,out}$	Mass adsorbed	g	0,83	1,02	1,37
X_{CO2}	Equilibrium loading	$kg_{CO2}/kg_{Adsorbent}$	0,028	0,034	0,046
q_{CO2}	Adsorption equilibrium	mol/kg	0,63	0,77	1,04

Table 12: Adsorption equilibrium at 25°C and 50% relative humidity for various partial pressure of CO_2

Partial pressure	Description	Unit	360 ppm	760 ppm	950 ppm	1800 ppm
$m_{CO2,in} - m_{CO2,out}$	Mass adsorbed	g	1,42	1,43	1,47	1,47
X_{CO2}	Equilibrium loading	$kg_{CO2}/kg_{Adsorbent}$	0,047	0,048	0,049	0,050
q_{CO2}	Adsorption equilibrium	mol/kg	1,07	1,08	1,11	1,14

A graphically descriptive interpretation of the equilibrium loading is given by the area between the breakthrough curve (adsorption) and the horizontally dashed line "c_{in}", which represents the input concentration, in Figure 36. Additionally, the data contained in Table 10, Table 11, Table 12 are compared in Figure 38 and Figure 39.

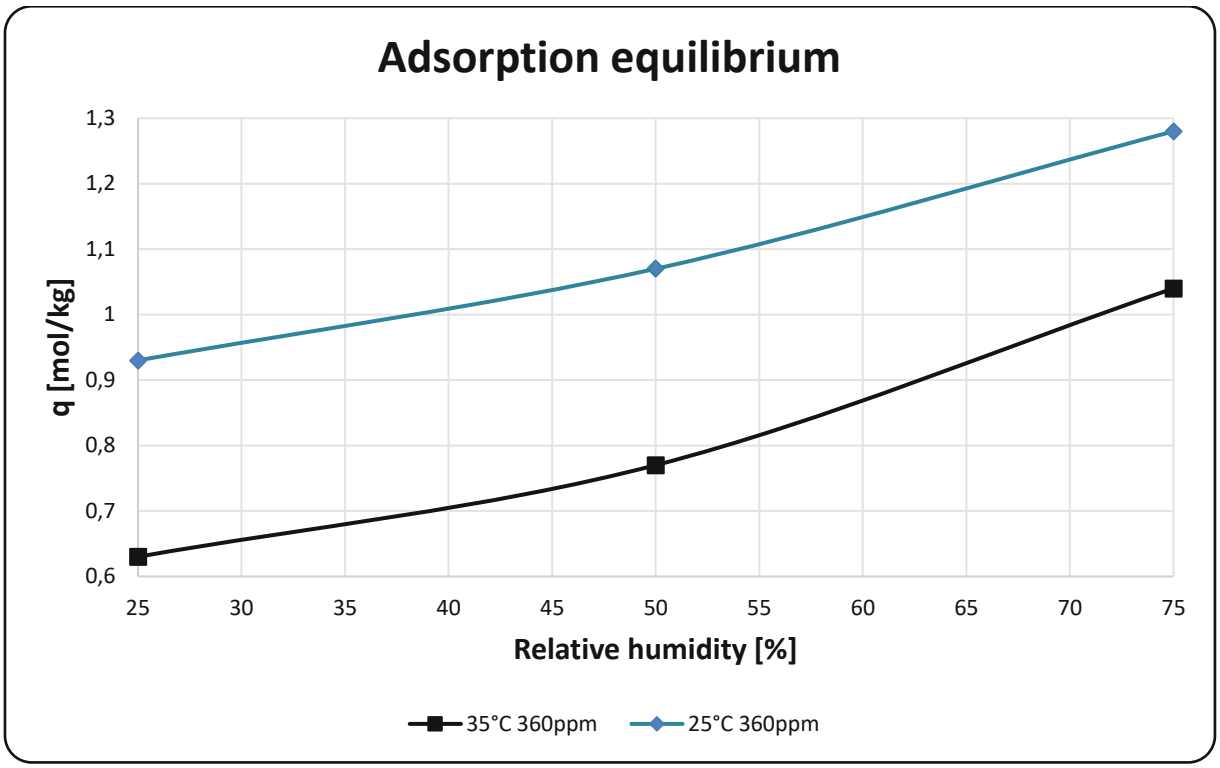

Figure 38: Adsorption equilibrium as a function of relative humidity for different temperatures (25/35°C)

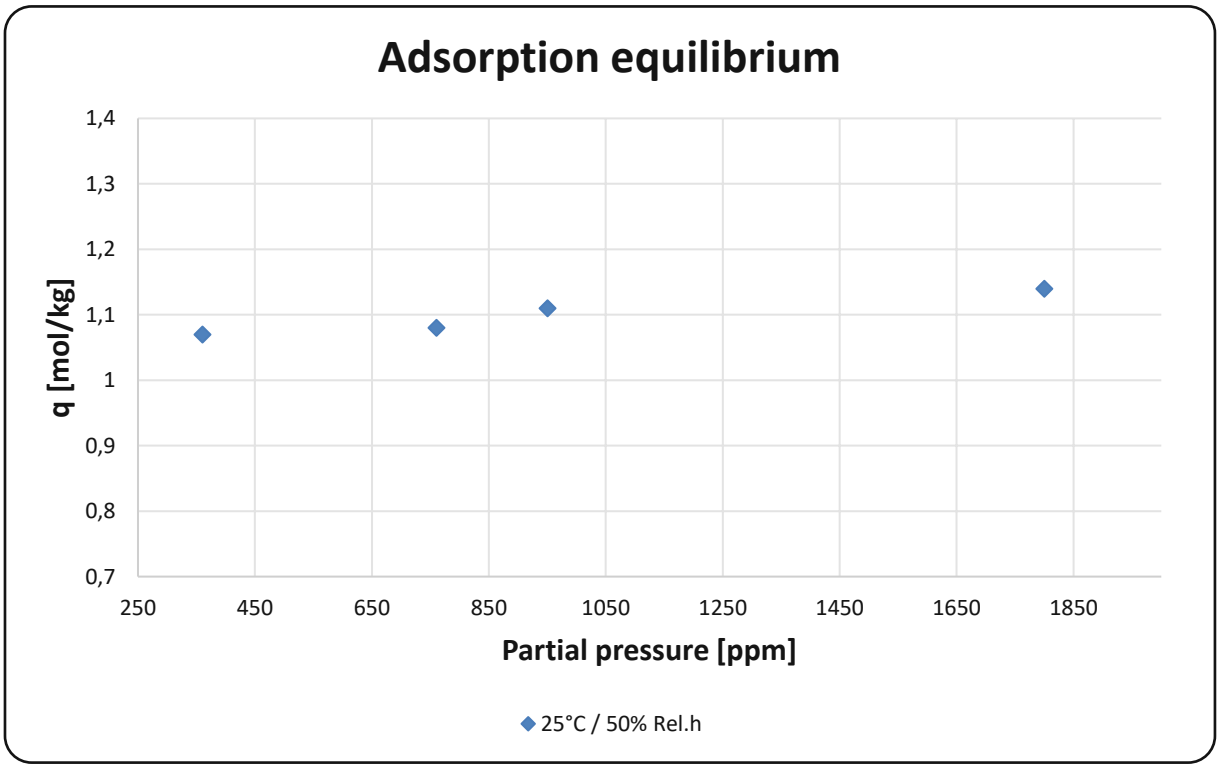

Figure 39: Adsorption equilibrium as a function of different CO_2 partial pressures (360/760/950/1800 ppm)

Table 13: Description of parameters for calculating adsorption equilibrium

Variable	Description	Unit
X_{CO2}	Equilibrium loading of component	g/g
$m_{CO2,ad}$	Adsorbed mass of CO_2	g
$m_{CO2,in}$/ $m_{CO2,out}$	Mass of CO_2 flowing in/out the reactor	g
$m_{adsorbent}$	Adsorbent mass	g
Δt	Discrete time interval	s
c_{CO2}	CO_2 concentration	ppm
$\dot{V}_{dry}$	Dry volumetric flow	Nm^3/s
p	pressure	Pa
M_{CO2}	Molar mass of CO_2	g/mol
R	Gas constant	J/molK
T	Temperature	K

3.4.3 Tentative kinetic evaluation

To evaluate the kinetic behaviour, the data are evaluated with regard to the time period after which 90 % of the determined equilibrium load is reached (26). Linear interpolation is performed between the first measured value at which 90 % of the equilibrium load is exceeded and the previous measured value.

$$\tau_{90} = t\left(\frac{X_{CO_2}(t)}{X_{CO_{2,eq}}(t)} \geq 0{,}9\right) \quad (26)$$

It should be noted that this determined criterion cannot be directly compared with the literature, since these measurements are not usually carried out in fixed-bed operation. For an assessment of the reaction kinetics, however, it is much more meaningful since possible measurement inaccuracies of the measuring probe or a parameter change of the air in the compressor have less influence.

In fixed bed operation, normally a combination of two criteria is measured: Time until the adsorbent is fully loaded (t_{ad}) and breakthrough time (t_{bt}). This data is calculated following equations (27) and (28) and is presented in the following tables (Table 14,Table 15,Table 16). A graphical illustration of the data is given in chapter 4.

$$\tau_{ad} = t\left(\frac{X_{CO_2}(t)}{X_{CO_{2,eq}}(t)} = 1\right) \quad (27)$$

$$\tau_{bt} = t\left(\frac{c_{CO_2}(t)}{c_{CO_{2,eq}}(t)} = 0\right) \quad (28)$$

Table 14: Adsorption kinetics at 25°C

Relative humidity	Description	Unit	25 %	50 %	75 %
τ_{bt}	Breakthrough time	min	69	121	135
τ_{90}	90% Adsp. time	min	340	359	436
τ_{ad}	Full adsp. time	min	385	410	496

Table 15: Adsorption kinetics at 35°C. Missing data is explained in chapter 4

Relative humidity	Description	Unit	25 %	50 %	75 %
τ_{bt}	Breakthrough time	min	18	34	(29)
τ_{90}	90% Adsp. time	min	267	370	/
τ_{ad}	Full adsp. time	min	560	453	/

Table 16: Adsorption kinetics at 25°C and 50% relative humidity in min

Partial pressure	Description	Unit	360 ppm	760 ppm	950 ppm	1800 ppm
τ_{bt}	Breakthrough time	min	121	0	0	3
τ_{90}	90% Adsp. time	min	359	223	227	99
τ_{ad}	Full adsp. time	min	410	262	255	103

Table 17: Description of adsorption kinetic parameters

Variable	Description	Unit
X_{CO2} (t)	Loading of CO_2 at time t	g/g
τ_{90}	Duration for reaching 90% of the equilibrium load	min
τ_{ad}	Duration until full loading	min
τ_{bt}	Duration until breakthrough	min
c_{CO2} (t)	CO_2 concentration at time t	ppm
$c_{CO2,eq}$ (t)	CO_2 concentration at equilibrium	ppm

3.4.4 Quality of the measurement data

The recording of the measurement data has a few problems which are important to mention. For instance, a measurement point is only taken every 2 seconds. This works well at low rates of change since there will be no serious jumps in measurement data between the measuring points. However, at high rates of change, it is possible that peaks in partial pressure of CO_2 might not be recorded. This source of error together with the low measurement reliability of the measuring device led to a large uncertainty of the values, especially in desorption. For example, the tolerance of the Measuring device for a CO_2 content of 5000 ppm is +-350ppm. A similarly large measurement tolerance is given for the measurement of relative humidity.

3.5 Experimental DAC plant setup

The first experimental plant is built based on the findings and results of the laboratory plant and the literature review considered in this work. The main focus of the design of this plant is to obtain parameters for the simulation of a DAC prototype plant. These parameters are essential to be able to generate adsorption isotherms. In addition, it is possible to generate mass and energy balances over the system boundary and thus to check the DAC process for economic efficiency.

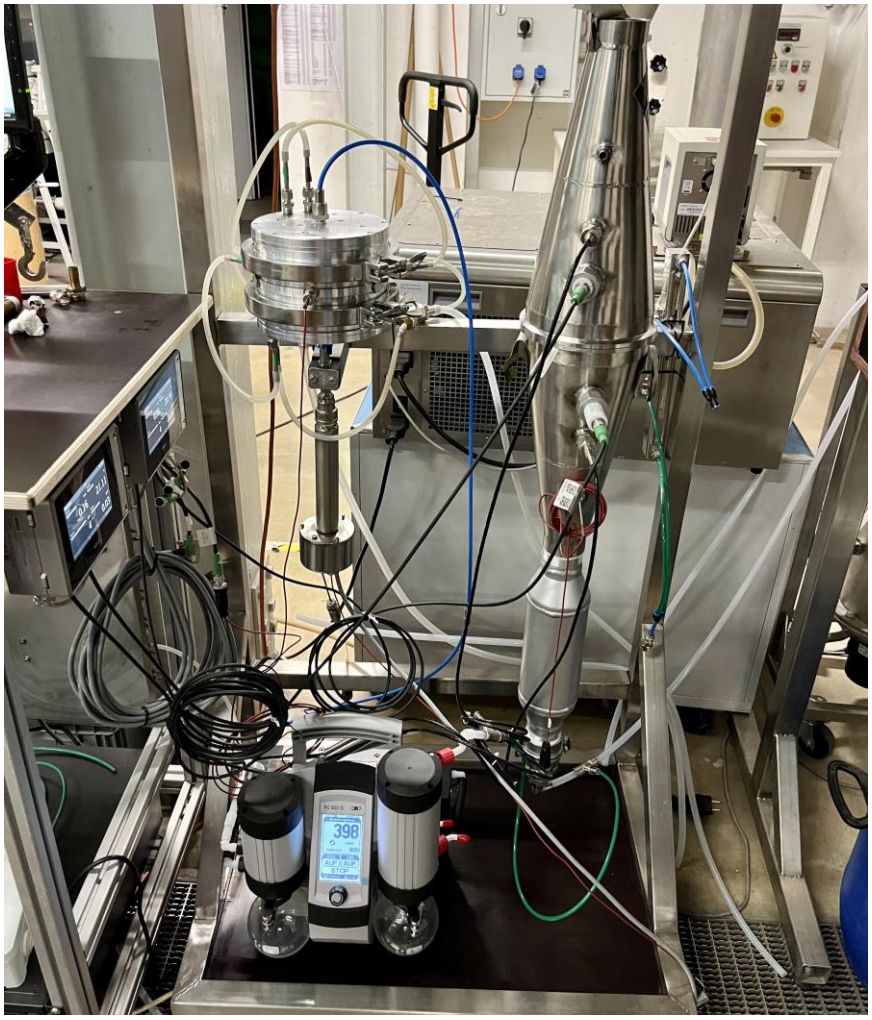

Figure 40: Experimental DAC plant set up in the Technikum at TU Wien. The system is shown in desorption mode. In the lower part of the picture, the vacuum pump can also be seen operating at 398 mbar.

3.5.1 Adsorption mode

As in the laboratory plant, dried compressed air is used for the adsorption tests. Nitrogen can be added as needed to reduce the CO_2 content in the feed gas stream. Equivalently, to increase the CO_2 content, pure CO_2 can be supplied either via a needle valve or via an MFC. A bubbler is used to increase the humidity of the air. The gas flow is split into a partial flow that passes through the bubbler and a partial flow that bypasses the bubbler. The division can be adjusted again via two float type flow meters. In addition, the temperature of the bubbler can be adjusted and thus influence the water loading.

After setting the CO_2 and water content of the feed gas, the inflow temperature is set. To accomplish that, a honeycomb heat exchanger with a large surface area is used. On the water side, the heat exchanger is connected to a cryostat to enable precise temperature control. Furthermore, the heat exchanger has a temperature measurement facility in both water connections.

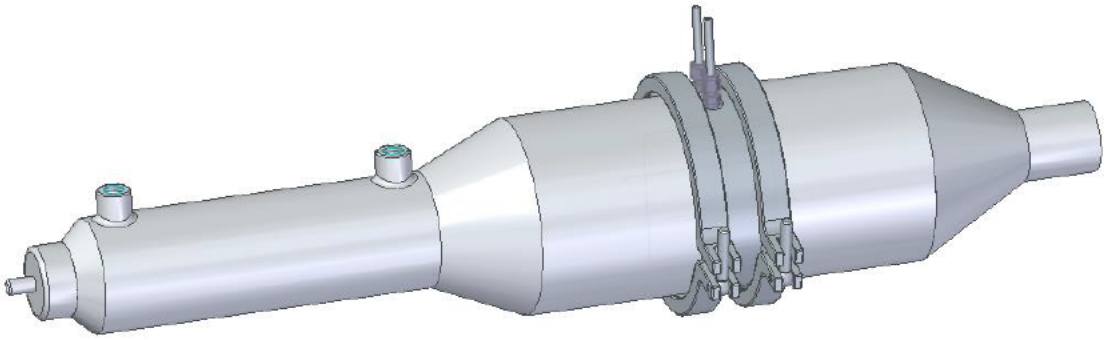

Figure 41: 3D drawing of the prototype in adsorption mode

The heat exchanger is directly connected to the inlet cone of the adsorption apparatus. The following measuring possibilities are available in the cone:

- Temperature
- Pressure
- CO_2 content
- Relative/Absolute humidity

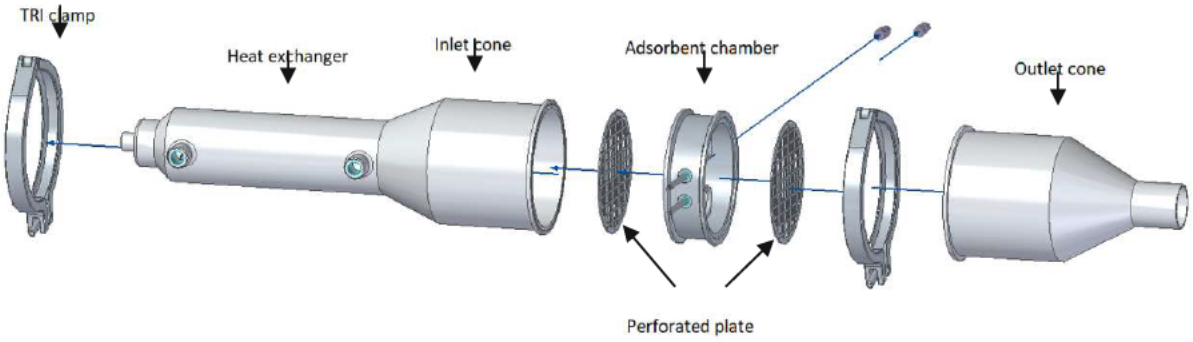

Figure 42: Exploded-view drawing of the prototype in adsorption mode

The inlet cone is mounted on the table using pipe clamps and is thus the fixed part. The fixed bed plate is mounted on the inlet cone by means of a TRI clamp. The fixed bed plate consists of an aluminium rotating part with TRI Clamp flanges on both sides. Both sides are closed with a perforated plate and fine mesh, forming the adsorbent chamber. A heat exchanger (bent 6mm tube) is also placed in the fixed bed, which can be operated in series with the air heat exchanger in adsorption mode. Distributed around

the circumference of the aluminium rotary part are 3 G¼" holes. One of these holes is used to measure the fixed bed temperature and another hole is used to fill or drain the adsorbent. On the outlet side of the fixed bed, the outlet cone is mounted by means of a TRI clamp as well. In the outlet cone the same measuring equipment is available as in the inlet cone.

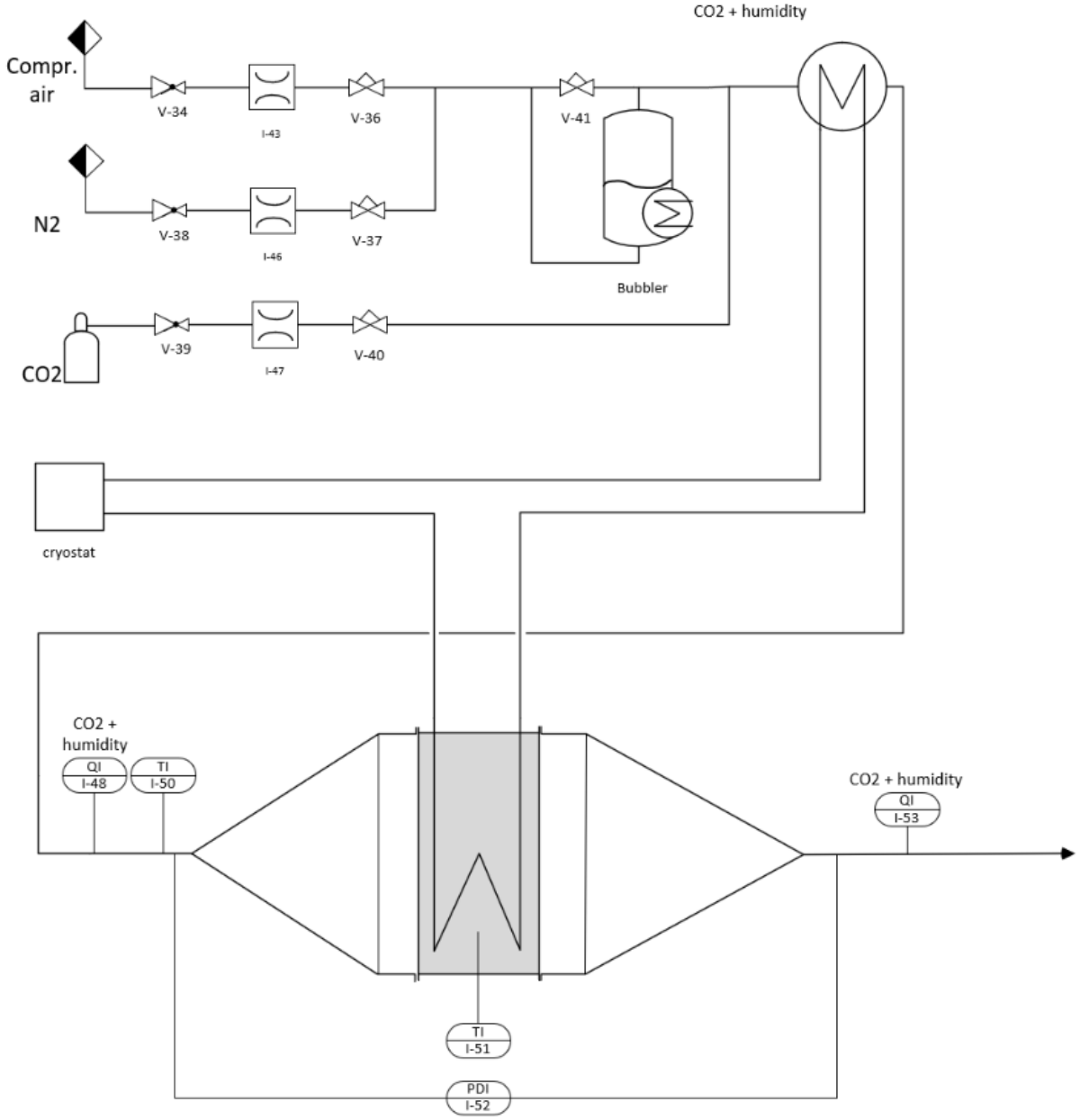

Figure 43: Adsorption setup of prototype

3.5.2 Desorption mode

For regeneration, the air supply is interrupted, and the outlet cone and the adsorbent bed are removed. The lower heating plate is mounted on the frame of the test stand and the adsorbent bed can be fixed to it with a clamp. The same applies to the upper heating plate, which in turn is fixed to the adsorbent bed with a clamp.

The heating plates have fine holes through which the released gas can be extracted. Likewise, the heating

plates have water channels that allow heating by means of a cryostat or thermal oil system. In this case, the two heating plates are connected in series with the internal heat exchanger. The released gas is not drawn off at both plates, but only at one side. Therefore, it is possible to introduce a purge gas such as nitrogen or steam at the opposite plate. During regeneration, the influence of this purge gas on the process is to be investigated. For this purpose, the apparatus is equipped with a steam generator and a membrane pump.

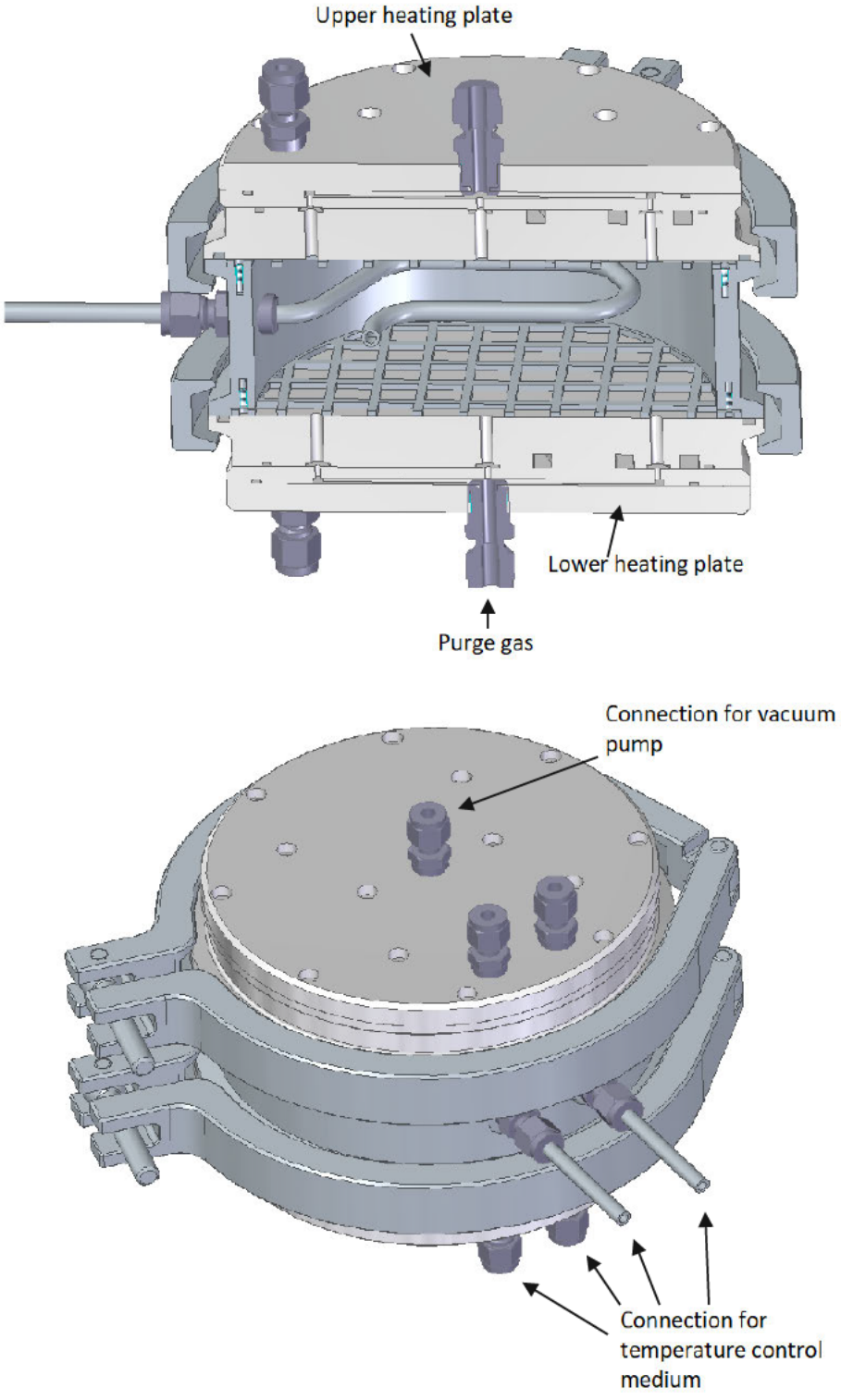

Figure 44: 3D drawing of the prototype in desorption mode

The released gas mixture is pumped off via a downstream vacuum pump. To prevent condensation in the pump and as a carrier gas flow for quantity determination, a defined volume flow of nitrogen can be introduced at the vacuum pump on the suction side as well as after the pump by means of an MFC. The nitrogen flow is selected so that the downstream CO_2 measurement operates in the intended measuring range (0-10000 ppm). From N_2 flow, moisture measurement and CO_2 concentration, statements can finally be made about the absolute amount of CO_2 and water in the originally extracted gas flow. After the vacuum pump, the gas can be cooled down to condensate remaining water in a heat exchanger, if necessary, before it is discharged into the environment.

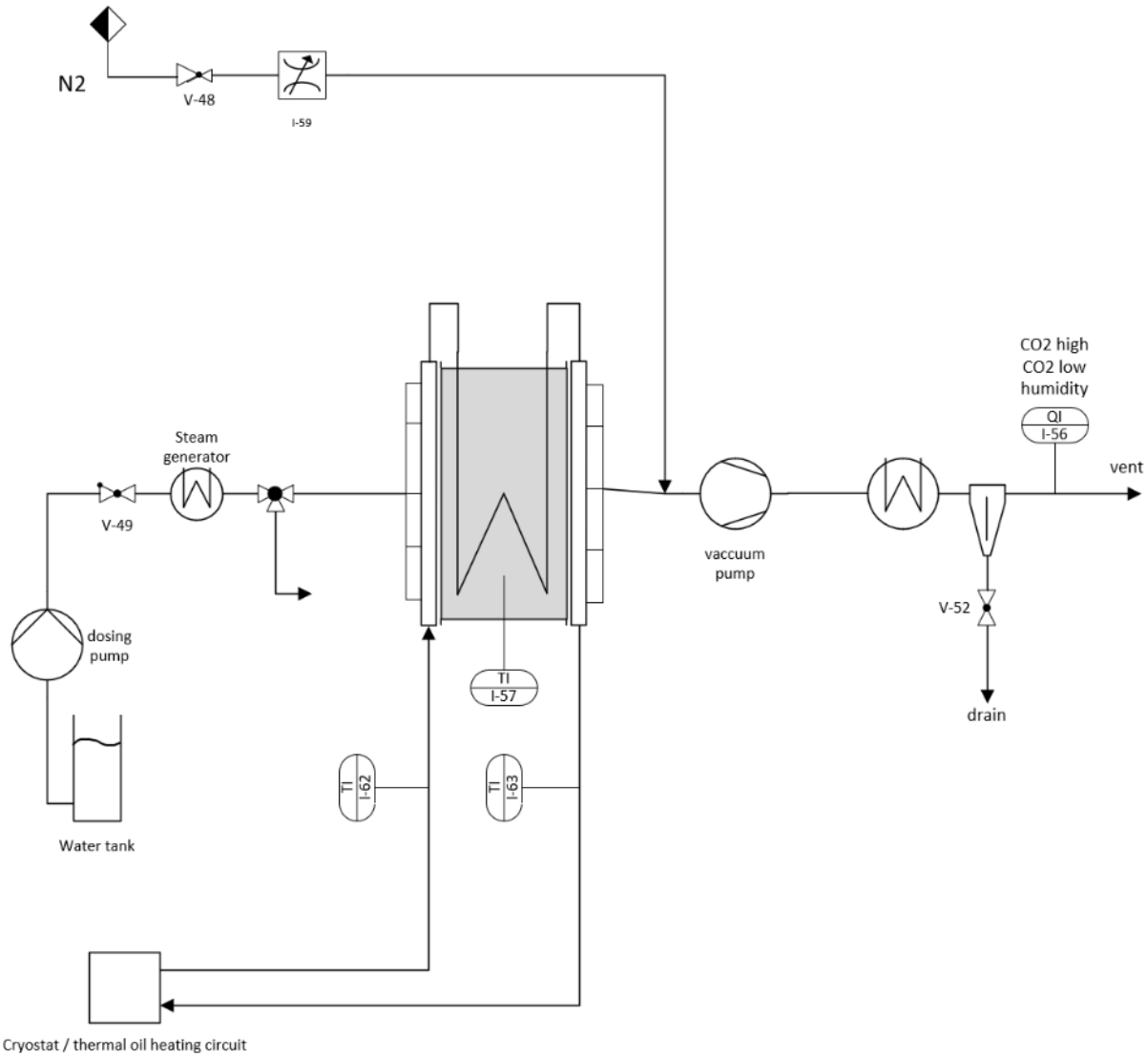

Figure 45: Desorption setup of prototype

4 Discussion of laboratory plant data

4.1 Desorption

Desorption takes place as discussed in 3.3.1 after each adsorption under constant conditions. Figure 46 shows the CO_2 concentration in the exhaust gas stream for three different desorption processes. These desorption processes are part of the first series of experiments in which adsorption was carried out at 25°C and different relative humidity's.

Since different loadings were achieved in the previously held adsorption cycles, the amount of CO_2 that is desorbed also changes. Although the desorption parameters were always kept constant, it can be seen very clearly that the CO_2 content in the nitrogen purge gas stream varies greatly.

A strong variation of the desorption temperature is a possibility, which can influence the desorption time and CO_2 concentration in the exhaust gas. However, Figure 47 contradicts this thesis, since the temperature curves for all desorption cycles are similar. Likewise, the amount of purge gas was always kept constant.

This confirms the assumption made before the start of the test work that little or no meaningful data can be collected via desorption. In this test apparatus, desorption is used exclusively for regeneration of the adsorbent.

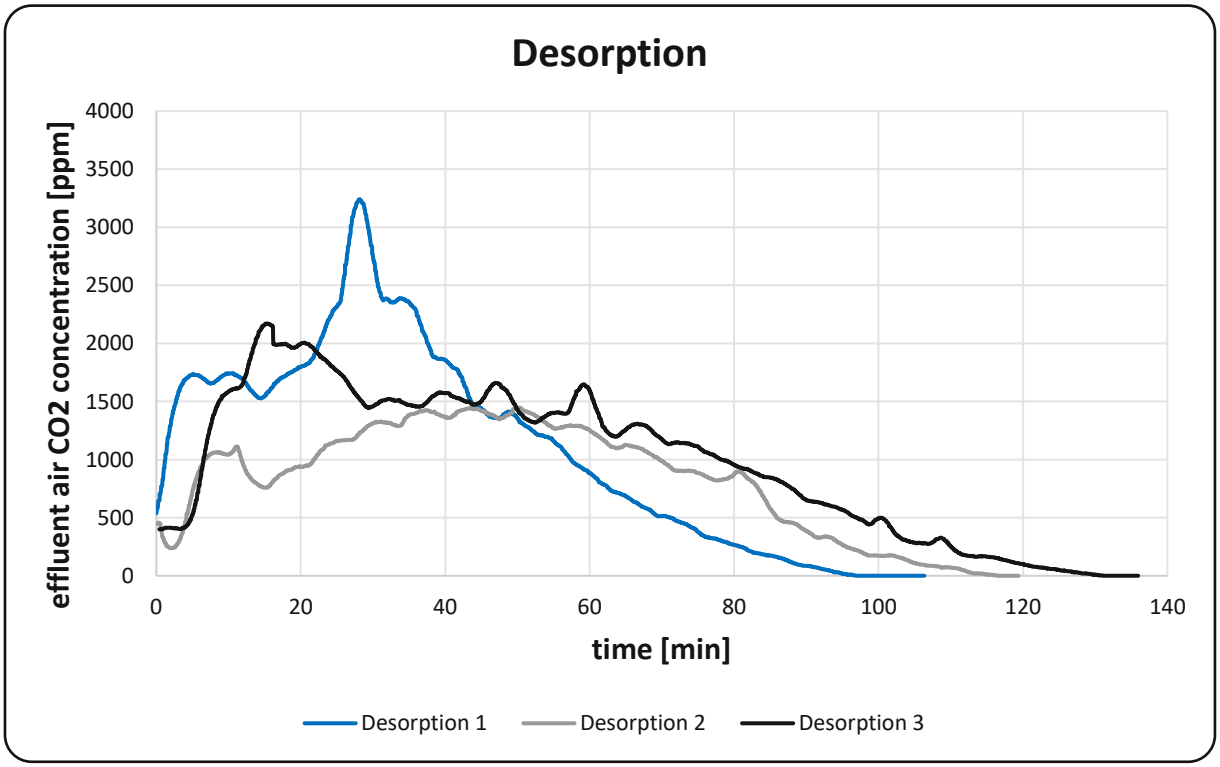

Figure 46: CO_2 concentration of effluent airstream over time for three different desorption cycles. CO_2 content measured in N_2 purge gas flow of 0.5 Nm^3/h

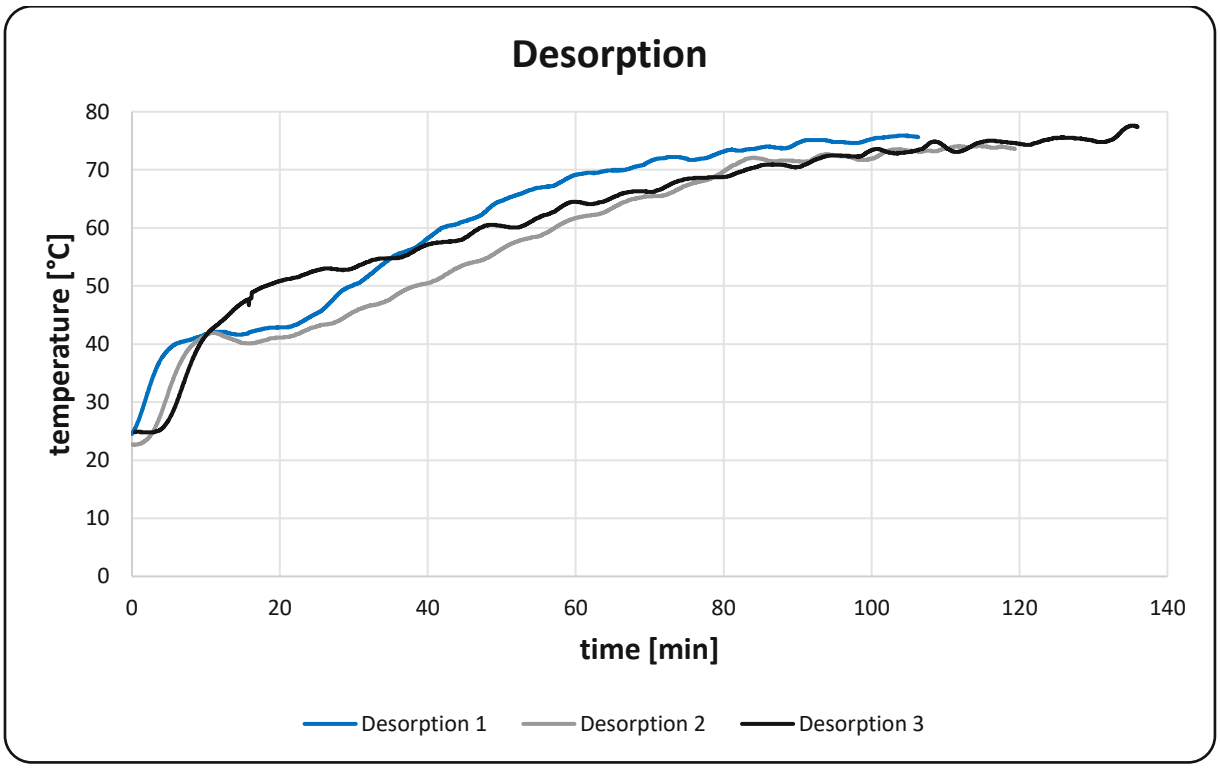

Figure 47: Temperature over time for three different desorption cycles

Figure 48 shows a desorption cycle in which the system has already reached the optimum temperature at the start of desorption. It can be seen very clearly that the desorption enthalpy strongly removes heat from the fixed bed. Furthermore, significantly more CO_2 is released from the fixed bed in the initial phase, compared to the desorption cycles where the plant could only be heated up during the test.

It should be noted, however, that in a range where very high CO_2 partial pressure is measured, the measuring device reaches its limits. Since the measuring instrument has an upper measuring limit of 10000ppm, the curve in this range must be interpolated when evaluating the data.

Implementing this desorption cycle for all experimental runs would not be feasible, as the reactor would have to be disassembled after each adsorption to remove the pebble and the adsorbent placed on top. Additionally, it would be impossible to separate the adsorbent from the pebble. In other words, new pebble and adsorbent would have to be used for each experimental cycle.

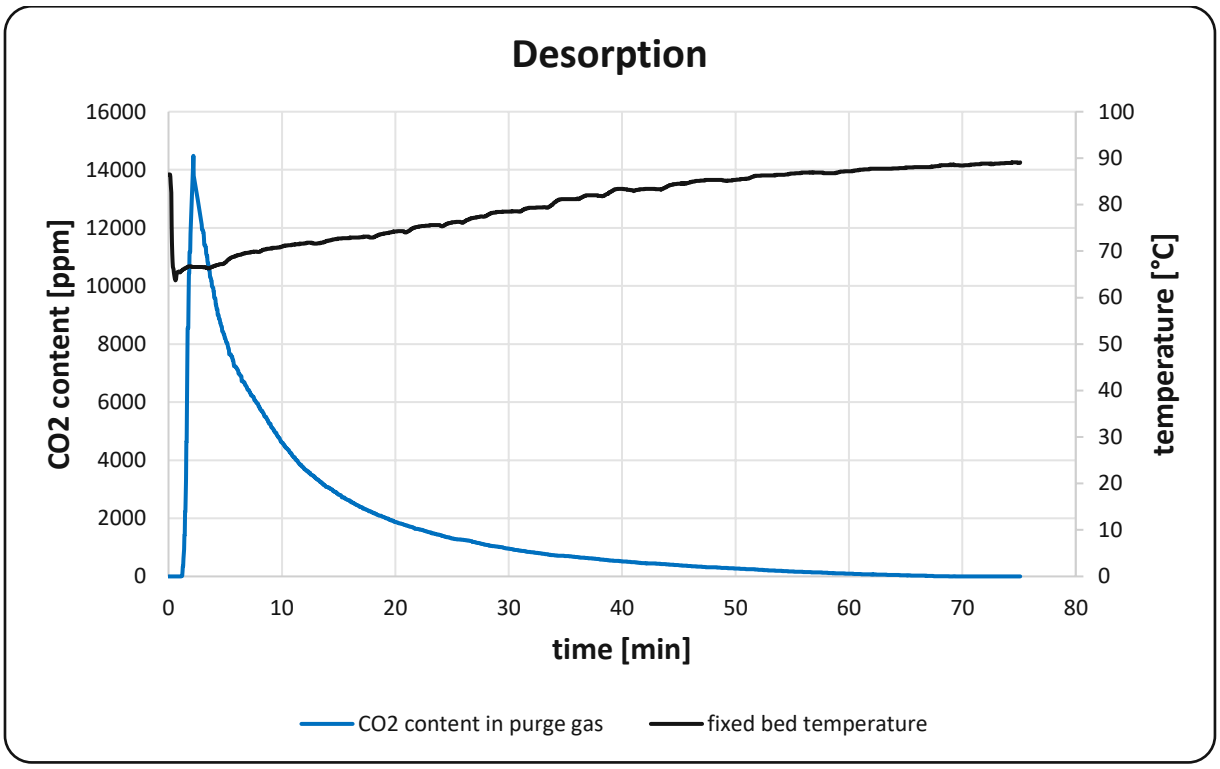

Figure 48: Desorption cycle with optimal bed temperature inside fixed bed. CO_2 content measured in N_2 purge gas flow of 0.5 Nm^3/h

4.2 Adsorption

As already discussed in 3.3.2 adsorption was implemented in three different test series. For this purpose, comparisons are made between the tests, which differ only in the parameter investigated, under otherwise identical or averaged conditions.

4.2.1 Influence of relative humidity

Figure 49 and Figure 50 represent the first test series of the adsorbent. The fixed bed was kept at a constant temperature of 25 °C and the relative humidity of the feed was varied. Significant differences in breakthrough time were obtained as can be seen in Table 14. At a relative humidity of 25%, the breakthrough time was 52 minutes shorter than at 50% rel.h and 66 minutes shorter compared to 75% rel.h.

The reason for this is the significantly higher equilibrium loading of the adsorbent with increasing moisture content. No general statements can be made about the influence of moisture on the reaction rate, since the largest occurring differences of τ_{90} can be explained better by the different equilibrium loadings.

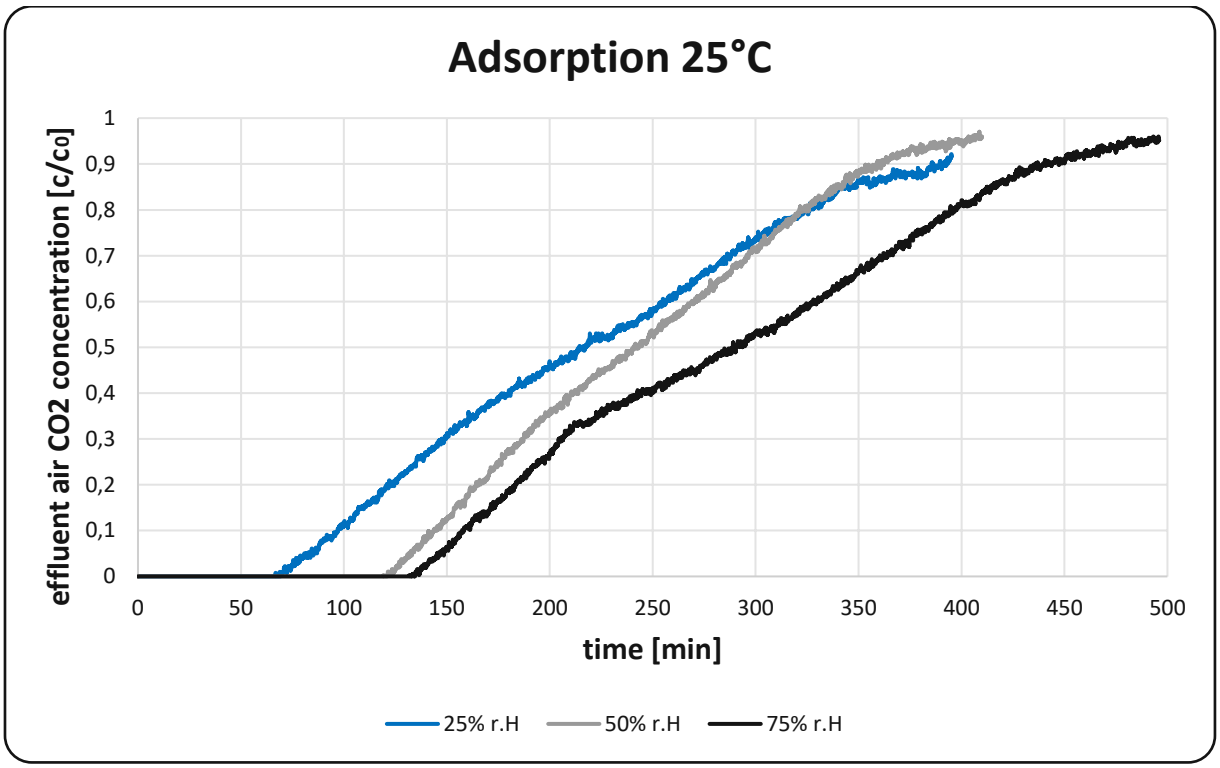

Figure 49: Adsorption breakthrough curve at 25°C for different relative humidity's

A comparison of Figure 49 and Figure 50 also shows that co-adsorption of water takes place, but it is completed much faster than the adsorption of CO_2. Since water was continuously fed into the system via the membrane pump during desorption in order not to dry out the adsorbent, it was not possible to achieve a constant moisture content in the waste gas stream at the start of adsorption. Therefore, it is not possible to make a mass balance of the water adsorption of the adsorbent.

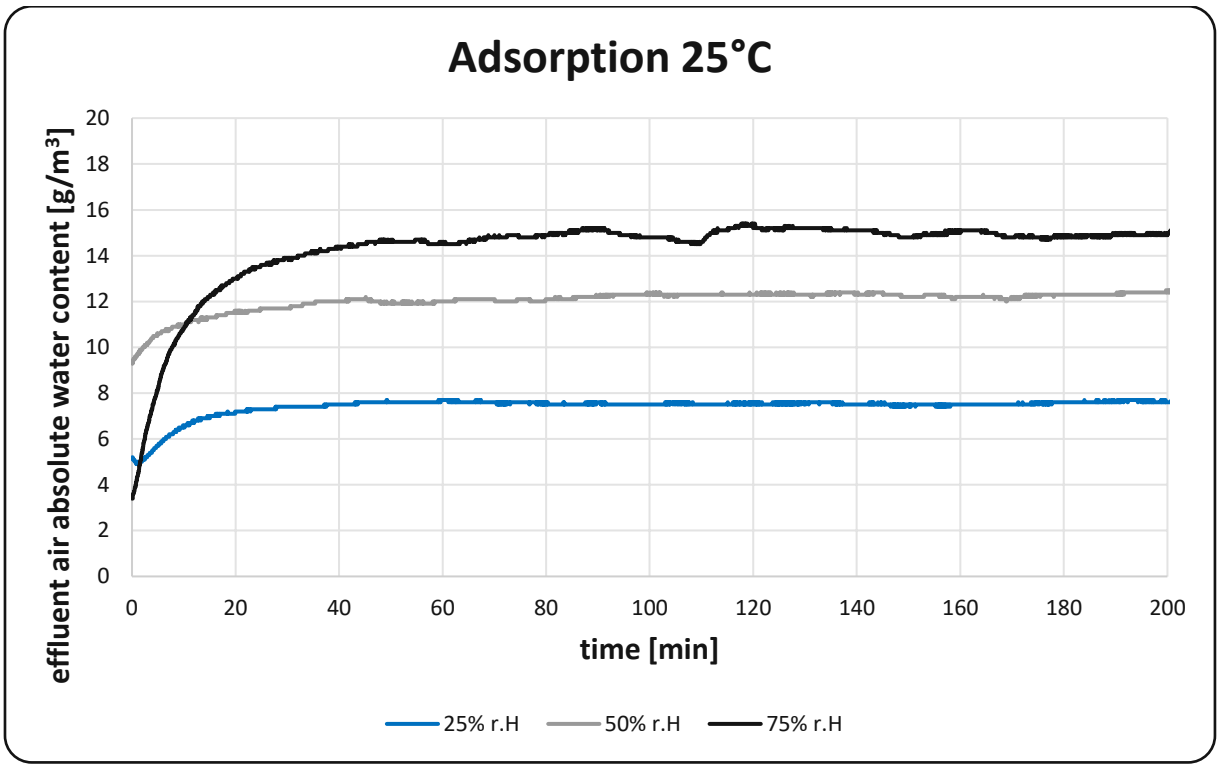

Figure 50: Measured absolute water content of effluent air (25°C; 25-75% r.H)

4.2.2 Influence of temperature

The second test series followed the same scheme as the first test series, but with a modified adsorption temperature. A comparison of Table 14 and Table 15 shows a significant decrease in breakthrough time independent of the moisture content and thus a much lower equilibrium loading of the adsorbent. Furthermore, a decrease in the reaction kinetics can also be observed. In particular, reaching full loading of the adsorbent takes much longer than at lower temperatures. This result is also consistent with findings from literature for chemisorbents.

The adsorption at 35°C and 75% rel.h. was stopped prematurely because the adsorption time exceeded the maximum duration of the measurement data recording, and the data would not have been saved. Measurement fluctuations can also be detected in all the data of this series of experiments. A possible cause for this is a malfunction of the wash bottle in the cryostat. A fluctuation in the relative moisture content of the feed stream would explain this measurement error in both the breakthrough curve and the recording of the absolute water content in the exhaust gas stream.

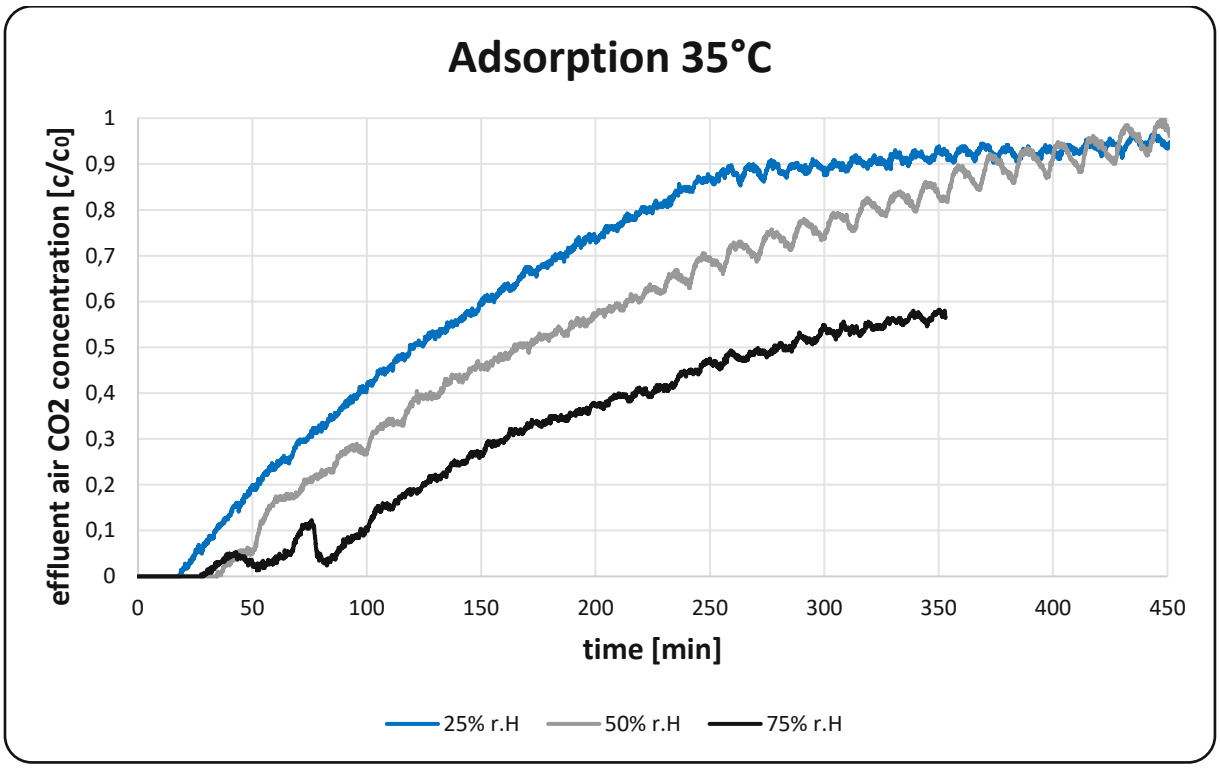

Figure 51: Adsorption breakthrough curve at 35°C for different relative humidity

Another problem that occurred during this series of tests was the partial condensation of water in the exhaust gas stream. Since the measuring probe could unfortunately not be installed in or directly after the reactor, the exhaust gas stream cooled down in the exhaust gas line. This is also confirmed by the data from the thermocouples in the reactor and in the measuring probe. In Figure 52 the absolute humidity directly after the fixed bed is assumed and shown as a dashed line.

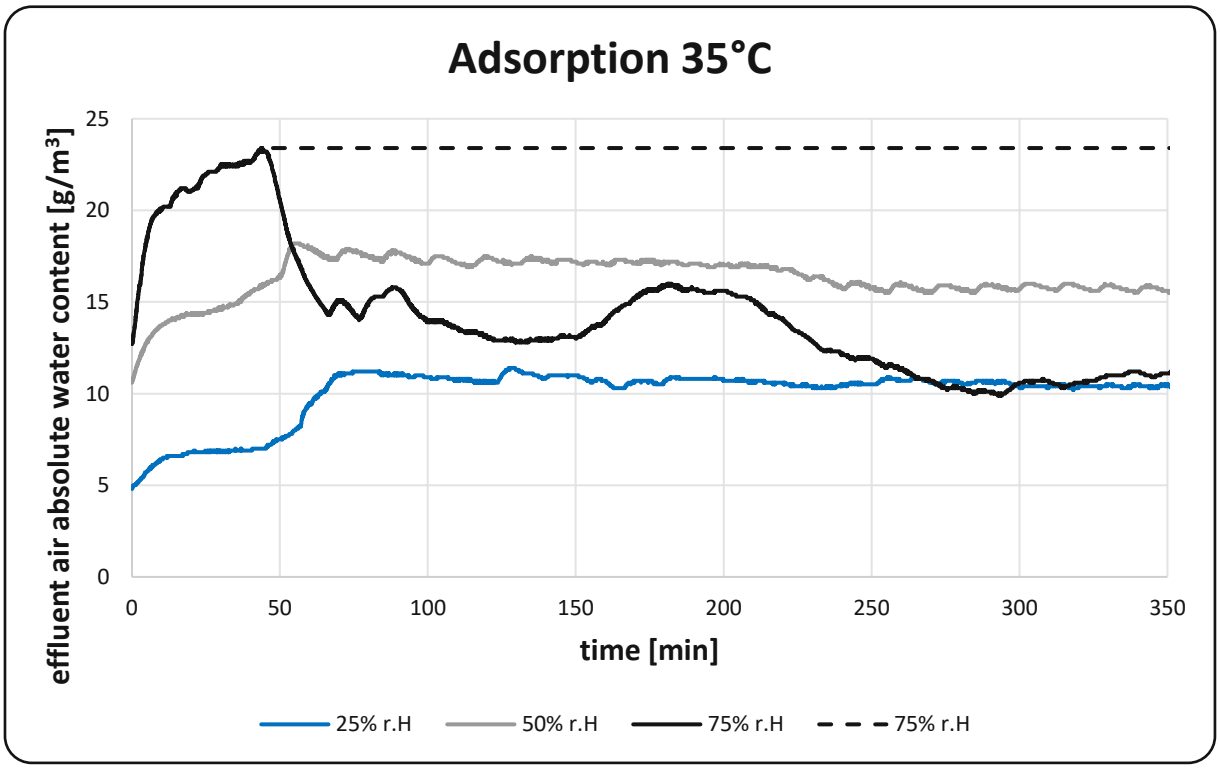

Figure 52: Measured absolute water content of effluent air (35°C; 25-75% rel.h)

4.2.3 Influence of partial pressure

In the third series of experiments, the effect of increasing the partial pressure of CO_2 is investigated. The temperature in the fixed bed and the relative humidity in the feed stream are kept constant. The equilibrium loadings, for the experimental cycles compared in Figure 53 can be read in Table 12. The data clearly shows that as the partial pressure of CO_2 increases, the equilibrium loading only increases very little. In the experimental data, an equilibrium loading of 1.07 mmol/g is obtained for a CO_2 content of 360 ppm in the carrier gas and 1.14 mmol/g at 1800 ppm.

However, a clear acceleration of the adsorption time can be verified when the partial pressure is increased. Interestingly, the breakthrough curve completely disappears for all experiments with CO_2 contents above 360ppm. The time to complete adsorption also varies widely between this series of experiments. This ranges from 410 min at 360ppm CO_2 to 103 min at 1800 ppm. A clear influence of the partial pressure on the adsorption kinetics is generally difficult to detect.

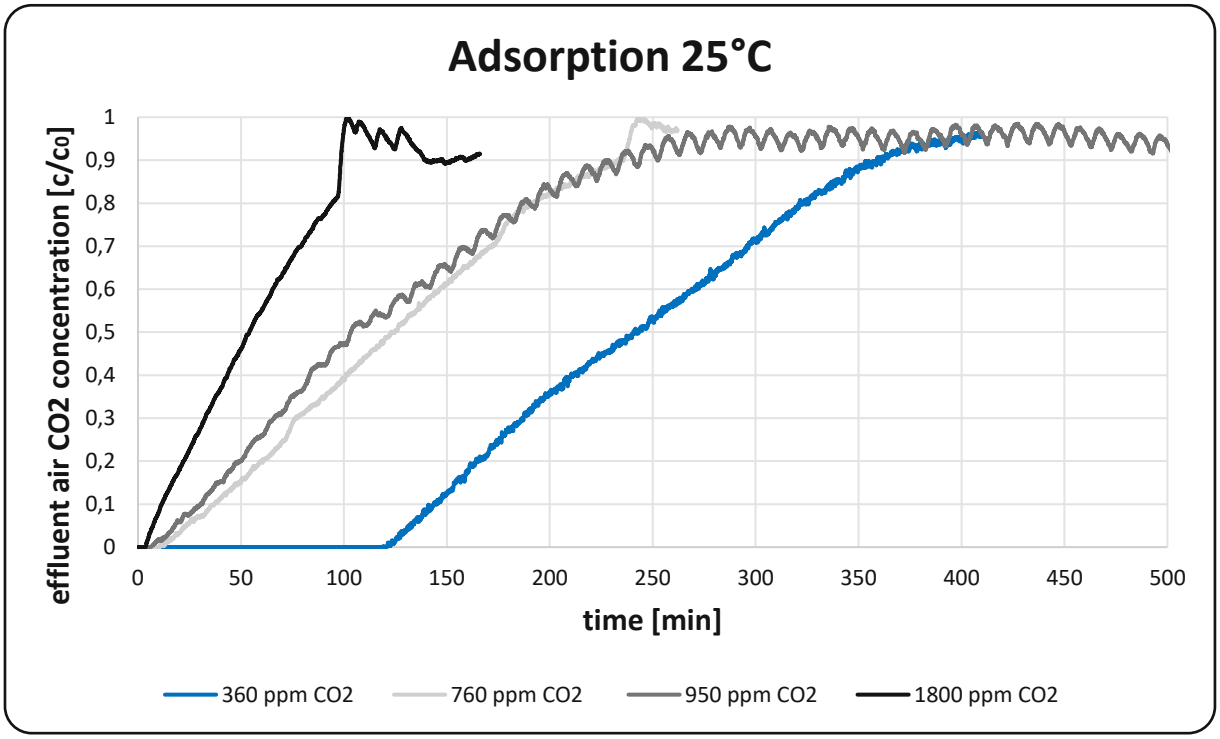

Figure 53: Adsorption breakthrough curve at 25°C and 50% r.H for different partial pressure of CO_2

4.3 Data validation with experimental DAC plant

The first tests of the experimental DAC plant are used to determine the pressure loss of the fixed adsorbent bed as the volume flow increases. This data is very important, as it will be used to determine the fan used for the prototype DAC plant. It also provides information on the energy consumption to be expected for the fan.

In order to validate the measured pressure difference, the pressure drop in the fixed bed was calculated on the basis of fluid mechanical principles as follows:

$$\frac{\Delta p}{H} = 180 * \frac{(1-\varepsilon)^2}{\varepsilon^3} * \frac{\mu * U}{{d_{sv}}^2} \quad (29)$$

The Carman-Kozeny equation, has been shown to be useful for Reynolds numbers less than 1[65][66]. The Reynolds number is to be calculated as follows:

$$Re = \frac{U * \rho_g * d_{sv}}{\mu} \quad (30)$$

As a model conception, it is usually presumed that the flow through the fixed bed takes place in parallel, twisted channels with a changing cross-sectional area.

For Reynolds numbers > 1, the turbulent term must also be taken into account. In this case, the equation according to Ergun has proven itself to be accurate enough[63]:

$$\frac{\Delta p}{H} = 150 * \frac{(1-\varepsilon)^2}{\varepsilon^3} * \frac{\mu * U}{{d_{sv}}^2} + 1{,}75 + \frac{1-\varepsilon}{\varepsilon^3} * \frac{\rho_g * U^2}{{d_{sv}}^2} \quad (31)$$

Table 18: Description of parameters for pressure drop calculation

Variable	Description	Unit
Δp	Pressure drop across fixed bed	bar
H	Height of fixed bed	m
μ	Dynamic viscosity	kg/ms
U	Empty pipe velocity	m/s
d_{sv}	Surface/Volume related diameter	m
ε	Porosity	-

Figure 54 clearly shows that the calculated pressure drop is somewhat lower than the actual measured pressure drop. On the one hand, this may be related to an inconsistent particle size distribution, on the other hand, the mesh and the perforated plates sealing the fixed bed may also cause an increased flow resistant.

Another important finding, which can be seen in Figure 54, is that the pressure drop can be very strongly influenced by varying the particle size. Therefore, the next step is to determine at which particle size and the associated pressure drop the adsorption performance is sufficient.

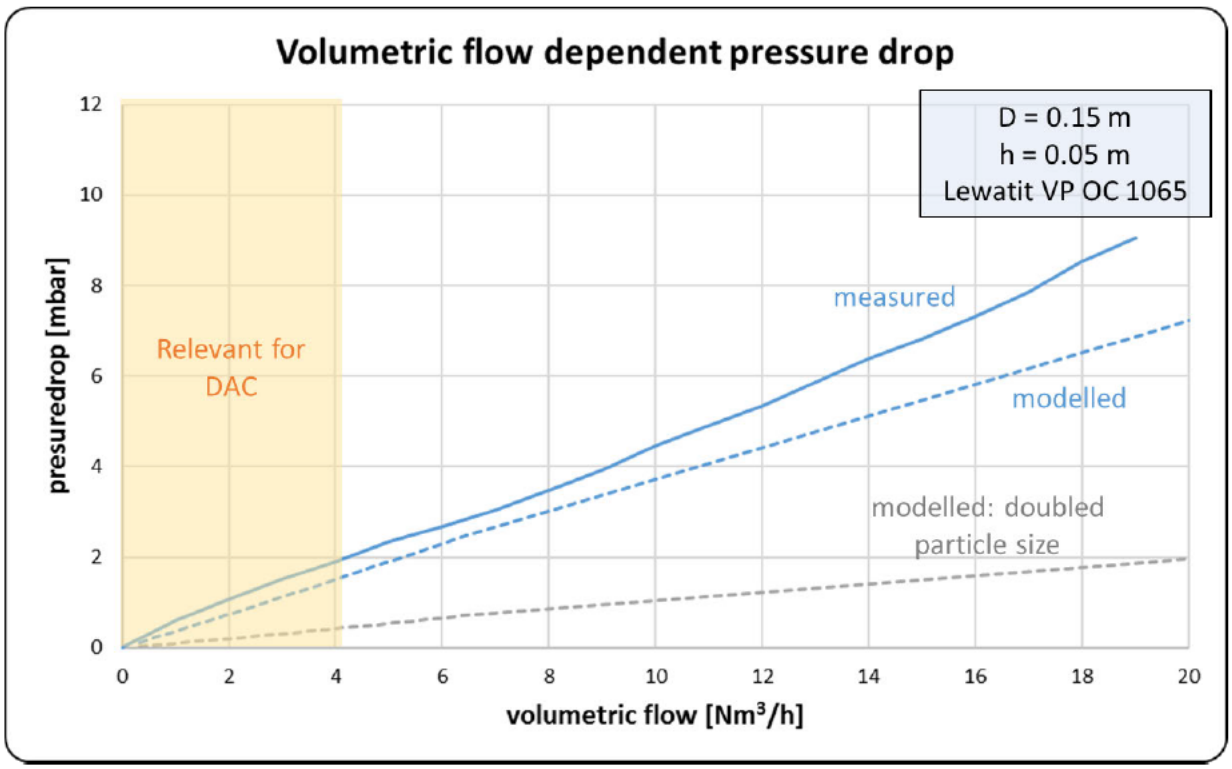

Figure 54: Volumetric flow dependent pressure drop

Another task of the experimental test facility is to validate the adsorption data obtained from the laboratory tests. For this purpose, the adsorption data were recorded for three different volume flows and the adsorption equilibrium was calculated as in 3.4.2.

These results not only confirm the laboratory plant data, they also coincide with the data from the available literature.[37] The small deviation of the CO_2 capacity can be attributed to the influence of the relative humidity. As shown in 3.5.1 a part of the dry volume flow is led through the bubbler, where it absorbs water. The higher this volume flow is, the less water can be absorbed by the air flowing through and the relative humidity during adsorption decreases. Chapter 3.4.2 shows that with increasing relative humidity, the maximum CO_2 capacity also increases.

Figure 55 and Figure 56 show the CO_2 and H_2O breakthrough curves at three different volume flows. As was already clearly visible in the laboratory plant data, the loading of the adsorbent with water is completed much faster than that with CO_2.

Table 19: Adsorption equilibrium and CO_2 capacity from experimental plant at 20°C

Vol. flow [Nm³/h]	5	10	15
Rel. h [%]	35,8	33,4	31,9
q_{CO2} [mmol/g]	1,21	1,19	1,18

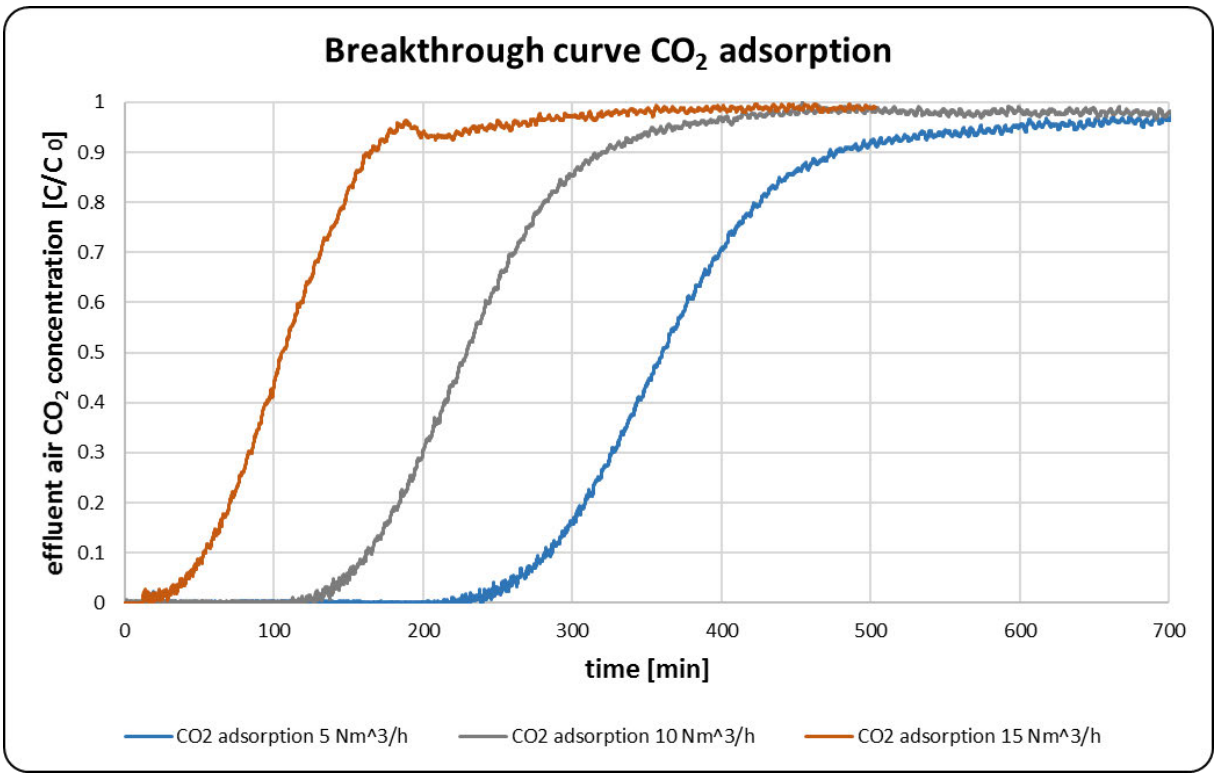

Figure 55: CO_2 Adsorption breakthrough curve at 20°C for different volume flowrates

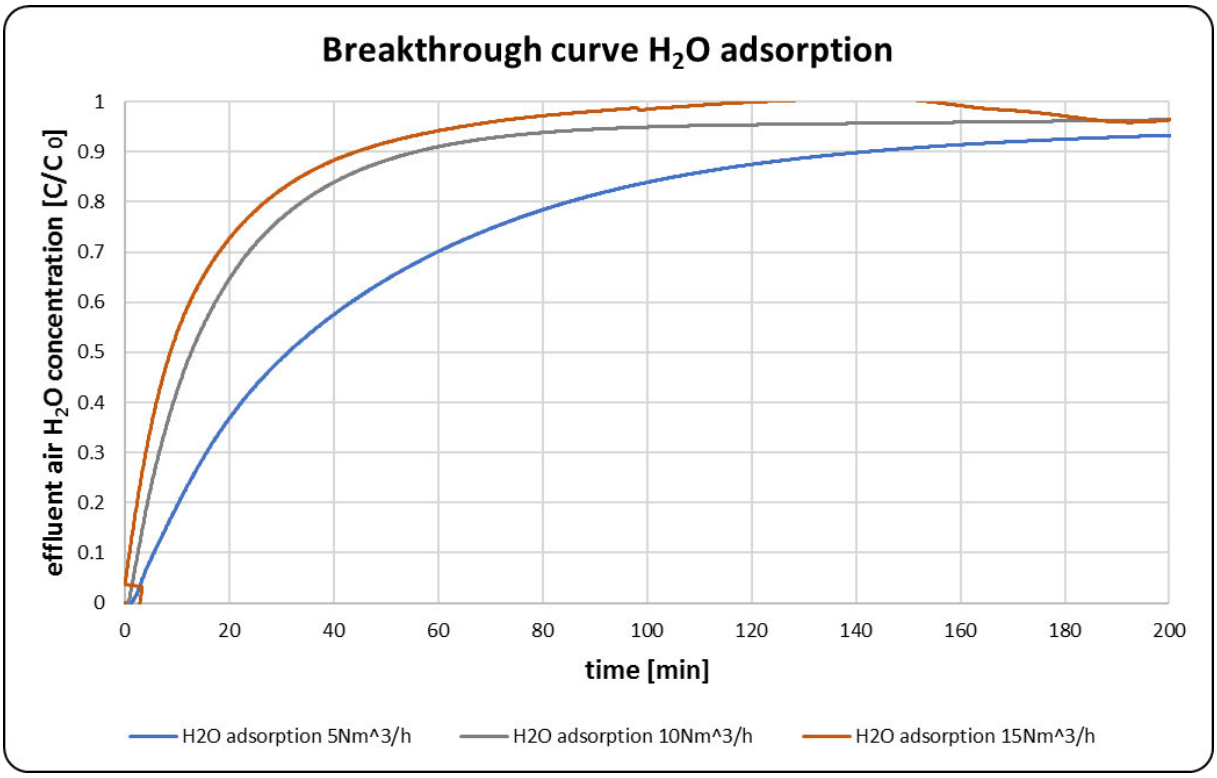

Figure 56: H_2O Adsorption breakthrough curve at 20°C for different volume flowrates

5 Conclusion

In this section, the results are summarized with respect to the set task and opportunities for further research are identified. Based on the research questions presented in Chapter 1, this thesis conducted a comprehensive literature review on direct air capture technology and related adsorption. In addition, an evaluation of the competition was carried out and first experimental data from a test plant was evaluated and presented.

1. **DAC technology:** Based on the research results of the carbon capture theory from concentrated sources, three technologies have become established for applications at very low CO_2 partial pressures (DAC). Direct air capture through aqueous liquid solvents, solid amine sorbents and electrochemical carbon dioxide capture. For both aqueous and solid adsorbents, a large amount of data from literature already exists and the basic mechanisms and parameters on which to build a DAC process are in place. However, the electrochemical recovery of CO_2 is still unexplored and far from being commercially viable. Nevertheless, this approach shows promising results regarding energy consumption which is one of the main problems of DAC that need to be tackled.
2. **Adsorption:** Based on the fundamentals of adsorption, a distinction can be made between physisorption and chemisorption for direct air capture processes. Although the adsorption enthalpy and the associated energy input for chemisorption is significantly higher than that for physisorption, the stronger bonds also typically enable higher adsorption capacities at lower partial pressures which is essential for DAC. The isotherm models are adequately described in the literature for pure component adsorption of CO_2 and H_2O and the adsorbent Lewatit VP OC 1065. For the adsorption of CO_2, the Toth-model has proven to be most accurate especially at low partial pressure ranges. Equally accurate, the GAB model describes the adsorption equilibrium of H_2O adsorption onto solid species. For the co-adsorption of CO_2 and H_2O there is currently no model that can be applied without a coarse adjustment. To explain the co-adsorption of CO_2 and H_2O onto solid sorbents mathematically, the underlying chemical mechanism needs further research. For the first calculation, an empirical solution based on the Toth model could be applied.
3. **Competitors:** The DAC start-ups can be divided into three technology areas (solid sorbent, liquid solvent, electrochemical), as already mentioned in DAC technology. Very clearly, companies based on solid sorbent technology predominate the sector. The reason for this might be that the underlying research is significantly more advanced compared to electrochemical DAC. Furthermore, the investment costs are significantly lower compared to liquid solvents. Another interesting observation is that those start-ups which have emerged from university research groups or at least have a university background, are the most successful and receive the most funding from investors and governments.

4. **Experimental work:** Over three different test series, the adsorbent Lewatit VP OC 1065 was investigated in the laboratory of the TU Wien regarding its adsorption and desorption behaviour in fixed-bed operation. The following adsorption parameters were investigated: temperature (25|35 °C), CO_2 content of the gas stream (360|760|950|1800 ppm) and humidity (25|50|75% rel.H). The results of these investigations were first presented (Chapter 3) and then discussed (Chapter 4). Trends with respect to the varied parameters were examined and compared with literature data. The results confirmed that with increasing the relative humidity the equilibrium loading increases. Furthermore, the data shows that a significantly lower equilibrium loading is achieved with increased temperatures. Finally, the influence of the partial CO_2 pressure on the equilibrium loading was investigated and no significant improvement or deterioration was found.

   Furthermore, the laboratory plant data was validated by adsorption experiments with the novel experimental DAC plant.

5. **Outlook:** Based on the data and results of the laboratory plant, an experimental plant was built at TU Wien. Since the laboratory plants focus is the variation of adsorption parameters, the regeneration of the adsorbent only works with nitrogen purging. The goal of the experimental plant is to investigate different desorption parameters. The unit can be operated with different purge gases (nitrogen/steam) and partial pressures. In addition, by means of comprehensive measurement data recording it is possible to draw mass and energy balances over the entire system and thus generate initial data for the economic operation of a DAC process. Based on this experimental system, a first DAC prototype will be planned, built, and commissioned in the Technikum of the TU Wien.

6 Directories

6.1 List of abbreviations and symbols

Abbreviation/Symbol	
DAC	Direct air capture
HVAC	Heating, ventilation and air conditioning
UN	United Nations
TGA	Thermogravimetric analysis
NET	Negative emissions technologies
IPCC	Intergovernmental panel on climate change
TVSA	Temperature-vacuum swing adsorption
HAS	Hyperbranched amino silica
BPM	Bipolar membrane
AEL/CEL	Anion/Cation exchange layer
GDE	Gas diffusion electrodes
TSA	Temperature swing adsorption
PSA	Pressure swing adsorption
CSA	Composition swing adsorption
GAB	Guggenheim-Anderson-de Boer
BET	Brunauer–Emmett–Teller
CO_2	Carbon dioxide
ppm	Parts per million
Gt	gigatonnes
Na_2CO_3	Sodium carbonate
$NaHCO_3$	Sodium hydrogen carbonate
$Ca(OH)_2$	Calcium hydroxide
$CaCO_3$	Calcium carbonate
H_2O	Water
CaO	Calcium oxide
KOH	Potassium hydroxide
K_2CO_3	Potassium carbonate
$KHCO_3$	Potassium bicarbonate
H_2SO_4	Sulfuric acid
KH_2PO_4	Monopotassium phosphate
H_3PO_4	Phosphoric acid

PEH	Pentaethylenehexamine
TEP	Tetraethylenepentamine
MEA	Monoethanolamine
DEA	Diethanolamine
PEI	Ployethylenimines

6.2 List of tables

Table 1: Description of parameters for adsorption Isotherms 19

Table 2: Description of parameters for H_2O isotherms 20

Table 3: List of Climeworks partners 22

Table 4: Technical specifications of Soletair's DAC unit 26

Table 5: Technical data for Testo measuring device and measuring probe 32

Table 6: Material data of Lewatit [55] 33

Table 7: Description of parameters for calculation of the fixed bed operation 38

Table 8: Desorption parameters 39

Table 9: Adsorption parameters 41

Table 10: Adsorption equilibrium at 25°C 45

Table 11: Adsorption equilibrium at 35°C 45

Table 12: Adsorption equilibrium at 25°C and 50% relative humidity for various partial pressure of CO_2 45

Table 13: Description of parameters for calculating adsorption equilibrium 47

Table 14: Adsorption kinetics at 25°C 48

Table 15: Adsorption kinetics at 35°C. Missing data is explained in chapter 4 48

Table 16: Adsorption kinetics at 25°C and 50% relative humidity in min 48

Table 17: Description of adsorption kinetic parameters 48

Table 18: Description of parameters for pressure drop calculation 62

Table 19: Adsorption equilibrium and CO_2 capacity from experimental plant at 20°C 63

6.3 List of figures

Figure 1: Global surface temperature increase since 1850-1900 as a function of cumulative CO_2 emissions [7] 2

Figure 2: Types of carbon capture scenarios[8] 3

Figure 3: Schematic of a membrane separation process[10] 4

Figure 4: (a) Cumulative number of patents and patent applications and (b) Total number of publications on Direct Air Capture since 2018[19] 5

Figure 5:Simplified flowsheet of a DAC process with a liquid solvent [22][23] 7

Figure 6:Schematic of a solar fluidized-bed reactor for the consecutive conduction of the carbonation and calcination steps using solar energy (ETH Zurich)[21] 8

Figure 7: Display of the three classes of amine adsorbent materials[25] 9

Figure 8: a) Linear PEI structure and b) branched PEI structure[21] 10

Figure 9: Variation of cyclic CO_2 adsorption (open symbols) and desorption (closed symbols) capacity of SI-AEATPMS as a function of: (a) adsorption humidity, (b) desorption pressure and (c) desorption temperature [28] 11

Figure 10: Cyclic regenerability of the HAS4 adsorbent compared to a representative class 2 adsorbent[29] 11

Figure 11: Schematic of water electrolysis. [30] 12

Figure 12: (a) BPMED schematic. (b) BPMED for CO_2 recovery; (ES) electrode solution = KOH; (AS) acid solution of KH_2PO_4 +H_3PO_4; (BS) base solution of six different mixtures of $KHCO_3$,K_2CO_3 and KOH.[30] 13

Figure 13: (a) Electrochemical CO_2 separation using gas diffusion electrodes (GDE) through binding with quinone redox-active carrier (i.e., no pH-swing is created). (b) Combination of pH-swing with the chemistry of redox active carriers through (PCET) reaction using mixture of hydroquinone, quinone, and sodium bicarbonate [30] 14

Figure 14: Adsorption and Desorption system of a two-component gas phase on a solid sorbent material. Extracted from Keller and Staudt [34] 15

Figure 15: Adsorption isotherms of a physisorbent (left, active char) and a chemisorbent (right, amine functionalized sorbent)[36] 16

Figure 16: Schematic diagram of an idealized temperature swing adsorption (TSA) process[39] 18

Figure 17:IUPAC classification of physisorption isotherms. Extracted from Sing et al. [43] 19

Figure 18: Representative process flow diagram for solid sorbent DAC. Green lines represent gaseous flows and blue lines liquid flows [6] 23

Figure 19:Process chemistry and thermodynamics of Carbon Engineering's DAC process[22] 24

Figure 20: Representative process flow diagram for the solvent process.[6] 25

Figure 21: Stages of TVSA operation of the DAC unit. (a) Adsorption. (b) Purging. (c) Heating. (d) Desorption[52] 27

Figure 22: Electrochemical DAC membrane (RepAir)[53] 28

Figure 23: Overview of existing DAC Start-up companies 29

Figure 24: Testing facility Technikum TU Vienna 30

Figure 25: Flow diagram of the fixed bed adsorption (upper) and desorption (lower) apparatus 31

Figure 26: Testo measuring device and measuring probe 32

Figure 27: Cryostat with gas washing bottle 33

Figure 28:Molecular structure and surface of Lewatit VP OC 1065 34

Figure 29: Calculated CO2 capacity at direct air capture conditions for VP OC 1065[59] 34

Figure 30:Effect of temperature in dry air exposure on the CO_2 adsorption capacity (evaluated at 15 vol % CO_2, 40 °C) as a function of treatment time[60] 35

Figure 31: CO_2 adsorption isotherms for Lewatit obtained from FB and TGA measurements [37] 36

Figure 32: Thermal stability of Lewatit 37

Figure 33: Minimum fluidization velocity[64] 37

Figure 34: Display of desorption enthalpy influence 40

Figure 35: Displayed water adsorption of the adsorbent 42

Figure 36: Typical adsorption curve 43

Figure 37: Typical desorption curve. CO_2 content measured in N_2 purge gas flow of 0.5 Nm^3/h 44

Figure 38: Adsorption equilibrium as a function of relative humidity for different temperatures (25/35°C) 46

Figure 39: Adsorption equilibrium as a function of different CO_2 partial pressures (360/760/950/1800 ppm) 46

Figure 40: Experimental DAC plant set up in the Technikum at TU Wien. The system is shown in desorption mode. In the lower part of the picture, the vacuum pump can also be seen operating at 398 mbar..... 50

Figure 41: 3D drawing of the prototype in adsorption mode 51

Figure 42: Exploded-view drawing of the prototype in adsorption mode..... 51

Figure 43: Adsorption setup of prototype 52

Figure 44: 3D drawing of the prototype in desorption mode 53

Figure 45: Desorption setup of prototype..... 54

Figure 46: CO_2 concentration of effluent airstream over time for three different desorption cycles. CO_2 content measured in N_2 purge gas flow of 0.5 Nm^3/h 55

Figure 47: Temperature over time for three different desorption cycles..... 56

Figure 48: Desorption cycle with optimal bed temperature inside fixed bed. CO_2 content measured in N_2 purge gas flow of 0.5 Nm^3/h..... 57

Figure 49: Adsorption breakthrough curve at 25°C for different relative humidity's..... 58

Figure 50: Measured absolute water content of effluent air (25°C; 25-75% r.H) 59

Figure 51: Adsorption breakthrough curve at 35°C for different relative humidity..... 60

Figure 52: Measured absolute water content of effluent air (35°C; 25-75% rel.h) 60

Figure 53: Adsorption breakthrough curve at 25°C and 50% r.H for different partial pressure of CO_2 61

Figure 54: Volumetric flow dependent pressure drop 63

Figure 55: CO_2 Adsorption breakthrough curve at 20°C for different volume flowrates 64

Figure 56: H_2O Adsorption breakthrough curve at 20°C for different volume flowrates 64

6.4 Literature

[1] A. Hubbard, "Adsorption: Theory, Modeling and Analysis. Edited by Jozsef Toth," *J. Colloid Interface Sci.*, vol. 260, no. ISSN: 0021-9797, 2003.

[2] S. Brunauer, P. H. Emmett, and E. Teller, "Adsorption of Gases in Multimolecular Layers," *J. Am. Chem. Soc*, vol. 60, no. ISSN: 0002-7863, p. 319, 1938.

[3] A. Samanta, A. Zhao, G. Shimizu, P. Sarkar, and R. Gupta, "Post-Combustion CO_2 Capture Using Solid Sorbents: A Review," *Ind. Eng. Chem. Res.*, vol. 51, Nov. 2011.

[4] H. D. Matthews and K. Caldeira, "Stabilizing climate requires near-zero emissions," vol. 35, no. December 2007, pp. 1–5, 2008.

[5] S. Solomon, G. Plattner, R. Knutti, and P. Friedlingstein, "Irreversible climate change due to carbon," *Proc. Natl. Acad. Sci. U. S. A.*, no. February 2014, 2009.

[6] N. McQueen, K. V. Gomes, C. McCormick, K. Blumanthal, M. Pisciotta, and J. Wilcox, "A review of direct air capture (DAC): scaling up commercial technologies and innovating for the future," *Prog. Energy*, vol. 3, no. 3, p. 032001, 2021.

[7] P. Zhai, "AR6 Climate Change 2021: The Physical Science Basis," 2021.

[8] P. K. Wong, A. Rajendran, I. A. Karimi, "Carbon capture and storage/utilisation technology primer: a summary," pp. 1–12, 2011.

[9] E. P. Fernando Vega, Luz M. Gallego Fernández, S. C. Mercedes Cano, and B. Navarrete, "Solvents for Carbon Dioxide Capture," *Intech*, vol. 11, no. tourism, p. 13, 2016.

[10] Y. Wang, L. Zhao, A. Otto, M. Robinius, and D. Stolten, "A Review of Post-combustion CO_2 Capture Technologies from Coal-fired Power Plants," *Energy Procedia*, vol. 114, no. November 2016, pp. 650–665, 2017.

[11] J. Xu, "Post-combustion CO_2 capture with membrane process: Practical membrane performance and appropriate pressure," *J. Memb. Sci.*, vol. 581, no. November 2018, pp. 195–213, 2019.

[12] K. S. Lackner, H. Ziock, and P. Grimes, "Carbon capture from air, is it an option?," *AIDS Read.*, vol. 18, no. 6, p. 292, 2008.

[13] F. S. Zeman and K. S. Lackner, "Capturing carbon dioxide directly from the atmosphere," *World Resour. Rev.*, vol. 16, no. 2, pp. 157–172, 2004.

[14] D. W. Keith, M. Ha-Duong, and J. K. Stolaroff, "Climate strategy with CO_2 capture from the air," *Clim. Change*, vol. 74, no. 1–3, pp. 17–45, 2006.

[15] R. Baciocchi, G. Storti, and M. Mazzotti, "Process design and energy requirements for the

capture of carbon dioxide from air," *Chem. Eng. Process. Process Intensif.*, vol. 45, no. 12, pp. 1047–1058, 2006.

[16] F. Zeman, "Energy and material balance of CO_2 capture from ambient air," *Environ. Sci. Technol.*, vol. 41, no. 21, pp. 7558–7563, 2007.

[17] K. S. Lackner, "Capture of carbon dioxide from ambient air," *Eur. Phys. J. Spec. Top.*, vol. 176, no. 1, pp. 93–106, 2009.

[18] E. S. Sanz-Pérez, C. R. Murdock, S. A. Didas, and C. W. Jones, "Direct Capture of CO_2 from Ambient Air," *Chem. Rev.*, vol. 116, no. 19, pp. 11840–11876, 2016.

[19] M. Ozkan, "Direct air capture of CO_2: A response to meet the global climate targets," *MRS Energy Sustain.*, no. 0123456789, pp. 1–6, 2021.

[20] A. Goeppert, M. Czaun, G. K. Surya Prakash, and G. A. Olah, "Air as the renewable carbon source of the future: An overview of CO 2 capture from the atmosphere," *Energy Environ. Sci.*, vol. 5, no. 7, pp. 7833–7853, 2012.

[21] X. Shi, "Sorbents for the Direct Capture of CO_2 from Ambient Air," *Angew. Chemie - Int. Ed.*, vol. 59, no. 18, pp. 6984–7006, 2020.

[22] D. W. Keith, G. Holmes, D. St. Angelo, and K. Heidel, "A Process for Capturing CO_2 from the Atmosphere," *Joule*, vol. 2, no. 8, pp. 1573–1594, 2018.

[23] F. Sabatino, "Evaluation of a Direct Air Capture Process Combining Wet Scrubbing and Bipolar Membrane Electrodialysis," *Ind. Eng. Chem. Res.*, vol. 59, no. 15, pp. 7007–7020, 2020.

[24] S. Han, M. Yoo, D. Kim, and J. Wee, "Carbon Dioxide Capture Using Calcium Hydroxide Aqueous Solution as the Absorbent," *Energy & Fuels*, pp. 3825–3834, 2011.

[25] S. A. Didas, S. Choi, W. Chaikittisilp, and C. W. Jones, "Amine − Oxide Hybrid Materials for CO 2 Capture from Ambient Air," *ACS Sustain. Chem. Eng.*, 2015.

[26] A. Goeppert, M. Czaun, R. B. May, G. K. S. Prakash, G. A. Olah, and S. R. Narayanan, "Carbon dioxide capture from the air using a polyamine based regenerable solid adsorbent," *J. Am. Chem. Soc.*, vol. 133, no. 50, pp. 20164–20167, 2011.

[27] Y. Belmabkhout and A. Sayari, "Effect of pore expansion and amine functionalization of mesoporous silica on CO_2 adsorption over a wide range of conditions," *Adsorption*, vol. 15, no. 3, pp. 318–328, 2009.

[28] J. A. Wurzbacher, C. Gebald, and A. Steinfeld, "Separation of CO 2 from air by temperature-vacuum swing adsorption using diamine-functionalized silica gel," *Energy Environ. Sci.*, vol. 4, no. 9, pp. 3584–3592, 2011.

[29] S. Choi, H. Drese, P. M. Eisenberger, and C. W. Jones, “Application of Amine-Tethered Solid Sorbents for Direct CO 2 Capture from the Ambient Air,” pp. 2420–2427, 2011.

[30] R. Sharifian, R. M. Wagterveld, I. A. Digdaya, C. Xiang, and D. A. Vermaas, “Electrochemical carbon dioxide capture to close the carbon cycle,” *Energy Environ. Sci.*, vol. 14, no. 2, pp. 781–814, 2021.

[31] S. Stucki, A. Schuler, and M. Constantinescu, “Coupled CO_2 Recovery from the atmosphere and water electrolysis,” *Int. J. Hydrog. Energ-*, vol. 20, no. 8, pp. 653–663, 1995.

[32] H. Xie, Y. Wu, T. Liu, F. Wang, B. Chen, and B. Liang, “Low-energy-consumption electrochemical CO_2 capture driven by biomimetic phenazine derivatives redox medium,” *Appl. Energy*, vol. 259, no. November 2019, p. 114119, 2020.

[33] D. Bathen and M. Breitbach, *Adsorptionstechnik*. Berlin [u.a.]: Springer, 2001.

[34] J. Keller and R. Staudt, “Gas Adsorption Equilibria: Experimental Methods and Adsorptive Isotherms B,” *J. Am. Chem. Soc.*, vol. 127, no. 20, pp. 7655–7656, 2005.

[35] A. W. Adamson, “The physical chemistry of surfaces, second edition: by Arthur W. Adamson,” *J. Colloid Interface Sci.*, vol. 28, no. 2, p. 340, 1968.

[36] A. H. Berger and A. S. Bhown, “Comparing physisorption and chemisorption solid sorbents for use separating CO_2 from flue gas using temperature swing adsorption,” *Energy Procedia*, vol. 4, no. May, pp. 562–567, 2011.

[37] H. Hofbauer, G. Schöny, and E. Zerobin, “Development of a temperature swing adsorption process for biogas upgrading,” TU Vienna, 2019.

[38] R. Goedecke, *Fluidverfahrenstechnik*. 2006.

[39] J. A. Mason, K. Sumida, Z. R. Herm, R. Krishna, and J. R. Long, “Evaluating metal-organic frameworks for post-combustion carbon dioxide capture via temperature swing adsorption,” *Energy Environ. Sci.*, vol. 4, no. 8, pp. 3030–3040, 2011.

[40] R. Veneman, N. Frigka, W. Zhao, Z. Li, S. Kersten, and W. Brilman, “Adsorption of H2O and CO_2 on supported amine sorbents,” *Int. J. Greenh. Gas Control*, vol. 41, pp. 268–275, 2015.

[41] J. Young, E. García-Díez, S. Garcia, and M. van der Spek, “ The impact of binary water–CO 2 isotherm models on the optimal performance of sorbent-based direct air capture processes ,” *Energy Environ. Sci.*, vol. 14, no. 10, pp. 5377–5394, 2021.

[42] M. Hefti and M. Mazzotti, “Modeling water vapor adsorption / desorption cycles,” *Springer Sci.*, no. October 2013, pp. 359–371, 2014.

[43] K. Sing, “Reporting Physisorption Data for Gas/Solid Systems with Special Reference to the

Determination of Surface Area and Porosity," *Pure Appl. Chem.*, vol. 54, pp. 2201–2218, Jan. 1982.

[44] V. Stampi-Bombelli, M. van der Spek, and M. Mazzotti, "Analysis of direct capture of CO 2 from ambient air via steam-assisted temperature–vacuum swing adsorption," *Adsorption*, vol. 26, no. 7, pp. 1183–1197, 2020.

[45] J. A. Wurzbacher, C. Gebald, S. Brunner, and A. Steinfeld, "Heat and mass transfer of temperature-vacuum swing desorption for CO_2 capture from air," *Chem. Eng. J.*, vol. 283, pp. 1329–1338, 2016.

[46] J. Young, E. Garcı, and S. Garcia, "The impact of binary water– CO_2 isotherm models on the optimal performance of sorbent-based direct air capture processes," *Energy Environ. Sci.*, pp. 5377–5394, 2021.

[47] C. Beuttler, L. Charles, and J. Wurzbacher, "The Role of Direct Air Capture in Mitigation of Anthropogenic Greenhouse Gas Emissions," *Front. Clim.*, vol. 1, no. November, pp. 1–7, 2019.

[48] C. Gebald, J. A. Wurzbacher, P. Tingaut, and A. Steinfeld, "Stability of amine-functionalized cellulose during temperature-vacuum-swing cycling for CO_2 capture from air," *Environ. Sci. Technol.*, vol. 47, no. 17, pp. 10063–10070, 2013.

[49] C.E.Ltd,"Carbon Engineering: Our story." [Online]. Available: https://carbonengineering.com/our-story/.

[50] P. Eisenberger, "System and method for carbon dioxide capture and sequestration," 2017.

[51] U. Satish, M. J. Mendell, K. Shekhar, T. Hotchi, and D. Sullivan, "Concentrations on Human Decision-Making Performance," *Environ. Health Perspect.*, vol. 120, no. 12, pp. 1671–1678, 2012.

[52] F. V. Vázquez, "Power-to-X technology using renewable electricity and carbon dioxide from ambient air: SOLETAIR proof-of-concept and improved process concept," *J.* CO_2 *Util.*, vol. 28, no. September, pp. 235–246, 2018.

[53] Y. Yushan and B. Setzler, "Electrochemical devices and fuel cell systems," 2020.

[54] A. P. Tirio and R. Wagner, "Process and apparatus for carbon dioxide and carbonyl sulfide capture via ion exchange resins," 2015.

[55] Lanxess, "Lewatit VP OC 1065 Technical Datasheet," pp. 3–6, 2017.

[56] R. Veneman, T. Hilbers, D. W. F. Brilman, and S. R. A. Kersten, "CO_2 capture in a continuous gas-solid trickle flow reactor," *Chem. Eng. J.*, vol. 289, pp. 191–202, 2016.

[57] E. Sonnleitner, G. Schöny, and H. Hofbauer, "Assessment of zeolite 13X and Lewatit® VP OC

1065 for application in a continuous temperature swing adsorption process for biogas upgrading," *Biomass Convers. Biorefinery*, vol. 8, no. 2, pp. 379–395, 2018.

[58] H. Hofbauer, G. Schöny, and F. Dietrich, "Experimental Studies on a Multi-Stage Fluidized Bed System for Post-Combustion CO 2 Capture," 2019.

[59] W. Buijs and S. De Flart, "Direct Air Capture of CO_2 with an Amine Resin: A Molecular Modeling Study of the CO_2 Capturing Process," *Ind. Eng. Chem. Res.*, vol. 56, no. 43, pp. 12297–12304, 2017.

[60] Q. Yu, J. D. L. P. Delgado, R. Veneman, and D. W. F. Brilman, "Stability of a Benzyl Amine Based CO_2 Capture Adsorbent in View of Regeneration Strategies," *Ind. Eng. Chem. Res.*, vol. 56, no. 12, pp. 3259–3269, 2017.

[61] Y. Li, H. Yi, X. Tang, F. Li, and Q. Yuan, "Adsorption Separation of CO_2/CH_4 Gas Mixture on the Commercial Zeolites at Atmospheric Pressure," *Chem. Eng. J.*, vol. 229, pp. 50–56, Aug. 2013.

[62] J. R. Grace, "Gas-Solid and Other Two-Phase Suspemmm," vol. 64, no. June, 1986.

[63] S. Ergun, "Fluid flow through packed columns," *Chemical enfineering progress*. pp. 89–94, 1952.

[64] J. Drake, "Hydrodynamic Characterization of 3D Fluidized Beds Using Noninvasive Techniques," no. January 2011, 2011.

[65] J. Kozeny, "Über kapillare Leitung des Wassers im Boden," *Akad. Wiss.Wien*, vol. 136, pp. 271–306, 1927.

[66] P. G. Carman, "Fluid flow through granular beds," *Chem. Eng. Res. Des.*, vol. 75, no. 1 SUPPL., pp. S32–S48, 1997.